



Pandian, Chenthamarai (2018) *Orbit manipulation of two closely-passing asteroids using a tether*. MSc(R) thesis.

<https://theses.gla.ac.uk/8953/>

Copyright and moral rights for this work are retained by the author

A copy can be downloaded for personal non-commercial research or study, without prior permission or charge

This work cannot be reproduced or quoted extensively from without first obtaining permission in writing from the author

The content must not be changed in any way or sold commercially in any format or medium without the formal permission of the author

When referring to this work, full bibliographic details including the author, title, awarding institution and date of the thesis must be given

Enlighten: Theses

<https://theses.gla.ac.uk/>
research-enlighten@glasgow.ac.uk

ORBIT MANIPULATION OF TWO CLOSELY-PASSING ASTEROIDS USING A TETHER

CHENTHAMARAI PANDIAN

Submitted in fulfilment of the requirements for the
Degree of Master of Science (Research)

School of Engineering
University of Glasgow



©2018 Chenthamarai Pandian

Chenthamarai Pandian: Orbit manipulation of two closely-passing asteroids using a tether.

Submitted in fulfilment of the requirements for the Degree of Master of Science (Research)
School of Engineering
University of Glasgow

©2018 Chenthamarai Pandian

ADVISORS:

Dr Matteo Ceriotti

Dr Patrick Harkness

Glasgow, Scotland, United Kingdom

Abstract

Asteroids can be considered both a threat as well as a source of mineral resources. Either way, asteroids have become a point of interest for scientists, space enthusiasts and private industries. Whether it be for protecting Earth from an asteroid strike or to obtain an asteroid for the prospect of mining, it is essential that we understand and identify a method to manipulate the orbital trajectory of an asteroid. There are quite some numbers of proposed methods to achieve a change in the orbital trajectory of an asteroid; some of the notable ones are gravity tractors, low thrust propulsion devices, kinetic impactors, and tethers.

In this thesis we will manipulate the orbital trajectory of an asteroid by transferring orbital energy between the asteroid in question and another closely-passing asteroid. The energy and momentum transfer are achieved by connecting the asteroids through a tether at their closest point of approach leading to the formation of a dumbbell system. The formation of the dumbbell system results in the transfer of some of the linear kinetic energy of both asteroids into rotational kinetic energy, which causes the dumbbell system to rotate about its centre of mass with an angular velocity leading to a rotational angular momentum. Disconnecting the tether at a point in time leads to the disruption of the dumbbell system and the asteroids gain or lose angular momentum and orbital energy from the system. The distribution of the orbital energy between the system and the asteroids determines the resulting orbit of the asteroids. A study on how parameters such as the length of the tether, the eccentricity of the asteroids at the time of tether connection and the mass of the asteroid affects the distribution of energy and angular momentum between the asteroids and the system is carried out. A detailed analysis with some selected combination of the above discussed parameters, such as how long to wait before tether disconnection to achieve maximum or minimum deflection from the initial orbit is carried out. This is done by modelling the dynamics of the asteroid-dumbbell system in MATLAB, where in the physics involving the orbital and attitude dynamics of the system are set up.

Some of the main results showed that the model specific error in orbital energy reduced with the reduction of the tether length, a gradual change in orbital energy for increase in tether length w.r.t angular displacement can be noticed for the dumbbell system, compared to periodic change for individual asteroids, and that there exists multiple opportunities for orbital change of the asteroids in the dumbbell system for a single heliocentric orbital motion of the centre of mass and a more desired orbit change can be achieved with multiple heliocentric orbits of the centre of mass of the dumbbell system.

Contents

Abstract	v
List of Figures	ix
List of Tables	x
Acknowledgement	xi
Declaration	xiii
Symbols	xv
Acronyms	xxi
1. Introduction	1
1.1 Asteroids.....	1
1.1.1 Description, Etymology and History.....	1
1.1.2 Detection and Classification	5
1.1.3 Reference Frames and Coordinate Systems.....	10
1.1.4 Celestial Dynamics.....	12
1.2 Asteroid Orbit Manipulation	28
1.2.1 Nuclear Detonation	29
1.2.2 Kinetic Impactor.....	30
1.2.3 Gravity Tractor.....	30
1.2.4 Focused Solar Energy	30
1.2.5 Mass Driver	31
1.2.6 Tether Assisted Deflection.....	31
1.3 Motivation	49
1.3.1 Asteroid Mining	51
1.3.2 In-Situ Resource Utilization.....	52
1.3.3 Scientific Missions	52
1.3.4 Economics	53
1.4 Concept used in this research	54
1.5 Objectives	54
1.5.1 Study on parameters	55
2. Model Description	57
2.1 Assumption.....	57
2.2 Representation	58
2.3 Dumbbell System	59
2.3.1 Attitude Dynamics	60

2.3.2	Orbital Dynamics	60
2.3.3	Dumbbell Propagation	63
3.	Parameters Affecting Orbit Manipulation.....	65
3.1	Energy and Angular Momentum.....	65
3.2	Variation of parameters	67
3.2.1	Length of the tether	67
3.2.2	Mass Ratio	72
3.2.3	Eccentricity	75
4.	Resulting Orbits and Wait Times.....	77
4.1	Energy Distribution over an Orbit.....	77
4.2	Wait Time.....	78
4.2.1	Single Orbit	78
4.2.2	Multiple Orbits	86
5.	Conclusion	101
5.1	Summary	101
5.2	Objectives Achieved.....	102
5.3	Remarks.....	102
5.4	Feasibility of the Idea	103
5.4.1	Asteroids	103
5.4.2	Tether	104
5.5	Future Work	104
5.5.1	Orbital Energy Range.....	104
5.5.2	Other Future Research.....	105
	References	107

List of Figures

FIG 1.1 CERES, PICTURE CAPTURED BY NASA’S DAWN SPACECRAFT ON APRIL 14, 2015.	2
FIG 1.2 JUPITER AFTER SHOEMAKER-LEVY 9 COLLISION.....	4
FIG 1.3 COMPARISON ON THE NUMBER OF ASTEROIDS DISCOVERED BETWEEN 1950 AND 2015 ^[19]	5
FIG 1.4 ASTEROID CLASSIFICATION BASED ON DYNAMICS.....	9
FIG 1.5 ASTEROID CLASS DISTRIBUTION.....	9
FIG 1.6 DEGREES OF FREEDOM OF AN ASTEROID.....	12
FIG 1.7 CONIC SECTIONS	15
FIG 1.8 REPRESENTATION OF AN ELLIPSE.....	16
FIG 1.9 REPRESENTATION OF THE CLASSICAL ORBITAL ELEMENTS.....	18
FIG 1.10 REPRESENTATION OF A PERIFOCAL FRAME	23
FIG 1.11 ARTIST’S DEPICTION OF A GRAVITY TRACTOR IN ACTION.....	30
FIG 1.12 DUMBBELL SATELLITE SYSTEM WITH AN IN-PLANE MOTION.....	34
FIG 1.13 DUMBBELL SATELLITE SYSTEM WITH AN OUT-OF-PLANE MOTION.....	39
FIG 1.14 EARTH’S GRAVITY WELL	43
FIG 1.15 LEGEND FOR FIG 1.16 AND FIG 1.17	46
FIG 1.16 ANGULAR DISPLACEMENT VS ORBITAL ENERGY OF SATELLITE1.....	46
FIG 1.17 ANGULAR DISPLACEMENT VS ORBITAL ENERGY OF SATELLITE2.....	46
FIG 1.18 NEA DISCOVERIES BY SURVEY (CREDIT: MPC)	50
FIG 2.1 REPRESENTATION OF THE MODEL.....	58
FIG 3.1 ERROR PERCENTAGE PLOT FOR VARIOUS TETHER LENGTHS.....	69
FIG 3.2 ENERGY OF ASTEROID1 AFTER TETHER DISCONNECTION FOR VARYING TETHER LENGTH AND ANGULAR DISPLACEMENT	71
FIG 3.3 ENERGY OF ASTEROID2 AFTER TETHER DISCONNECTION FOR VARYING TETHER LENGTH AND ANGULAR DISPLACEMENT	71
FIG 3.4 ENERGY OF DUMBBELL SYSTEM AFTER TETHER DISCONNECTION FOR VARYING TETHER LENGTH AND ANGULAR DISPLACEMENT	72
FIG 3.5 PLOT LEGEND FOR INITIAL ORBITS IN CASE1, CASE2 AND CASE3.....	73
FIG 3.6 ORBITS AT TETHER CONNECTION WITH MASS RATIO 1:1	73
FIG 3.7 ORBITS AT TETHER CONNECTION WITH MASS RATIO 1:2.....	74
FIG 3.8 ORBITS AT TETHER CONNECTION WITH MASS RATIO 2:1	74
FIG 3.9 ORBITS AT TETHER CONNECTION WITH $e_1 = 0.5$ AND $e_2 = 0$.....	76
FIG 3.10 ORBITS AT TETHER CONNECTION WITH $e_1 = 0$ AND $e_2 = 0.5$.....	76
FIG 4.1 ORBITAL ENERGIES OF THE ASTEROIDS WITH RESPECT TO THE TRUE ANOMALY OF THE CENTRE OF MASS.....	78
FIG 4.2 LEGEND FOR THE RESULTING ORBIT PLOTS	79
FIG 4.3 INITIAL, DUMBBELL AND FINAL ORBITS OF THE ASTEROIDS FOR A TETHER CUT AT TRUE ANOMALY 30 DEGREES	80
FIG 4.4 INITIAL, DUMBBELL AND FINAL ORBITS OF THE ASTEROIDS FOR A TETHER CUT AT TRUE ANOMALY 60 DEGREES	80
FIG 4.5 INITIAL, DUMBBELL AND FINAL ORBITS OF THE ASTEROIDS FOR A TETHER CUT AT TRUE ANOMALY 90 DEGREES	81

FIG 4.6 INITIAL, DUMBBELL AND FINAL ORBITS OF THE ASTEROIDS FOR A TETHER CUT AT TRUE ANOMALY 120 DEGREES	82
FIG 4.7 INITIAL, DUMBBELL AND FINAL ORBITS OF THE ASTEROIDS FOR A TETHER CUT AT TRUE ANOMALY 150 DEGREES	82
FIG 4.8 INITIAL, DUMBBELL AND FINAL ORBITS OF THE ASTEROIDS FOR A TETHER CUT AT TRUE ANOMALY 180 DEGREES	83
FIG 4.9 INITIAL, DUMBBELL AND FINAL ORBITS OF THE ASTEROIDS FOR A TETHER CUT AT TRUE ANOMALY 210 DEGREES	83
FIG 4.10 INITIAL, DUMBBELL AND FINAL ORBITS OF THE ASTEROIDS FOR A TETHER CUT AT TRUE ANOMALY 240 DEGREES	84
FIG 4.11 INITIAL, DUMBBELL AND FINAL ORBITS OF THE ASTEROIDS FOR A TETHER CUT AT TRUE ANOMALY 270 DEGREES	84
FIG 4.12 INITIAL, DUMBBELL AND FINAL ORBITS OF THE ASTEROIDS FOR A TETHER CUT AT TRUE ANOMALY 300 DEGREES	85
FIG 4.13 INITIAL, DUMBBELL AND FINAL ORBITS OF THE ASTEROIDS FOR A TETHER CUT AT TRUE ANOMALY 330 DEGREES	85
FIG 4.14 INITIAL, DUMBBELL AND FINAL ORBITS OF THE ASTEROIDS FOR A TETHER CUT AT TRUE ANOMALY 360 DEGREES	86
FIG 4.15 INITIAL ORBIT PLOTS FOR THE TEST CASE	88
FIG 4.16 ZOOMED VIEW OF FIG 4.15	88
FIG 4.17 LEGENDS FOR FIG 4.18, FIG 4.19, FIG 4.20 AND FIG 4.21	92
FIG 4.18 ENERGY VARIATION OF ASTEROID1 AGAINST ANGULAR DISPLACEMENT OF THE TETHER FOR AN ECCENTRICITY VALUE OF 0	93
FIG 4.19 ENERGY VARIATION OF ASTEROID1 AGAINST THE ANGULAR DISPLACEMENT OF THE TETHER FOR AN ECCENTRICITY VALUE OF 0.0017.....	97
FIG 4.20 ENERGY VARIATION OF ASTEROID1 AGAINST THE ANGULAR DISPLACEMENT OF THE TETHER FOR AN ECCENTRICITY VALUE OF 0.0623.....	98
FIG 4.21 ENERGY VARIATION OF ASTEROID1 AGAINST THE ANGULAR DISPLACEMENT OF THE TETHER FOR AN ECCENTRICITY VALUE OF 0.9.....	99

List of Tables

TABLE 1.1 ORBITAL ENERGIES OF DIFFERENT ORBITS	14
TABLE 1.2 KEPLERIAN ORBITS, THEIR ECCENTRICITIES AND SEMIMAJOR AXIS	16
TABLE 3.1 ERROR PERCENTAGE COMPARISON FOR VARIOUS TETHER LENGTHS	68

Acknowledgement

First and foremost, I would like to thank my parents for their blessings, support and guidance. They have been my pillar of strength throughout my life, without them this would not have been possible, and this thesis is dedicated to them. I would like to thank my brother who has inspired, encouraged and guided me throughout my life. He is the primary reason of inspiration, through his ideas, moulded me to pursue the field of aerospace engineering.

I would like to thank my supervisors Dr Matteo Ceriotti and Dr Patrick Harkness, for accepting me as their student, for their constant guidance, and advice throughout my research. Their enormous support during a time of personal family crisis played a huge part in the successful completion of this thesis. Their novel ideas from the time of conceptualising this research and towards completion shaped this thesis. I have learnt a great deal not only in terms of academics, but a lot more from them. I cannot express my gratitude to them by mere words for their constant support of my research.

I would also like to thank Ms Elaine McNamara for the administrative support and guidance she provided during times when it mattered the most. I would like to thank Ms Heather Lambie and Ms Elizabeth Adams for all the encouragement, support and the multiple opportunities they provided for skill development through participation in curricular and extra-curricular activities not only within the University but throughout Scotland.

I would like to give my special thanks to Mavy for her support in acting as a source of strength and motivation in completing my Thesis during a difficult time. I would also like to thank my friends Aldo, Spencer, Alessandro, Joanna, Firat, James, Alex, Steve, Anne, Nel, and many others for making my time in Glasgow filled with fun. I will cherish those unforgettable memories for ever.

Finally, I would like to thank Mr Ramasamy, manager (Bank of India) for the trust and confidence he had in me to authorise the Loan to partially cover this endeavour.

Last but not the least, I would like to thank the University of Glasgow, for providing with tools, environment, freedom and the support to pursue this research and complete my Thesis.

Declaration

I hereby declare that this submission is my own work and that, to the best of my knowledge and belief, it contains no material previously published or written by another person nor material which to a substantial extent has been accepted for the award of any other degree or diploma of the university or other institute of higher learning, except where due acknowledgement has been made in the text.

Glasgow, Scotland, 21 March 2018.

Chenthamarai Pandian

Symbols

a	Orbital major radii or semimajor axis of the orbit	km
a_{COM}	Semimajor axis of the centre of mass	km
b	Orbital minor radii or semiminor axis of the orbit	km
c_0	Constant of integration	
\vec{e}	Eccentricity vector of the orbit of a body	
e	Eccentricity of the orbit of a body	
e_z	z axis component of the eccentricity vector	
e_1	Eccentricity of the orbit of Asteroid1	
e_2	Eccentricity of the orbit of Asteroid2	
E	Total energy of the dumbbell satellite system	
E_{per}	Percentage of error in the calculation of orbital energy	J
\vec{f}	Gravitational force vector between two bodies	N
F_T	Tether tension force	N
F_C	Centripetal force	N
f_{lag}, g_{lag}	Lagrange coefficients	
$f_{lag,COM}, g_{lag,COM}$	Lagrange coefficients for the centre of mass	
G	Universal gravitational constant	$km^3 kg^{-1}s^{-2}$
\vec{h}	Orbital angular momentum vector of a body per unit mass	$km^2 s^{-1}$
h	Specific orbital angular momentum of the orbiting body	$km^2 s^{-1}$
h_z	z axis component of the orbital angular momentum vector	$km^2 s^{-1}$
\vec{h}_i^{orb}	Orbital angular momentum vector of the respective asteroid	$kg m^2 s^{-1}$
i	Inclination of the orbit of a body	deg
i_1	Inclination of the orbit of Asteroid1	deg
i_2	Inclination of the orbit of Asteroid2	deg
i_{COM}	Inclination of the orbit of the Centre of mass	deg
\hat{K}	Unit vector in the direction of z axis in the reference frame of the orbit of an orbiting body	
K	Kinetic energy of the momentum exchange tether system	J
I	Moment of Inertia about the centre of mass of the dumbbell system	$kg m^2$
l	Length of the tether	km
l_1	Distance between Asteroid1 and the centre of mass	km
l_2	Distance between Asteroid2 and the centre of mass	km
L_1	Distance between Satellite1 and the centre of mass	km
L_2	Distance between Satellite2 and the centre of mass	km
m	Mass of the orbiting body	kg
m_1	Mass of the Asteroid1	kg
m_2	Mass of the Asteroid2	kg
m_i	Mass of the respective asteroid	kg
m_{db}	Mass of the dumbbell system	kg
M	Mass of the central body	kg
M_{Sun}	Mass of the Sun	kg
M_D	Mass of the total momentum exchange tether system	kg
\vec{N}	Node vector of the orbit of an orbiting body	
N	Magnitude of the node vector of the orbit of an orbiting body	
N_x	x axis component of the node vector	

N_y	y axis component of the node vector	
P	Orbital period of the body	s
P_D	Orbital period of the centre of mass of the momentum exchange tether system	s
p	Geometric parameter	
\vec{r}	Radial distance vector between the orbiting and central body	km
r	Magnitude of the radial distance vector between the orbiting and central body	km
r_1	Magnitude of the position vector of Asteroid1 with respect to Sun	km
r_2	Magnitude of the position vector of Asteroid2 with respect to Sun	km
$\vec{r}_{1(0)}$	Initial radius vector of Asteroid1 in Cartesian co-ordinates at time $t = 0$	km
$\vec{r}_{2(0)}$	Initial radius vector of Asteroid2 in Cartesian co-ordinates at time $t = 0$	km
$\vec{r}_{COM(0)}$	Initial radius vector of the centre of mass in Cartesian co-ordinates at time $t = 0$	km
$\vec{r}_{1(t)}$	The radius vector of Asteroid1 with respect to Sun in Cartesian co-ordinates at time t	km
$\vec{r}_{2(t)}$	The radius vector of Asteroid2 with respect to Sun in Cartesian co-ordinates at time t	km
$\vec{r}_{COM(t)}$	Initial radius vector of the centre of mass in Cartesian co-ordinates at time t	km
r_{COM}	Magnitude of the position vector of the centre of mass with respect to Sun (<i>km</i>)	km
\vec{r}_i	Radius vector of the respective asteroid with respect to sun.	km
r_i	Magnitude of the radius vector of the respective asteroid with respect to Sun	km
\vec{r}_t	Radius vector of a body after time t	km
\vec{r}_0	Radius vector of a body at $t = 0$	km
r_0	Magnitude of the radius vector at $t = 0$	km
r_D	Radius of the centre of mass of the momentum exchange tether system from the Sun	km
r_p	Radius at periapsis of the orbiting body	km
$r_{p,1}$	Radius at perihelion of Asteroid1	km
$r_{p,2}$	Radius at perihelion of Asteroid2	km
$r_{p,COM}$	Radius at perihelion of the centre of mass	km
\hat{r}_1	Unit vector for Asteroid1	
\hat{r}_2	Unit vector for Asteroid2	
$\vec{r}_{i_db(t)}$	The position vectors of the respective asteroid with respect to the centre of mass of the dumbbell system at time t in the reference frame <i>Ref B</i>	km
$\vec{r}_{i_orb(t)}$	The position vectors of the respective asteroid relative to the Sun at time t in the reference frame <i>Ref A</i>	km
\hat{r}_{COM}	Unit vector of the Centre of mass	
\vec{R}	Radius vector of the centre of mass of the dumbbell system in the operational context for momentum exchange tether system	km

R	Magnitude of the radius vector of the centre of mass of the dumbbell system in the operational contexts for momentum exchange tether system	km
\vec{R}_1	Radius vector of Satellite1 of the dumbbell system in the operational context for momentum exchange tether system	km
R_1	Magnitude of the radius vector of Satellite1 of the dumbbell system in the operational context for momentum exchange tether system	km
\vec{R}_2	Radius vector of Satellite2 of the dumbbell system in the operational context for momentum exchange tether system	km
R_2	Magnitude of the radius vector of Satellite2 of the dumbbell system in the operational context for momentum exchange tether system	km
t	Time	s
U	Potential energy of the momentum exchange tether system	J
\vec{v}	Orbital velocity vector of the orbiting body	$km\ s^{-1}$
v	Magnitude of the orbital velocity vector of the orbiting body	$km\ s^{-1}$
\vec{v}_t	Orbital velocity vector of a body after time t	$km\ s^{-1}$
v_D	Velocity of the momentum exchange tether	$km\ s^{-1}$
\vec{v}_0	Initial velocity vector of a body.	
v_r	Radial velocity component of the body's orbital velocity	$km\ s^{-1}$
$v_{r(0)}$	Radial velocity component at $t = 0$	
$v_{r,COM(0)}$	Radial velocity component of the centre of mass at $t = 0$	$km\ s^{-1}$
v_{\perp}	Transverse velocity component in the dumbbell system in the momentum exchange tether operational context	$km\ s^{-1}$
$\vec{v}_{1(0)}$	Initial velocity vector of Asteroid1 in Cartesian co-ordinates at time $t = 0$	$km\ s^{-1}$
$\vec{v}_{2(0)}$	Initial velocity vector of Asteroid2 in Cartesian co-ordinates at time $t = 0$	$km\ s^{-1}$
$\vec{v}_{COM(0)}$	Initial velocity vector of the centre of mass in Cartesian co-ordinates at time $t = 0$	$km\ s^{-1}$
$\vec{v}_{COM(t)}$	Velocity vector of the centre of mass in Cartesian co-ordinates at time t	$km\ s^{-1}$
$\vec{v}_{1(t)}$	The orbital velocity vector of Asteroid1 with respect to Sun in Cartesian co-ordinates at time t	$km\ s^{-1}$
$\vec{v}_{2(t)}$	The orbital velocity vector of Asteroid2 with respect to Sun in Cartesian co-ordinates at time t	$km\ s^{-1}$
v_1	Magnitude of the orbital velocity of Asteroid1 with respect to Sun	$km\ s^{-1}$
v_2	Magnitude of the orbital velocity of Asteroid2 with respect to Sun	$km\ s^{-1}$
V_o	Orbital velocity of the centre of mass of the momentum exchange tether system	$km\ s^{-1}$
v_{COM}	Magnitude of the orbital velocity of the centre of mass with respect to Sun	$km\ s^{-1}$
$v_{1,rot}$	Magnitude of the rotational velocity of Asteroid1 relative to the centre of mass	$km\ s^{-1}$
$v_{2,rot}$	Magnitude of the rotational velocity of Asteroid2 relative to the centre of mass	$km\ s^{-1}$
\vec{v}_i	Orbital velocity vector of the respective asteroid with respect to the Sun	$km\ s^{-1}$

v_i	Magnitude of the orbital velocity vector of the respective asteroid with respect to Sun	$km\ s^{-1}$
$\vec{v}_{i_rot}(t)$	Rotational velocity vector of the respective asteroid with respect to the centre of mass of the dumbbell system at time t in the reference frame <i>Ref B</i>	$km\ s^{-1}$
$\vec{v}_{i_orb}(t)$	Orbital velocity vector of the respective asteroid with respect to the centre of mass of the dumbbell system at time t in the reference frame <i>Ref A</i>	$km\ s^{-1}$
X	Universal anomaly	
X_{COM}	Universal anomaly for the centre of mass	
X_0	Universal anomaly with initial trail value	
μ	Standard gravitational parameter of a body	$km^3\ s^{-2}$
μ_S	Standard gravitational parameter of Sun	$km^3\ s^{-2}$
μ_E	Standard gravitational parameter of Earth	$km^3\ s^{-2}$
α	Angle between the tether and the y axis of the local reference frame in context 2 of the momentum exchange tether system	<i>rad</i>
$C(z), S(z)$	Stumpff functions	
β_x	Rotational motion of the asteroid about the x-axis	<i>deg</i>
β_y	Rotational motion of the asteroid about the y-axis	<i>deg</i>
β_z	Rotational motion of the asteroid about the z-axis	<i>deg</i>
Δ_x	Translation motion of the asteroid along the x-axis	<i>km</i>
Δ_y	Translation motion of the asteroid along the y-axis	<i>km</i>
Δ_z	Translation motion of the asteroid along the z-axis	<i>km</i>
ε	Total specific orbital energy of an orbiting body	Jkg^{-1}
ε_{cir}	Specific orbital energy for a body in a circular orbit	Jkg^{-1}
ε_{eli}	Specific orbital energy for a body in an elliptical orbit	Jkg^{-1}
ε_{par}	Specific orbital energy for a body in a parabolic orbit	Jkg^{-1}
ε_{hyp}	Specific orbital energy for a body in a hyperbolic orbit	Jkg^{-1}
ε_1^{orb}	Orbital energy of Asteroid1	<i>J</i>
ε_2^{orb}	Orbital energy of Asteroid2	<i>J</i>
ε_1^{pot}	Potential energy of Asteroid1	<i>J</i>
ε_2^{pot}	Potential energy of Asteroid2	<i>J</i>
ε_1^{kin}	Kinetic energy of Asteroid1	<i>J</i>
ε_2^{kin}	Kinetic energy of Asteroid2	<i>J</i>
ε_{db}^{orb}	Orbital energy of the dumbbell system	<i>J</i>
ε_{db}^{pot}	Potential energy of the dumbbell system	<i>J</i>
ε_{db}^{kin}	Kinetic energy of the dumbbell system	<i>J</i>
$\varepsilon_{db}^{rot_kin}$	Rotational (kinetic) energy of the dumbbell system	<i>J</i>
ε_{db}^{total}	Total energy of the dumbbell system	<i>J</i>
$\varepsilon_1^{orb,BTC}$	Orbital Energy of Asteroid1 before tether connection	<i>J</i>
$\varepsilon_2^{orb,BTC}$	Orbital Energy of Asteroid2 before tether connection	<i>J</i>
$\varepsilon_1^{orb,ATD}$	Orbital Energy of Asteroid1 after tether disconnection	<i>J</i>
$\varepsilon_2^{orb,ATD}$	Orbital Energy of Asteroid2 after tether disconnection	<i>J</i>
ε_i^{orb}	Orbital Energy of the respective asteroid	<i>J</i>
ε_i^{kin}	Kinetic Energy of the respective asteroid	<i>J</i>
ε_i^{pot}	Potential Energy of the respective asteroid	<i>J</i>
θ	True anomaly of the orbiting body	<i>deg</i>
θ_{COM}	True anomaly of the centre of mass	<i>deg</i>
θ_1	True anomaly of Asteroid1	<i>deg</i>

θ_2	True anomaly of Asteroid2	<i>deg</i>
θ_{COM}	True anomaly of the Centre of mass	<i>deg</i>
Θ	Angular displacement of the tether	<i>rad</i>
ϕ	Angle between the tether and z axis of the local coordinate in context 1 of the momentum exchange tether system	<i>rad</i>
\emptyset	Angle between the tether and x axis of the local coordinate in context 2 of the momentum exchange tether system	<i>rad</i>
Ω	Longitude of the ascending node of the orbit	<i>deg</i>
Ω_1	Longitude of the ascending node of Asteroid1	<i>deg</i>
Ω_2	Longitude of the ascending node of Asteroid2	<i>deg</i>
Ω_{COM}	Longitude of the ascending node of the Centre of mass	<i>deg</i>
ω	Argument of periapsis of the orbiting body	<i>deg</i>
ω_1	Argument of periapsis of Asteroid1	<i>deg</i>
ω_2	Argument of periapsis of Asteroid2	<i>deg</i>
ω_D	Orbital angular velocity of the centre of mass of the momentum exchange tether system	<i>rad s⁻¹</i>
ω_v	Angular velocity of the dumbbell system	<i>rad s⁻¹</i>
ω_{COM}	Argument of periapsis of the Centre of mass	<i>deg</i>

Acronyms

AIAA	American Institute of Aeronautics and Astronautics
AIDA	Asteroid Impact and Deflection Assessment.
ASI	Agenzia Spaziale Italiana / Italian Space Agency
ATD	After Tether Disconnection
AU	Astronomical Unit
BBC	British Broadcasting Corporation
BTC	Before Tether Connection
CCD	Charge-Coupled-Device
COPUOS	Committee on the Peaceful Uses of Outer Space
COM	Centre of Mass
GTO	Geostationary Transfer Orbit
IAU	International Astronomical Union
IAWN	International Asteroid Warning Network
ISRU	International Asteroid Warning Network
ISS	International Space Station
JAXA	Japanese Aerospace Exploration Agency
KISS	Keck Institute of Space Studies
LINEAR	Lincoln Near-Earth Asteroid Research
MATLAB	Matrix Laboratory
MOID	Minimum Orbit Intersection Distance
MPC	Minor Planet Center
MSFC	Marshal Space Flight Center
NASA	National Aeronautics and Space Administration
NEAs	Near-Earth Asteroids
NEAT	Near-Earth Asteroid Tracking
NEOs	Near-Earth Objects
NEOWISE	NEO Wide-field Infrared Survey Explorer
Pan-STARRS	Panoramic Survey Telescope and Rapid Response System.
PCAS	Palomar Planet-Crossing Asteroid Survey
PET	Polyethylene Terephthalate
PHAs	Potentially Hazardous Asteroids
SEDS	Small Expendable Deployer System
TiPS	Tether Physics and Survivability

TNT	Trinitrotoluene
TSS	Tethered Satellite System
UN	United Nations
UNO	United Nations Organisation

1. Introduction

The purpose of this chapter is to form the basis of the argument put forward in this thesis, leading to the motivation, objectives and structure of the thesis. To do this we start by explaining what asteroids are, how our view of asteroids has evolved over time (making it an important factor affecting life on our planet), dynamics involved in their propagation, followed by explaining the need to gain control in manipulating their trajectory, and ending this section by setting the methods of achieving our objectives through this research.

1.1 Asteroids

1.1.1 Description, Etymology and History

Asteroids are small, airless rocky bodies revolving around the Sun that are too small to be called planets^[1]. The actual origin and meaning of the word “*asteroid*” comes from the Greek word “*ἀστεροειδής (asteroeidés)*” (meaning “*Star like*”), coined by the German astronomer William Herschel^[2, 3]. They are also, sometimes, called as minor planets.

After the discovery of Ceres (**Fig 1.1**), the largest and the first asteroid to be discovered on 1st January 1801 by the Italian astronomer Giuseppe Piazzi, a new body of similar nature was discovered on 28 March 1802 by Heinrich Wilhelm Matthias Olbers, named as Pallas^[2, 3]. These bodies moved like planets yet were too small to be one, and they also looked like stars but moved fast in relation to the others. This discovery raised the possibility that they might be of a new category of bodies and that there could be more of them. After much deliberation, it was decided that they be named into a new category of celestial bodies called “*asteroids*”^[2].

“The bodies to be named are neither fixed stars, planets, nor comets, but have a great resemblance to all the three?” (Herschel, 1802c)

Though the discovery of asteroids was accidental while in the search for the missing planet (predicted by the Titus-Bode law) between Mars and Jupiter, the early days of their discoveries were exciting to the whole scientific community^[4]. During the latter part of the nineteenth century, dozens of asteroids were discovered, mainly due to the use of photography in astronomy. By the middle of the twentieth century hundreds were discovered, but now they were considered as “*junk*” or “*vermin of the skies*”^[4], as after their discovery there was nothing to be done, the little trail they made in astronomical photographs

were a nuisance. After the advent of the space age, the interest in asteroids started to grow again, the launching of numerous space probes and the advances in the astronomical techniques such as photometry, spectrophotometry, radiometry and polarimetry, due to which approximate determination of the size, shape and mineralogical composition of these bodies were made possible, contributed to some theories on the origin of the solar system^[4,5]. The way people viewed asteroids started to change as our understanding of these celestial bodies went deeper.



Fig 1.1 Ceres, picture captured by NASA’s Dawn spacecraft on April 14, 2015

[Credit: NASA/JPL-Caltech/UCLA/MPS/DLR/IDA]

Though the meteorite impact at Tunguska in 1908 was a massive event, it was largely ignored by the public, due to fact that it happened in a remote uninhabited part of the Earth. Clearly the Tunguska object would have wiped out the population, if it had hit a city, as it is believed that the Tunguska object was tens of metres in diameter and had an explosive energy equivalent to 10 – 20 megatons of Trinitrotoluene (TNT) ^[5].

Space-probe photographs of the cratered surface of Mercury and Mars made it evident that asteroid bombardment had been an important process in the formation and development of many of the planets, including the Earth ^[5]. In fact, the publication of “*Extraterrestrial cause for the Cretaceous–Tertiary extinction*” by Luis Alvarez and others in 1980 provided some conclusive evidence to the asteroid impact theory for the mass extinction of dinosaurs and other species of the Cretaceous period^[6].

This led to considerable interest among the scientific community on the dangers posed by the asteroids. Following this discovery, The National Aeronautics and Space Administration (NASA) convened a workshop, “*Collision of Asteroids and Comets with the Earth: Physical and Human Consequences*” in Snowmass, Colorado (July 13-16, 1981)^[9, 10].

Nine years later, on 23 March 1989, the close passage of a 300-meter-wide asteroid 1989 FC prompted the American Institute of Aeronautics and Astronautics (AIAA, 1990) to recommend studies to increase the detection rate of Near-Earth Asteroids (NEAs), and how to prevent such objects from striking Earth. The AIAA brought these recommendations to the House Committee on Science, Space, and Technology, leading to the United States Congressional mandate for this workshop included in the NASA 1990 Authorization Bill. The United States House of Representatives in its NASA Multiyear Authorization Act of 1990 ^[10] stated:

“The Committee believes that it is imperative that the detection rate of Earth-orbit-crossing asteroids must be increased substantially, and that the means to destroy or alter the orbits of asteroids when they threaten collision should be defined and agreed upon internationally.”

“The chances of the Earth being struck by a large asteroid are extremely small, but since the consequences of such a collision are extremely large, the Committee believes it is only prudent to assess the nature of the threat and prepare to deal with it. We have the technology to detect such asteroids and to prevent their collision with the Earth.”

“The Committee therefore directs that NASA undertake two workshop studies. The first would define a program for dramatically increasing the detection rate of Earth-orbit-crossing asteroids; this study would address the costs, schedule, technology, and equipment required for precise definition of the orbits of such bodies. The second study would define systems and technologies to alter the orbits of such asteroids or to destroy them if they should pose a danger to life on Earth. The Committee recommends international participation in these studies and suggests that they be conducted within a year of the passage of this legislation.”

This resulted in the “*Spaceguard survey*”, which led to the Spaceguard goal of detecting 90% of all the Near-Earth Objects (NEOs) larger than 1 km in 10 years.

The observation of the collision of Shoemaker-Levy 9 with Jupiter in 1994 heightened the public awareness about our vulnerabilities to NEOs^[8]. The event, observed through almost all Earth-based observatories and many orbiting and interplanetary spacecraft, including the Hubble Space Telescope (HST), Galileo, Ulysses, and Voyager 2 was the first collision of two solar system bodies ever to be observed ^[7]. The collision was far more powerful (**Fig 1.2**) than the disappearance of the dinosaurs 65 million years ago, but fortunately the Earth is smaller than Jupiter and hence does not attract objects like Jupiter does^[5].



Fig 1.2 Jupiter after Shoemaker-levy 9 collision

(Credit: Planetary Resources Inc.)

This incident and the Spaceguard survey report spread the focus internationally that the International Astronomical Union (IAU) working group on NEOs organized “*The Vulcano workshop: Beginning the Spaceguard survey*” in 1995 at Vulcano, Italy. In addition to this, the United Nations International Conference on Near-Earth Object was held at the United Nations (UN) Headquarters in New York, organized by the United Nations Office of NEOs, which sensitized member states to the potential threats due to NEOs and proposed an expansion of existing observation campaigns to detect and track NEOs ^[16].

In 2003, a NASA study indicated that with the goal of discovering 90% of asteroids 1 km and larger almost attained, and with new survey and detection available the goal should be revised. In response to this, the NASA Authorization Act of 2005 was passed by the United States Congress to provide an analysis of alternatives to discover, track, catalogue, and determine the physical characteristics of NEOs equal to or greater than 140 meters in diameter to assess the threat of such objects to Earth, and to find 90% of the NEOs within fifteen years. In 2001, The United Nations’ Committee on the Peaceful Uses of Outer Space (COPUOS) established the Action Team on Near-Earth Objects (Action Team 14) and on the recommendations^[16] of the working committee of Action Team 14, in 2013, International Asteroid Warning Network (IAWN) was established, to create an international group of organizations involved in detecting, tracking and characterizing NEOs. The IAWN is tasked with developing a strategy using well-defined communication plans and protocols to assist

Governments in the analysis of asteroid impact consequences and in the planning of mitigation responses. The combined effort of all these initiatives have given us an enormous amount of data on asteroids. While these data are being used to defend our planet, they have also shown us these asteroids have enormous amount of resources that can be harvested to replenish materials found in our planet. A bit more about asteroid mining and related topics will be covered at the end of this chapter.

1.1.2 Detection and Classification

Detection

Detecting asteroids requires surveys with telescopes^[35]. Well before the public and scientific awareness/concern on the threats posed by the NEOs, Eleanor F. Helin and Eugene M. Shoemaker initiated the Palomar Planet-Crossing Asteroid Survey (PCAS) in 1973, dedicated to the detection of Earth crossing NEOs. It detected 95 NEAs and 17 comets in addition to confirmation of previous discoveries until its discontinuation in June 1995 after 23 years of operation^[9].

Fig 1.3 shows the comparison of the number of asteroids discovered between 1950 and 2015, where the green dots represent the non-Earth-crossing asteroids, and the red dots represent the Earth-crossing asteroids.

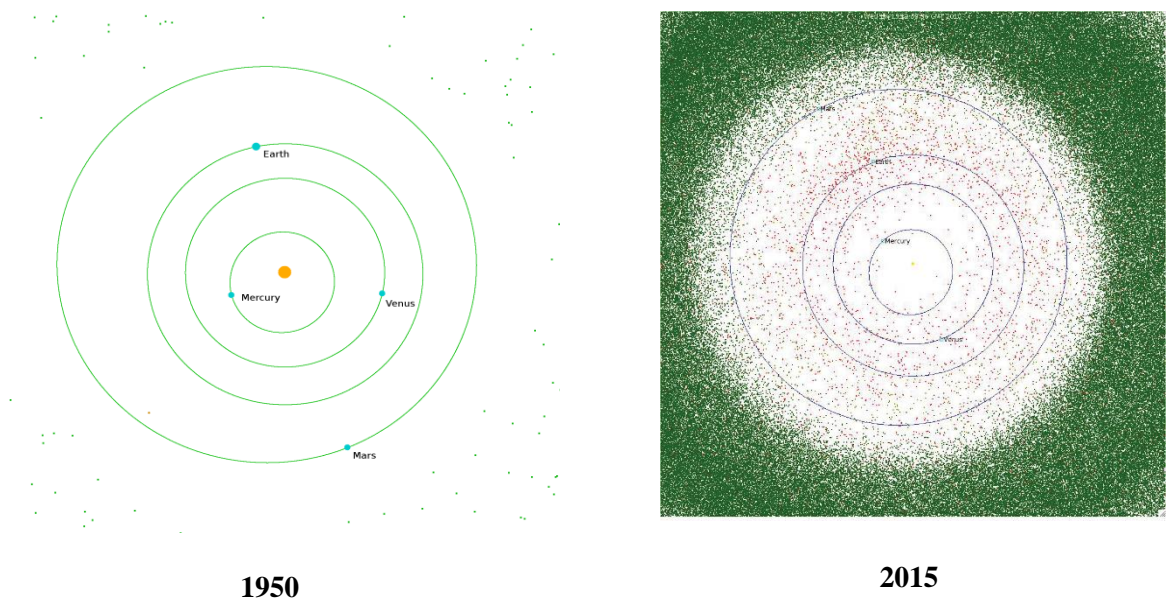


Fig 1.3 Comparison on the number of asteroids discovered between 1950 and 2015 ^[19]

[Credit: Armagh Observatory]

One of the reasons for this huge increase in the observation and discovery rate has been due to the use of Charge-Coupled-Device (CCD) based search systems^[17, 18]. It should be noted that the Minor Planet Center (MPC) is the official worldwide organization in charge of collecting observational data for minor planets (asteroids) and comets, calculating their orbits and publishing the information via the Minor Planet Circulars. Under the auspices of the IAU, it operates at the Smithsonian Astrophysical Observatory, which is part of the Centre for Astrophysics along with the Harvard College Observatory. Numerous surveys have been initiated since then and they could be classified based on the following two methods^[36]:

- 1) Ground-based surveys – They are in the optical band
- 2) Space-based surveys – They are in the thermal infrared band

Ground-Based Surveys

They are practical only in the optical band, mainly due to the affordability of very large optical detector arrays, the high atmospheric transparency and low background in the optical band. Some of the ground-based surveys are ^[17]:

- 1) Near Earth Asteroid Tracking (NEAT) program.
- 2) Catalina Sky Survey
- 3) Pan –STARRS
- 4) LINEAR
- 5) Spacewatch

Space-Based Surveys

One of the main advantages of a space-based survey is that they can be designed to work at any optimal wavelength for the task like X-ray, ultraviolet and far-infrared bands, which are absorbed by the atmosphere. There were two Hubble Space Telescope (HST) survey programs that have been used to image the illuminated portions of 10 asteroids^[36]. Some of the space-based surveys are ^[36]:

- 1) NEOWISE
- 2) Sentinel (Proposed)
- 3) NEOCam (Proposed)

Classification

Asteroids are broadly classified by two criteria:

- 1) Dynamical – based on their orbit
- 2) Spectral – based in their surface composition

Dynamical Classification

Dynamical classification is based on the orbital characteristics of the asteroids. These are sub-classified into groups and families named mostly after the discovery of the first member in that category. The term “asteroid families” is historically associated with the Japanese researcher Kiyotsugu Hirayama, who was the first to use the concept of orbital elements to identify asteroid groups characterised by similar orbits. He made the hypothesis that the near identical orbits could not be due to chance and that could be due to common origin^[17]. Groups are helpful in classifying asteroids that have broadly similar orbits, and families are used to classify asteroids that are usually fragments of past asteroid collisions. The following are broadly classified groups of asteroids:

- 1) Inner Solar system asteroids
 - a. Near-Earth Asteroids
 - i. Atiras
 - ii. Atens
 - iii. Apollos
 - iv. Amors
 - b. Near-Mars Asteroids
 - i. Hungarias
 - ii. Phocaeas
 - iii. Mars-crossers
- 2) Mid Solar system asteroids
 - a. Main Belt asteroids
 - b. Hildas
 - c. Jupiter Trojans
- 3) Outer Solar system asteroids
 - a. Centaurs
 - b. TNOs
 - c. Plutinos
 - d. Kuiper Belt
 - e. Scattered Disk

Near-Earth Asteroids

Technically, NEAs are defined as asteroids that come closer than 0.3 AU (45 million km) of Earth. New objects are brought into the swarm of NEOs by gravitational perturbations out of their orbits in the Kuiper belt and/or Oort cloud. Some objects currently classed as NEAs may in fact be devolatilized comets. Planet-crossing objects are removed from the population wither through collision with a planet or by gravitational perturbations that eject them into hyperbolic orbits. **Fig 1.4** and **Fig 1.5** show the orbit types and distribution of dynamically classified asteroids.

Atiras

These are inner Earth asteroids, meaning asteroids whose orbits are entirely contained within the orbit of the Earth, i.e. they have their aphelion less than 1 AU and perihelion of less than 0.983 AU. Asteroid 163693 Atira, discovered on the 11th of February 2003 by the LINEAR project, was the first asteroid of this class and hence the name to this group of asteroids.

Atens

These are asteroids which cross the orbit of the Earth at some point in their orbit and have an aphelion of less than 1 AU and a perihelion greater than 0.983 AU. 2062 Aten, discovered by E.F. Helin^[4] under the PCAS program on the 7th of January 1976, was the first asteroid of this class and hence the name to this group of asteroids. As of 2nd October 2014, there are 879 asteroids of this class^[22].

Apollos

These are asteroids which cross the orbit of the Earth at some point in their orbit and have an aphelion of greater than 1 AU and perihelion less than 1.017 AU. 1862 Apollo, discovered by Karl Reinmuth in 1932^[4], was the first asteroid of this group of asteroids. As of 2nd October 2014, there are 5669 asteroids of this class ^[22].

Amors

These are asteroids which never cross the orbit of the Earth and have an aphelion greater than 1 AU and perihelion greater than 1.017 AU but less than 1.3 AU. Even though 433 Eros a Mars-crossing asteroid, discovered on the 13th of August 1898 by Carl Gustav Witt, was the first discovered asteroid of this class, 1221 Amor, discovered on the 12th of March 1932 by E. Delporte^[4], was given the honour. As of 2nd October 2014, there are 4900 known asteroids of this class^[22].

Potentially Hazardous Asteroids

These are asteroids whose minimum orbit intersection distance (MOID) to Earth are less than 0.05 AU and have an absolute magnitude greater^[20] than 22.0. As of 2nd October 2014, there are 1505 potentially hazardous asteroids^[21].

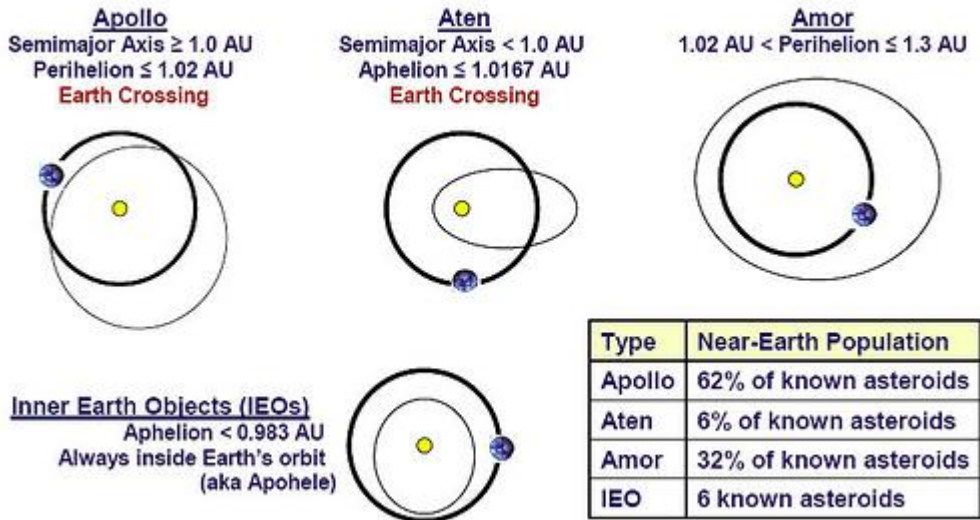


Fig 1.4 Asteroid classification based on dynamics

[Credit: NASA JPL]

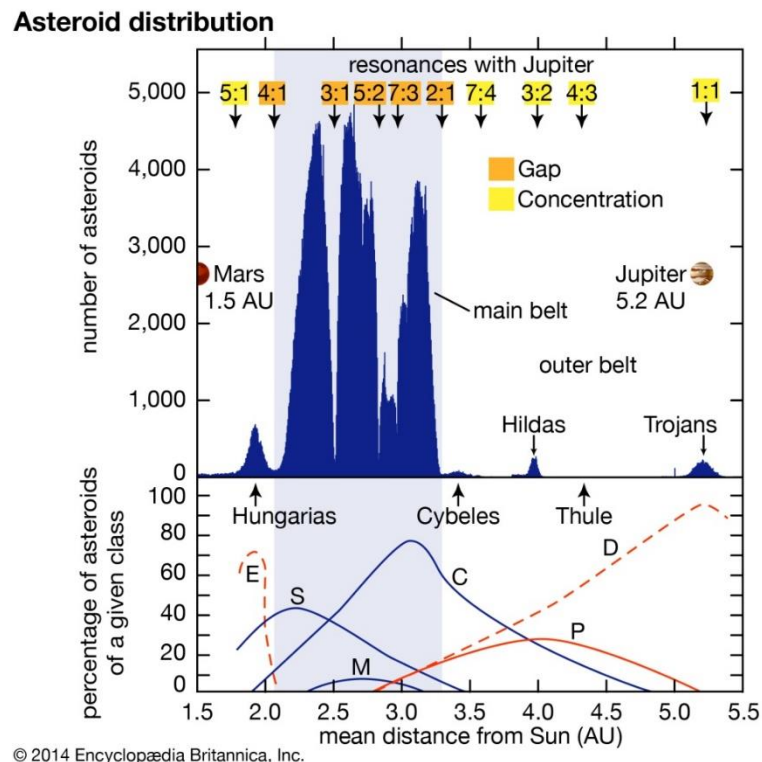


Fig 1.5 Asteroid class distribution

[Credit: Encyclopaedia Britannica, Inc.]

Asteroids that collide and disintegrate into smaller fragments make up most of these NEOs and these reach the Earth's atmosphere at the rate of 100 tons a day^[17] and the vast majority of those disintegrate upon entering the Earth's atmosphere. The Chelyabinsk asteroid was said to be 19 m^[58] in diameter and exploded 24-30 km altitude^[58] with the energy of ~30 atomic bombs equalling ½ megaton^[58] of TNT damaging windows, partly destroying buildings and injuring more than 1000 people^[17].

1.1.3 Reference Frames and Coordinate Systems

A reference frame along with a co-ordinate system and time provides a point of reference to standardise measurements in tracking an object in space. A reference frame can only be used to observe motion, but to quantify the motion and to perform algebra of vectors we need a coordinate system.

Reference Frames

A frame of reference is a structure of concepts, assumptions and values which helps in the observation of motion of a body from a point of reference. The following are some of the types of reference frames commonly used,

Inertial Reference Frame

A frame of reference fixed with respect to the fixed-stars, in which a point object subject to zero net external force moves in a straight-line with constant speed, is called as an inertial reference frame. Newton's laws of motion are valid only in an inertial reference frame. *Ref A* in **Fig 2.1** is an example of an inertial reference frame.

Non-inertial Reference Frame

A frame of reference that is rotating and/or accelerating with respect to the fixed-stars is called as a non-inertial reference frame. Newton's laws of motion are not valid in a non-inertial reference frame. *Ref B* in **Fig 2.1** is an example of a non-inertial reference frame.

Body fixed and Space-fixed Reference Frame

Body-fixed reference frames are a mostly in non-inertial state that has its origin usually fixed at the centre-point/centre of mass of a body. These can also be in a state of inertia in cases such as being fixed at the centre of mass of the Sun. It is convenient to express rotations in a coordinate system having its origin located at the centre-of-mass of the rigid body, and its

coordinate axes aligned along the principal directions for the body. This body-fixed frame then moves within a stationary space-fixed frame.

Space-fixed reference frames are fixed at a point in space with respect to the fixed-stars and is usually in an inertial state.

Coordinate Systems

A coordinate system uses coordinates to determine the position of a body in space or to describe the magnitude and direction of target velocity with respect to a specified reference frame. Coordinate systems can be grouped into orthogonal, celestial and geographic. Without going much into detail about all the different types of coordinate systems, commonly used coordinate systems that are closely related to this thesis will be discussed.

Orthogonal Coordinate System

If the vectors that define the coordinate frame are locally perpendicular in a Euclidian space, the coordinate frame is said to be orthogonal. Cartesian and Polar coordinate systems are two of the most commonly used orthogonal coordinate system.

Cartesian or rectangular Coordinate System

Cartesian coordinates use the units of linear distance along the different axes to measure the position of an object from the origin of the coordinate system.

Polar or Spherical coordinate system

Polar coordinates use the units of linear distance measured from the origin and angular distance measured from an axis to determine the position of a body in space.

Celestial or Astronomical Coordinate System

Celestial coordinates are usually spherical coordinate systems with origin placed at a celestial body or at a point in space in the celestial sphere and the defining axis placed as part of chosen plane. The linear distance is measured from the origin and the angular distance is measured from the respective plane. The Ecliptic coordinate system is one of the most commonly used celestial coordinate system

Ecliptic Coordinate System

The ecliptic coordinate system is used largely for studies involving planets and asteroids, as their motion is confined to the zodiac. The defining plane of the coordinate system is the ecliptic plane.

1.1.4 Celestial Dynamics

The dynamics of a celestial body involves translational (orbital) and rotational (spin) motions. An asteroid has six degrees of freedom ^[45] as shown in **Fig 1.6**, three degrees for translational (orbital) motion ($\Delta_x, \Delta_y, \Delta_z$) and three degrees for rotational (spin-up) motion ($\beta_x, \beta_y, \beta_z$). Spin-up dynamics is not within the scope of this research and hence we neglect the three degrees of freedom for rotational motion. While forces due to the solar radiation pressure, solar wind, Yarkovsky effect, Poynting-Robertson effect and YORP effect, contribute to the orbital motion of an asteroid, they are negligible compared to the force due to gravity and hence are not considered.

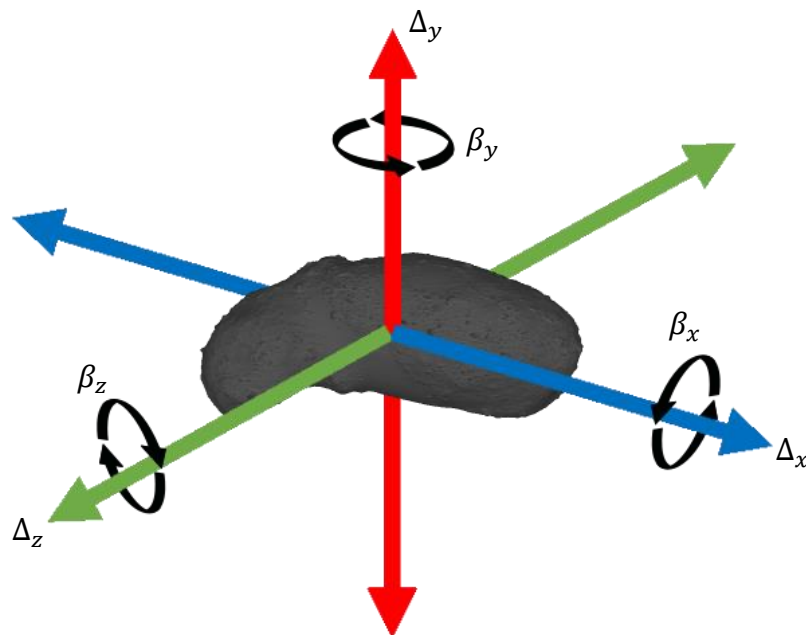


Fig 1.6 Degrees of freedom of an Asteroid

[Asteroid Credit: JAXA]

With the considerations specified before, an asteroid moves in the celestial space with the three degrees of freedom for orbital motion. The equation of motion is governed by Newton's law of motion and Newton's law of gravitation, which may also be used to define the laws observed by Kepler on the motion of planets.

$$\vec{f} = m \frac{d^2 \vec{r}}{dt^2} \quad (1)$$

$$\vec{f} = -\frac{GMm}{r^3} \vec{r} \quad (2)$$

Where:

$$G = 6.673 \times 10^{-20} \text{ km}^3 \text{ kg}^{-1} \text{ s}^{-2}$$

Equating equations (1) and (2), we get the two body equation of motion for the asteroid,

$$\frac{d^2 \vec{r}}{dt^2} = -\frac{GM}{r^3} \vec{r} \quad (3)$$

Johannes Kepler was the first astronomer to correctly describe the motion of the planets in the solar system^[48].

Kepler's Laws

The motion of the planets was found by Kepler to follow the three laws ^[25]:

1. The planetary orbits are all ellipses and the Sun lies at one of the foci of each ellipse
2. The radius vectors connecting each planet to the Sun sweeps out equal areas in equal time intervals
3. The square of the orbital periods of the planets are proportional to the cubes of their orbital major radii

$$P^2 \propto a^3 \quad (4)$$

Energy and Momentum

The transfer of orbital energy and momentum is discussed in the later chapters of this thesis, and hence it is better to look at these concepts related to the orbital motion of the asteroids or celestial bodies. An asteroid follows a heliocentric orbital motion and two of the most important quantities in the motion of a celestial body are energy and momentum. Assuming that the basic concepts of momentum and energy are well known, the fundamentals of these quantities are not discussed here. From the basic laws of physics, we know that an isolated two-body system is a conservative system, meaning both energy and momentum are conserved. Several fundamental properties of the different types of orbits are developed with the aid of the laws of conservation of momentum and energy. These properties include the period of elliptical orbits and the escape velocity associated with parabolic paths^[14].

Lagrange and Hamilton showed that the laws of motion can be replaced completely with an alternate description for the motion of dynamic systems based on energy principles^[46]. The

total orbital energy of an asteroid in a closed orbit in a central gravitational field is the sum of its potential energy per unit mass and kinetic energy per unit mass.

$$\varepsilon = \frac{v^2}{2} - \frac{\mu}{r} \quad (5)$$

Equation (5) is called as the visa viva equation. The specific orbital energies for different orbits are given in **Table 1.1**

Circular Orbit	$\varepsilon_{cir} = -\frac{\mu}{2r}$
Elliptical Orbit	$\varepsilon_{eli} = -\frac{\mu}{2a}$
Parabolic Orbit	$\varepsilon_{par} = 0$
Hyperbolic Orbit	$\varepsilon_{hyp} = \frac{\mu}{2a}$

Table 1.1 Orbital energies of different orbits

Here,

$$\mu = \mu_S = 1.32712440018 \times 10^{11} \text{ km}^3 \text{ s}^{-2}$$

The angular momentum of a body per unit mass is constant in time:

$$\vec{h} = \vec{r} \times \vec{v} \quad (6)$$

From the scalar product of the orbital angular momentum \vec{h} with the orbital radius vector \vec{r} , we obtain the equation of the plane, which passes through the origin and whose normal is parallel to \vec{h}

$$\vec{h} \cdot \vec{r} = 0 \quad (7)$$

Since \vec{h} is a constant vector, it always points in the same direction. Hence the motion of the bodies is confined to some fixed planes which pass through the origin^[49].

Orbit Equation

The orbit equation defines the path of a body around a central body in a two-body system derived by cross-multiplying equation for newton's second law with the specific angular

momentum of the orbiting body^[47]. This is the solution of the equation of motion expressed in polar coordinates (r, θ) .

$$r = \frac{h^2}{\mu} \frac{1}{1 + e \cos \theta} \quad (8)$$

Where, $\mu = \mu_S = 1.32712440018 \times 10^{11} \text{ km}^3 \text{ s}^{-2}$

The orbit equation describes conic sections, including ellipses, and hence it is a mathematical statement of Kepler's first law. The two-body problem deals with the motion of two bodies influenced solely by their mutual gravitational attraction.

A conic section is a curve formed by the intersection of a plane passing through a right circular cone. The path taken by a body in an orbit relative to another body is a conic section such as a circle, ellipse, parabola, hyperbola, and the shape of the orbit is determined by the eccentricity. As **Fig 1.7** shows, the angular orientation of the plane relative to the cone determines whether the conic section is a circle, ellipse, parabola, or hyperbola. The type of conic section is related to the eccentricity, the semimajor axis, and the specific mechanical energy. **Table 1.1** shows the relationships between energy and the type of conic section, while **Table 1.2** shows the relationship between eccentricity, semimajor axis and the type of conic section.

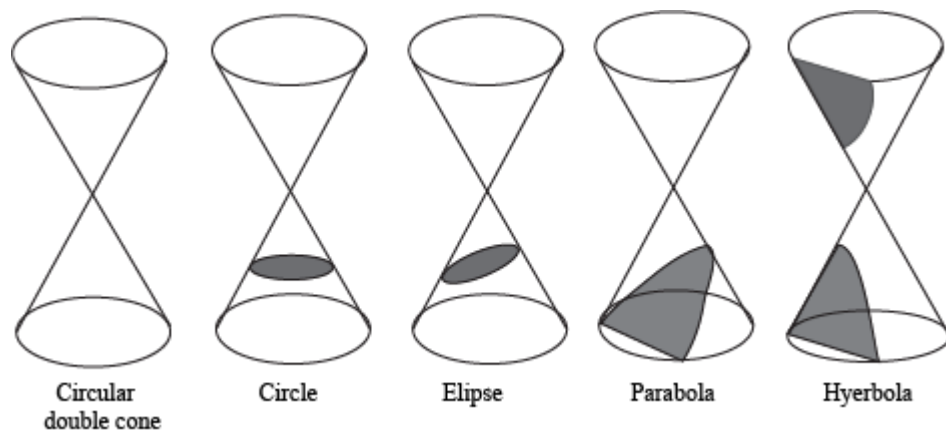


Fig 1.7 Conic sections

[credit: shmoop.com]

Keplerian Orbits

It is important to know that Keplerian motion is confined to the plane of orbit and all the celestial bodies in the solar system travel in an elliptical orbit around the Sun. In this thesis we will be dealing with circular and elliptical orbits and hence we would discuss these two

types of orbits. **Table 1.2** shows the properties of eccentricity and semimajor axis of Keplerian orbits.

Type of Keplerian Orbit	Eccentricity	Semimajor axis
Circular Orbit	$e = 0$	$a = r$
Elliptic Orbit	$0 < e < 1$	$a > 0$
Parabolic Orbit	$e = 1$	$a \approx \infty$
Hyperbolic Orbit	$e > 1$	$a < 1$

Table 1.2 Keplerian Orbits, their eccentricities and semimajor axis

Circular Orbit

As shown in **Table 1.1**, orbits with $e = 0$ are circular and the orbit equation (8) for a circular orbit results to,

$$r = \frac{h^2}{\mu} \quad (9)$$

Other parameters like velocity and period for a circular orbit are,

$$v = \sqrt{\frac{\mu}{r}} \quad (10)$$

$$P = \frac{2\pi}{\sqrt{\mu}} r^{\frac{3}{2}} \quad (11)$$

Elliptical Orbit

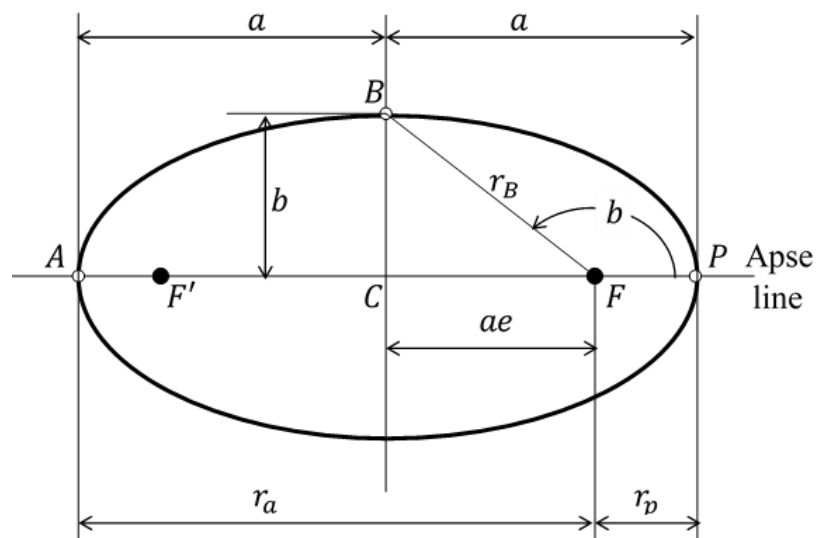


Fig 1.8 Representation of an Ellipse

[Credit: Recreated from Orbital Mechanics for Engineers, Howard Curtis]

An elliptical orbit is one in which $0 < e < 1$, the magnitude of the radius vector is the smallest at the periapsis and has the maximum value at apoapsis. Without going much into details about the derivations, the following are some of the important expressions of an elliptical orbit, represented by **Fig 1.8**

$$r_p = \frac{h^2}{\mu} \frac{1}{1 - e} \quad (12)$$

$$a = \frac{h^2}{\mu} \frac{1}{1 - e^2} \quad (13)$$

$$r_p = a(1 - e) \quad (14)$$

$$b = a\sqrt{1 - e^2} \quad (15)$$

$$P = \frac{2\pi}{\sqrt{\mu}} a^{\frac{3}{2}} \quad (16)$$

Orbital Trajectory

The first step in defining the orbital trajectory of an asteroid is the preliminary determination of the orbital state vectors. The preliminary determination is done through various methods of subsequent observations such as radar, telescope, etc. The term trajectory refers to the path of a body in space^[24] and the orbital state vectors are the Cartesian vectors of position (\vec{r}) and velocity (\vec{v}) at an epoch. Going into the different methods of preliminary determination which falls under the stream of astrometry is not within the scope of this research and hence it is assumed that an orbital state vector is already obtained. The position and velocity vectors at one point in time can be calculated from the position and velocity at any other given point in time. The next step is to determine the size, shape and orientation of the orbit and one way to achieve this is to find the classical orbital elements.

Classical Orbital Elements

The Keplerian or classical orbital elements are the six constants obtained from the integration of the solutions to the scalar, second order, nonlinear coupled, ordinary differential equations

of motions. This set of orbital elements can be divided into two groups: the dimensional elements and the orientation elements. The semimajor axis, eccentricity and the true anomaly are the dimensional elements and they specify the size and shape of the orbit and relate the position in the orbit to time. The inclination of the orbit plane, the longitude of the ascending node and the argument of periapsis are the orientation elements, also called as Euler angles and they specify the orientation of the orbit in space^[60]. **Fig 1.9** shows the representation of classical orbital elements on an inertial reference frame.

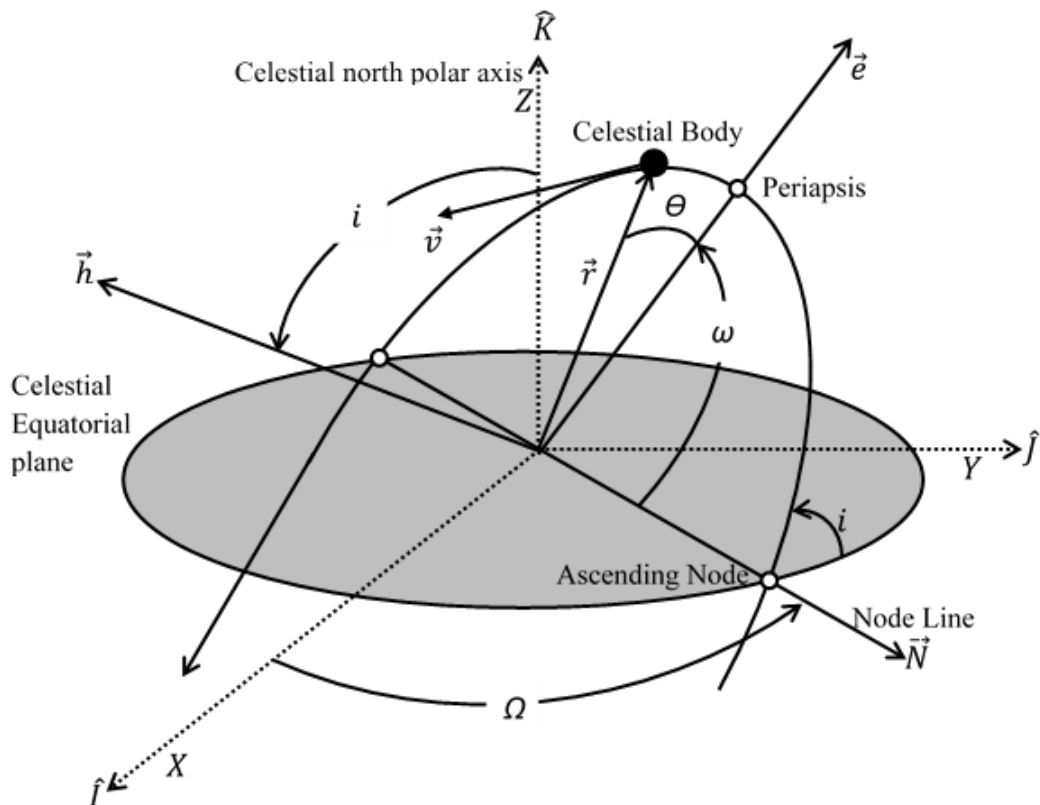


Fig 1.9 Representation of the Classical Orbital Elements

[Credit: Recreated from *Orbital Mechanics for Engineers*, Howard Curtis]

The classical orbital elements are listed and described as follows,

- 1) Semimajor axis (a) - defines the size of the orbit
- 2) Eccentricity (e) - defines the shape of the orbit
- 3) Inclination of the orbital plane (i) - defines the orientation of the orbital plane with respect to the reference plane
- 4) Longitude of the ascending node (Ω) - defines the shape of the orbit, and is the angle between the reference direction and the direction of the ascending node
- 5) Argument of periapsis (ω) - defines the position of the body in the orbit, measured from the ascending node to periapsis

- 6) True anomaly (θ) - defines the position of the body in orbit, relating position and time.

The classical orbital elements can be obtained from the orbital state vectors and the orbital state vectors can be calculated from the classical orbital elements^[14].

Orbital Elements from State vectors

The classical orbital elements could be used in defining an orbit to avoid the complications involved in keeping track of time in methods using state vectors. From **Fig 1.9** it can be noted that the inclination (i), longitude of ascending node (Ω), argument of periapsis (ω), and the true anomaly (θ) depend on, and hence be calculated from, the three fundamental vectors of the orbit \vec{h} , \vec{N} and \vec{e} . The angular momentum vector \vec{h} , is perpendicular to the plane of the orbit and we already have the expression for the angular momentum vector from (6). Hence, the next step is to find the node and eccentricity vector.

Node vector

The node vector extends from the origin of the celestial sphere through the ascending node and beyond. The vector falls on the node line, which is the line connecting the points at which the orbit of a celestial body intersects with the celestial equator. The point of intersection at which the celestial body, in its orbit, passes above the celestial equator is called the ascending node, and the point of intersection at which the celestial body, in its orbit, passes below the celestial equator is called as the descending node. It can be noted that the node vector is perpendicular to both the unit vector \hat{K} and angular momentum vector \vec{h} . By definition, that means \vec{N} is the cross product of \hat{K} and \vec{h} .

$$\vec{N} = \hat{K} \times \vec{h} \quad (17)$$

Eccentricity Vector

The eccentricity vector points from the centre of the celestial equatorial plane (focus of the orbit) to the periapsis with a magnitude equal to the eccentricity of the orbit. The expression for the eccentricity vector can be obtained by solving the trajectory equation and the general equation of a conic section, expressed in polar coordinates. Without going much into detail about the derivation, the expression can be expressed in (18).

$$\vec{e} = \frac{1}{\mu} \left[\left(v^2 - \frac{\mu}{r} \right) \vec{r} - r v_r \vec{v} \right] \quad (18)$$

The radial velocity (v_r) is the component of the body's velocity vector that points in the direction of the radius connecting the body and the focus point. It can be expressed as in equation (19)

$$v_r = (\vec{r} \cdot \vec{v}) / r \quad (19)$$

Inclination of the orbital plane.

From **Fig 1.9** it can be seen that the inclination (i) of the orbit is the dihedral angle between the orbital plane and the celestial equatorial plane, which is measured counter clockwise around the node line vector from the celestial equator to the orbit. This is also the angle between the positive z axis and the normal to the plane of the orbit or the angular momentum vector (\vec{h}). The inclination is a positive number between 0 and 180 degrees.

$$i = \cos^{-1} \left(\frac{h_z}{h} \right) \quad (20)$$

Longitude of the ascending Node

The angle between the positive side of the x axis and the node line is called as the longitude of the ascending node. It is a positive number lying between 0 and 360 degrees.

$$\Omega = \cos^{-1} \left(\frac{N_x}{N} \right) \quad (21)$$

$$\Omega = \begin{cases} \cos^{-1} \left(\frac{N_x}{N} \right) & (N_y \geq 0) \\ 360^\circ - \cos^{-1} \left(\frac{N_x}{N} \right) & (N_y < 0) \end{cases} \quad (22)$$

Argument of periapsis

It is the angle between the node line vector and the eccentricity vector measured in the plane of the orbit. It is a positive number between 0 and 360 degrees.

$$\omega = \cos^{-1} \left(\frac{\vec{N} \cdot \vec{e}}{Ne} \right) \quad (23)$$

$$\omega = \begin{cases} \cos^{-1}\left(\frac{\vec{N} \cdot \vec{e}}{Ne}\right) & (e_z \geq 0) \\ 360^\circ - \cos^{-1}\left(\frac{\vec{N} \cdot \vec{e}}{Ne}\right) & (e_z < 0) \end{cases} \quad (24)$$

True anomaly

The angle from the eccentricity vector to the position vector of the body, measured in the direction of body's motion. Alternately, we could use time since perigee passage.

$$\theta = \cos^{-1}\left(\frac{\vec{e} \cdot \vec{r}}{er}\right) \quad (25)$$

$$\theta = \begin{cases} \cos^{-1}\left(\frac{\vec{e} \cdot \vec{r}}{er}\right) & (v_r \geq 0) \\ 360^\circ - \cos^{-1}\left(\frac{\vec{e} \cdot \vec{r}}{er}\right) & (v_r < 0) \end{cases} \quad (26)$$

The angular momentum and the true anomaly are frequently replaced by the semimajor axis and the mean anomaly.

State Vectors as a Function of time

If the position and velocity of an orbiting body are known at one instance of time, then the position and velocity of the orbiting body at any other instance of time can be calculated from the known initial values. Classical formulation and universal formulation are two of the most commonly used methods to achieve this. While classical formulation uses eccentric and hyperbolic anomalies, the universal formulation uses universal anomaly to find state vectors as a function of time. Without going much into detail about the merits and demerits of both the formulations, we use the universal formulation to obtain the state vectors at time t from the initial state vectors.

The Keplerian motion of a body is confined to the plane of its orbit, hence we can assume that the initial state vectors of position and velocity and the final state vectors of position and velocity are all coplanar. According to the fundamental theorem of coplanar vectors, "If A , B & C are coplanar vectors, and A & B are not colinear, it is possible to express C as a linear combination of A and B "^[64]. Unless the motion of the body is rectilinear the state vectors are linearly independent of each other and hence they can be represented in a linear combination shown in (27) and (28).

$$\vec{r}_t = (f_{lag}\vec{r}_0) + (g_{lag}\vec{v}_0) \quad (27)$$

$$\vec{v}_t = (\dot{f}_{lag}\vec{r}_0) + (\dot{g}_{lag}\vec{v}_0) \quad (28)$$

The coefficients f_{lag} , g_{lag} , \dot{f}_{lag} , and \dot{g}_{lag} in (27) and (28) are coefficients of the linear combination mentioned earlier. The coefficients were first derived by Joseph Louis Lagrange and hence are called as the Lagrange coefficients. The Lagrange coefficients are functions of time and the initial conditions through which we can find the radius and velocity vectors of the orbiting body at a time elapsed after the initial time. It is convenient to find the expressions for the Lagrange coefficients using a perifocal frame of reference, from which the Lagrange coefficients in terms of the general frame of reference can be obtained.

Lagrange Coefficients in the Perifocal Frame of Reference

A perifocal frame is the ‘natural frame’ of orbit and is used to describe orbits in three dimensions^[65]. The frame is centred at the focus of the orbit. Here the fundamental plane is the orbital plane of the body. **Fig 1.10** shows the representation of a perifocal frame. The coordinate axes are named \bar{x} , \bar{y} and \bar{z} , where the \bar{x} axis points towards the periapsis, the \bar{y} axis is rotated 90 degrees in the direction of orbital motion and lies in the orbital plane and the \bar{z} axis is perpendicular to the plane of the orbit in the direction of the angular momentum vector \vec{h} completing a right-handed perifocal system. \hat{p} , \hat{q} and \hat{w} are the unit vectors in the direction of \bar{x} , \bar{y} and \bar{z} axis respectively. The coordinates of the perifocal frame are represented as,

$$\bar{x} = r \cos \theta \quad (29)$$

$$\bar{y} = r \sin \theta \quad (30)$$

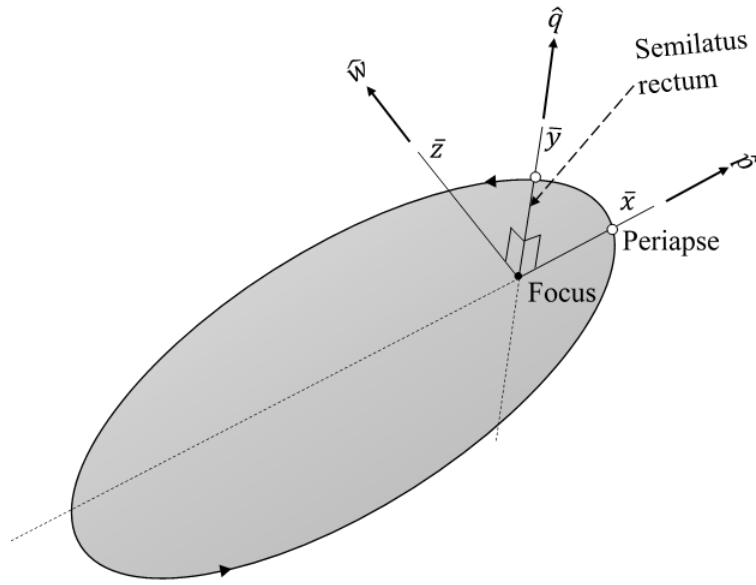


Fig 1.10 Representation of a Perifocal frame

[Credit: Recreated from *Orbital Mechanics for Engineers*, Howard Curtis]

In the perifocal frame, the position vector \vec{r} and the velocity vector \vec{v} are represented by (31) and (32) ,

$$\vec{r} = \bar{x} \hat{p} + \bar{y} \hat{q} \quad (31)$$

$$\vec{v} = \dot{\bar{x}} \hat{p} + \dot{\bar{y}} \hat{q} \quad (32)$$

Expressing (31) and (32) at time $t = 0$ we obtain the expression,

$$\vec{r}_0 = \bar{x}_0 \hat{p} + \bar{y}_0 \hat{q} \quad (33)$$

$$\vec{v}_0 = \dot{\bar{x}}_0 \hat{p} + \dot{\bar{y}}_0 \hat{q} \quad (34)$$

Without going much into the details of derivation, we obtain the values of the Lagrange coefficients in the perifocal reference from by solving (27), (28), (33) and (34) as done by bate et al^[64],

$$f_{lag} = \frac{\bar{x} \dot{\bar{y}}_0 - \bar{y} \dot{\bar{x}}_0}{h} \quad (35)$$

$$g_{lag} = \frac{-\bar{x} \bar{y}_0 + \bar{x} \bar{y}_0}{h} \quad (36)$$

And the derivative of the equation (35) and (36) gives,

$$\dot{f}_{lag} = \frac{\dot{\bar{x}} \bar{y}_0 + \bar{y} \dot{\bar{x}}_0}{h} \quad (37)$$

$$\dot{g}_{lag} = \frac{-\dot{\bar{x}} \bar{y}_0 + \bar{y} \dot{\bar{x}}_0}{h} \quad (38)$$

The expression for the Lagrange coefficients obtained in (35), (36), (37) and (38) are in the perifocal frame of reference. To obtain their expressions in terms of the general frame of reference, we relate the perifocal coordinates to the general coordinates.

Universal Anomaly

To relate the perifocal coordinates to the general coordinates, the angular momentum and energy are related to the geometrical parameters p and a respectively. Here p is compared to h by equating the trajectory equation and general equation of a conic section in polar coordinates, the derivation of both are beyond the scope of this thesis. From (5) and Table 1.1, we obtain the relationship between energy and a in (40),

$$h = r^2 \dot{\theta} = \sqrt{\mu p} \quad (39)$$

$$\varepsilon = \frac{1}{2} v^2 - \frac{\mu}{r} = \frac{-\mu}{2a} \quad (40)$$

Resolving v into its radial component, \dot{r} , and its transverse component, $r\dot{\theta}$, the energy equation (40) can be written as,

$$\frac{1}{2} \dot{r}^2 + \frac{1}{2} (r\dot{\theta})^2 - \frac{\mu}{r} = \frac{-\mu}{2a} \quad (41)$$

Solving for \dot{r}^2 and setting $(r\dot{\theta})^2 = \frac{\mu p}{r^2}$, we get

$$\dot{r}^2 = \frac{-\mu p}{r^2} + \frac{2\mu}{r} - \frac{\mu}{a} \quad (42)$$

Since the solution is not obvious we introduce an independent variable, X defined as

$$\dot{X} = \frac{\sqrt{\mu}}{r} \quad (43)$$

This independent variable X , is the universal anomaly. Solving (42) and (43) by dividing we can find the expression of r and t in terms of X .

$$r = a \left(1 + e \sin \frac{X + c_0}{\sqrt{a}} \right) \quad (44)$$

$$\sqrt{\mu} t = aX - ae\sqrt{a} \left(\cos \frac{X + c_0}{\sqrt{a}} - \cos \frac{X + c_0}{\sqrt{a}} \right) \quad (45)$$

Here c_0 is a constant of integration. Solving (44) and (45) introducing two more variables (46) and (47), while assuming $X = 0$ and $t = 0$, we obtain the expression for r and t omitting the constant of integration c_0 ,

$$z = \gamma X^2 \quad (46)$$

$$\gamma = \frac{1}{a} \quad (47)$$

$$\sqrt{\mu} t = \left[\frac{\sqrt{z} - \sin \sqrt{z}}{\sqrt{z}^3} \right] X^3 + \frac{r_0 v_{r,0}}{\sqrt{\mu}} X^2 \left[\frac{1 - \cos \sqrt{z}}{z} \right] + \frac{r_0 X \sin z}{\sqrt{z}} \quad (48)$$

$$r = \frac{X^2}{2} + \frac{r_0 v_{r,0}}{\sqrt{\mu}} \frac{X}{\sqrt{z}} \sin \sqrt{z} \quad (49)$$

Stumpff Functions

(48) and (49) are indeterminate for $z = 0$, so we introduce two functions, substituting $\left[\frac{1-\cos\sqrt{z}}{z}\right]$ and $\left[\frac{\sqrt{z}-\sin\sqrt{z}}{\sqrt{z}^3}\right]$ in (48), called as the Stumpff functions (50) and (51) to remedy this.

$$C(z) = \begin{cases} \frac{(1 - \cos \sqrt{z})}{z} & (z > 0) \\ \frac{(\cosh \sqrt{-z} - 1)}{-z} & (z < 0) \\ \frac{1}{2} & (z = 0) \end{cases} \quad (50)$$

$$S(z) = \begin{cases} \frac{(\sqrt{z} - \sin \sqrt{z})}{\sqrt{z}^3} & (z > 0) \\ \frac{(\sinh \sqrt{-z} - \sqrt{-z})}{\sqrt{-z}^3} & (z < 0) \\ \frac{1}{6} & (z = 0) \end{cases} \quad (51)$$

Using (50) and (51), with (48) and (49) we get,

$$\sqrt{\mu} t = X^3 S(z) + \frac{r_0 v_{r,0}}{\sqrt{\mu}} X^2 C(z) + r_0 X (1 - z S(z)) \quad (52)$$

$$r = \sqrt{\mu} \frac{dt}{dx} = X^2 C(z) + \frac{r_0 v_{r,0}}{\sqrt{\mu}} X (1 - z S(z)) + r_0 (1 - z C(z)) \quad (53)$$

We solved for X when time $t = 0$, now we need to solve for X when time is known, in order to find the radius and velocity vectors at a later time. From r_0 , v_0 and the energy equation (40), you can obtain the semi-major axis, a (as part of the expression for z in (52)). But we cannot get X from itself in (52), since (52) is transcendental for X , so an iterative trial and error solution is used to obtain the value of X by using an initial value of X denoted as X_0 . Without going much into the details of obtaining the initial value of X , we can use initial value of X as suggest by V. A. Chobotov^[67],

$$X_0 = \sqrt{\mu} |\gamma| t \quad (54)$$

We can use the Newton Raphson method (55) for the iteration.

$$X_{n+1} = X_n - \frac{F(X)}{F'(X)} \quad (55)$$

If we let $t = 0$ and choose a trial value for X , then rewriting (52) we get,

$$F(X) = \frac{r_0 v_{r,0}}{\sqrt{\mu}} X^2 C(z) + (1 - \gamma r_0) X^3 S(z) + r_0 X - \sqrt{\mu} t \quad (56)$$

And the derivation of (56) yields,

$$F'(X) = \frac{r_0 v_{r,0}}{\sqrt{\mu}} X (1 - \gamma X^2 S(z)) + (1 - \gamma r_0) X^2 C(z) + r_0 \quad (57)$$

Now using (56) and (57) in (55) we get,

$$X_{n+1} = X_n - \frac{\frac{r_0 v_{r,0}}{\sqrt{\mu}} X_n^2 C(z_n) + (1 - \gamma r_0) X_n^3 S(z_n) + r_0 X_n - \sqrt{\mu} t}{\frac{r_{COM,0} v_{r,0}}{\sqrt{\mu}} X_n (1 - \gamma X_n^2 S(z_n)) + (1 - \gamma r_{COM,0}) X_n^2 C(z_n) + r_{COM,0}} \quad (58)$$

Where t is the time corresponding to the given r_0 , v_0 , a and X_0 , while $z_n = \alpha X_n^2$

Now with the value of X obtained, we can get the expression for the coordinates of the perifocal frame in terms of X . To do this, we use an expression (59) obtained from the standard conic equation,

$$r e \cos \theta = a(1 - e^2) - r \quad (59)$$

Combining equation (59) and (44) in (29), we get the expression for the coordinates of the perifocal frame in terms of X .

$$\bar{x} = r \cos \theta = -a \left(e + \sin \frac{X + c_0}{\sqrt{a}} \right) \quad (60)$$

Since $\bar{y}^2 = r^2 - \bar{x}^2$ and solving it with (60), we get,

$$\bar{y} = a\sqrt{1-e^2} \cos \frac{X+c_0}{\sqrt{a}} \quad (61)$$

Differentiating equations (60) and (61), and using the definition for the universal variable X , we get the coordinate $\dot{\bar{x}}$ and $\dot{\bar{y}}$,

$$\dot{\bar{x}} = -\frac{\sqrt{\mu a}}{r} \cos \frac{X+c_0}{\sqrt{a}} \quad (62)$$

$$\dot{\bar{y}} = -\frac{h}{r} \sin \frac{X+c_0}{\sqrt{a}} \quad (63)$$

Lagrange Coefficients Related to the General Frame of Reference

Solving by substituting the values of (60), (61), (62) and (63) in (35), (36), (37) and (38) and using the values for X , and through the expressions for z , $C(z)$ and $S(z)$ we get the expressions for the Lagrange coefficients in terms of the general frame of reference. The Lagrange coefficients are not independent and knowing any three of the coefficients, the fourth coefficient can be found [63].

$$f_{lag} = 1 - \frac{X^2}{r_0} C(z) \quad (64)$$

$$g_{lag} = t - \frac{1}{\sqrt{\mu}} X^3 S(z) \quad (65)$$

$$\dot{f}_{lag} = \frac{\sqrt{\mu}}{r r_0} (z S(z) - 1) X \quad (66)$$

$$\dot{g}_{lag} = 1 - \frac{X^2}{r} C(z) \quad (67)$$

Using (64),(65),(66) and (67) in (27) and (28), along with values of the initial state vectors $[\vec{r}_0$ and $\vec{v}_0]$, the value of state vectors at a later time $[\vec{r}$ and $\vec{v}]$ can be obtained.

1.2 Asteroid Orbit Manipulation

The physics of manipulating the orbital trajectory of an asteroid involves the application of force either perpendicular to, or along (speeding up or slowing down the orbital velocity of

the asteroid relative to the sun) the direction of motion of the asteroid^[38]. Different methods of asteroid deflection have been proposed over the years, but they can be broadly classified into “impulsive” and “continuous (slow push or pull)” deflection. The impulsive method involves imparting an instantaneous amount of force to change the velocity vector of the asteroid. Slow push or pull method involves exerting a small but steady amount of force continuously to the object for a time interval causing small changes to the trajectory of the body relative to its nominal orbit^[42].

The trajectory manipulation of an asteroid could be carried out for various reasons, but two of the most prominent ones are to deflect them from impacting with earth and to shepherd them to a desirable orbit for accessing them.

There are several means of inducing perturbations in the orbit of an asteroid, discussing all of them would be an enormous task and not in the scope of this thesis, and hence only a few methods would be discussed here.

1.2.1 Nuclear Detonation

This is one of the earliest and also one of the most well-known methods, and a nuclear device can be detonated in three ways to achieve a deflection:

1. A nuclear standoff method where a nuclear explosive is detonated on flyby near the surface of an asteroid via proximity fuse
2. A nuclear explosive is detonated on the surface of an asteroid via contact fuse
3. A nuclear explosive is detonated beneath the surface of an asteroid by driving the explosive device into the asteroid

A nuclear standoff detonation would cause a deflection through the influence of radiation, while a detonation on the surface or beneath the surface would have an additional cause deflection by the impulse imparted by ejecta from the explosion^[38]. According to NASA analysts, nuclear explosions are assessed to be 10-100 times more effective than non-nuclear alternatives, but it should be noted that because of restrictions found in *Article IV* of the “*Treaty on Principles Governing the Activities of States in the Exploration and Use of Outer Space, including the Moon and Other Celestial Bodies*”, use of a nuclear device would require prior international consideration^[27].

1.2.2 Kinetic Impactor

A kinetic impactor is where a massive object, whether it is an asteroid, a rocket, a spacecraft, is made to impact the object to change its course. NASA calls this approach a most mature approach^[27]. The European Space Agency's AIDA and Don Quixote are two of the kinetic impactors designed for test around 2020. One of the major problems with this is fragmentation and hence increasing the threat if the fragments impact the Earth. This is where the composition of the asteroids comes into play, a dense metallic asteroid would not fragment easily but a less dense asteroid would^[38].

1.2.3 Gravity Tractor

A gravity tractor moves the asteroid by pulling it using gravitational force slowly over time, this could result in sufficient deflection depending on the scenario. A spacecraft with an ion thruster is one of the possibilities. Small but constant thrust would get the asteroid to move slightly which would result in a considerable distance over time. The spacecraft hovers near the asteroid with thrusters angled outward so the exhaust does not impinge on the surface. This deflection method is insensitive to the structure, surface properties and rotation state of the asteroid ^[39].

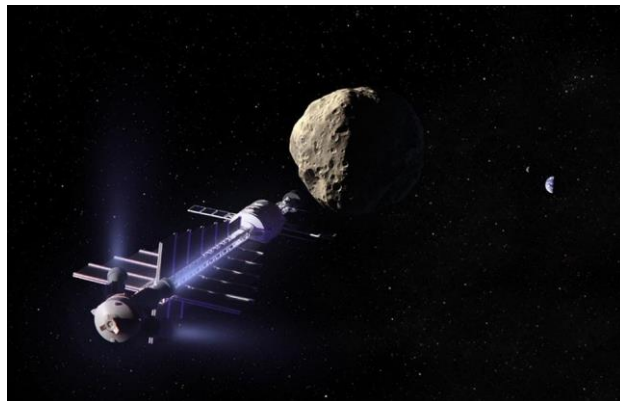


Fig 1.11 Artist's depiction of a gravity tractor in action
[Credit Dan Durda (FIAAA, B612 Foundation)]

1.2.4 Focused Solar Energy

Solar energy can be used for manipulating the orbit of an asteroid, by deploying a large, thin-film mirror surface to collect sunlight and focusing that on to the surface of the asteroid, a small thrust can be created from the vaporization of the material over the surface of the object. This method requires a long-term planning, and development. This method can also be tried by using solar sails, as solar sails suffer from very low thrust (roughly $10^{-5} Nm^{-2}$

of collector surface at 1 AU) and the mechanical difficulty of tethering the sail to a rotating asteroid, they could be used to focus sunlight onto the surface of the asteroid to generate thrust as the asteroid's surface sublimates^[41].

1.2.5 Mass Driver

This method was originally developed in support of space settlement projects in the mid-1970s. A mass driver, as the name suggests ejects the mass^[37] on the surface of the asteroid into space in the right direction to apply a consistent acceleration along the asteroid's orbital path.

1.2.6 Tether Assisted Deflection

The use of tethers to deflect an asteroid is not new in concept, multiple methods of tether assisted deflection have been proposed over the years. This thesis proposes a different method of tether assisted deflection, making use of asteroid-to-asteroid close encounters, connecting two closely passing asteroids with a tether.

Space Tethers

Space tethers are long cables that connect two bodies whether be it satellites or celestial bodies where the length of the space tethers exceed the size of the connected bodies. Space tethers are usually made up of thin strands of high strength conducting wires or fibres, the desired tether material properties depend upon the intended application. Some desirable properties for a tether include high tensile strength and low density. A protective coating may be necessary to avoid being affected by exposure to ultraviolet radiation. Some of the common materials used for building space tethers include Kevlar, ultra-high molecular weight polyethylene, carbon nanotubes, M5 fibre and diamond^[50]. The idea of using space tethers was first proposed for the creation of artificial gravity from the centrifugal force of inertia, proposed by Tsiolkovsky^[50].

Types of Space Tethers

Depending on the features, objective, etc. space tethers can be grouped into different types. Some of them are ^[50]:

- 1) Static tethers – In which the quantity and lengths of tethers, the quantity and weights of objects, and their relative position and orientation remain constant during activity
- 2) Dynamic tethers – Which can significantly change configurations and structures

- 3) Electrodynamic tethers – They include conductive materials which actively interact with Earth’s magnetic field and ionosphere, no matter whether the tether is static or dynamic
- 4) Momentum exchange tethers – These can be either static or dynamic that capture an arriving body and then releases it at a later time into a different velocity. Momentum exchange tethers can be used for orbital manoeuvring, by transferring momentum or energy between connected bodies

Momentum Exchange Tethers

Momentum exchange tethers are highly suitable for applications involving orbital trajectory manipulation such as deflection. Inter-orbital manoeuvres can be carried out by the continuous action of a constraint force upon a system’s elements, and at the expense of constraint provided by a tether [51].

Two bodies are coupled in such a way that there is momentum or energy transfer between them. This is achieved by taking advantage of the gravity gradient force that exists due to the differential gravitational force between the two ends of the tether. This force helps in keeping a high tether tension, by pulling the ends apart in opposite direction. Releasing one end of the tether will transfer momentum from one body to another. The body that is closer to the central body will experience more gravitational force and less centrifugal force while the body that is farther from the central body will experience more centrifugal force and less gravitational force comparatively. To simplify, this model could be considered, to be in a dumbbell configuration [50].

The gravitational and centrifugal forces are equal and balanced only at the dumbbell system’s centre of mass. Equating the gravitational and centrifugal force at the centre of mass:

$$\frac{GM_{Sun}M_D}{r_D^2} = M_D r_D \omega_D^2 \quad (68)$$

Since,

$$\omega_D = \frac{v_D}{r_D} \quad (69)$$

$$\omega_D = \frac{2\pi}{P_D} \quad (70)$$

Substituting (69) in (68) and (70) in (68) we get (71) and (72) respectively,

$$v_D^2 = \frac{GM_{Sun}}{r_D} \quad (71)$$

$$P_D^2 = \frac{4\pi^2 r_D^3}{GM_{Sun}} \quad (72)$$

Where,

$$G = 6.673 \times 10^{-20} \text{ km}^3 \text{ kg}^{-1} \text{ s}^{-2}$$

From the above equations it can be noted that the orbital velocity, orbital period and angular velocity depend on the orbital radius and are independent of the system mass.

Equations of motion

In order to understand the dynamics of momentum exchange tethers, we derive the equation of motion for a system using momentum exchange tethers in two different operational contexts. The most common and widely studied system is the dumbbell system. So, let us base both the operational contexts on the dumbbell system.

For simplification we can assume the tether to be massless and inelastic, the end masses as point masses and gravitational force of the central body as the only force acting on the system.

Context 1

In this context we use a dumbbell satellite system in an elliptical earth orbit, with only in-plane motion for the attitude dynamics.

The dumbbell satellite system is modelled with two reference frames, an inertial geocentric reference frame X, Y, Z fixed to the centre of the earth E and a non-inertial local reference frame x, y, z fixed to the centre of mass of the dumbbell system O with a generalised coordinate ϕ , which is the angle between the tether and the z axis. \vec{R} is the radius vector of the centre of mass of the dumbbell satellite system, θ is the true anomaly of the centre of mass, m_1 and m_2 are the masses of the satellites, M_E the mass of the earth and L as the length of the tether, which is the distance between m_1 and m_2 .

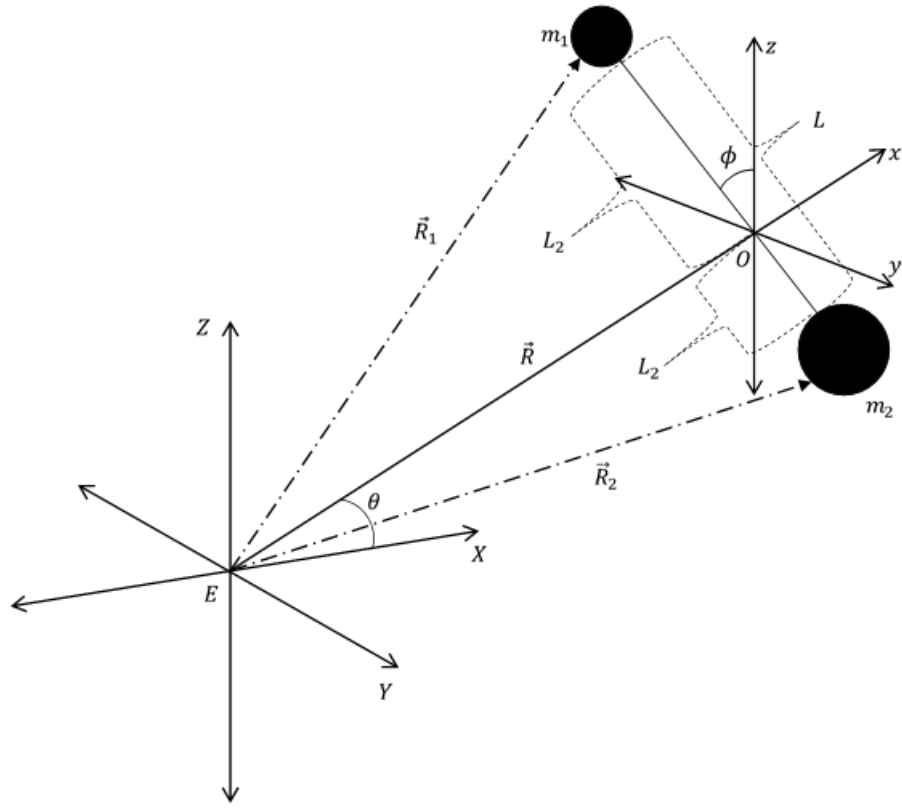


Fig 1.12 Dumbbell Satellite System with an in-plane motion

From (3), the two body second order differential equation of relative motion between two bodies can be written as (73) for the centre of mass of the dumbbell system.

$$\frac{d^2 \vec{R}}{dt^2} = - \frac{\mu_E \vec{R}}{R^3} \quad (73)$$

In this context let us derive the equation of motion in relation to the rate of change of the true anomaly of the orbital motion. To obtain the expression for the orbital motion of the centre of mass of the dumbbell system in terms of the rate of change of true anomaly, we first relate the rate of change of the true anomaly, the radius of the centre of mass and the angular momentum. From the expression for the specific angular momentum (74), we obtain the relation.

$$\vec{h} = \vec{R} \frac{d\vec{R}}{dt} \quad (74)$$

$$\frac{d\vec{R}}{dt} = R \frac{d\theta}{dt} \hat{\theta} + \frac{dR}{dt} \hat{R} \quad (75)$$

$$\vec{h} = \vec{R} \left(R \frac{d\theta}{dt} \hat{\theta} + \frac{dR}{dt} \hat{R} \right) = R^2 \frac{d\theta}{dt} \hat{h} \quad (76)$$

$$h = R^2 \frac{d\theta}{dt} \quad (77)$$

$$\frac{d\theta}{dt} = \frac{h}{R^2} \quad (78)$$

Considering the dumbbell satellites to travel in an elliptical orbit, we obtain the expression for an elliptical orbit, and so, from **(8)** the orbit formula for the conic section can be expressed for the dumbbell system as,

$$R = \frac{h^2}{\mu_E} \frac{1}{1 + e \cos \theta} \quad (79)$$

Without going much into the details of derivation, we obtain the following relation from the geometry of the ellipse,

$$R = \frac{a(1 - e^2)}{1 + e \cos \theta} \quad (80)$$

$$h^2 = \mu_E a(1 - e^2) \quad (81)$$

$$v_r = \frac{\mu_E}{h} e \sin \theta \quad (82)$$

$$v_{\perp} = \frac{\mu_E}{h} (1 + e \cos \theta) \quad (83)$$

Substituting **(80)** and **(81)** in **(78)**, we get

$$\frac{d\theta}{dt} = \frac{\sqrt{\mu_E} (a(1-e^2))^{\frac{1}{2}}}{(a(1-e^2))^2} (1+e \cos \theta)^2 \quad (84)$$

$$\frac{d\theta}{dt} = \frac{\sqrt{\mu_E}}{(a(1-e^2))^{\frac{3}{2}}} (1+e \cos \theta)^2 \quad (85)$$

Equation **(85)** is the Keplerian motion of the centre of mass of the dumbbell system for an elliptical orbit in terms of the rate of change of true anomaly. Similarly, substituting **(81)** into the expression for the radial **(82)** and tangential **(83)** velocity components of the orbital velocity and solving, we find the expression for the orbital velocity **(86)** of the centre of mass of the dumbbell satellite system in the elliptical orbit.

$$\left(\frac{dR}{dt}\right)^2 = \frac{\mu_E}{a(1-e^2)} (1+e^2+2e \cos \theta) \quad (86)$$

From the position vectors R_1 and R_2 of the satellites in the dumbbell system in the local reference frame and using the generalised coordinate ϕ , we can obtain the coordinates of the satellites,

$$x_1 = (1-\delta)L \sin \phi \quad (87)$$

$$z_1 = (1-\delta)L \cos \phi \quad (88)$$

$$x_2 = -\delta L \sin \phi \quad (89)$$

$$z_2 = -\delta L \cos \phi \quad (90)$$

$$\delta = \frac{m_1}{m_1 + m_2} \quad (91)$$

The equation of motion can be obtained with the use of the Lagrange equation using ϕ as a generalised coordinate, where K represents the kinetic energy and U represents the potential energy of the dumbbell satellite system.

$$\frac{d}{dt} \frac{\partial K}{\partial \dot{\phi}} - \frac{\partial K}{\partial \phi} + \frac{\partial U}{\partial \phi} = 0 \quad (92)$$

First, we find the kinetic energy of the dumbbell system from the kinetic energy of the center of mass of the dumbbell system added with the kinetic energy of each satellites,

$$K = \frac{1}{2} m \left(\frac{dR}{dt} \right)^2 + \frac{1}{2} \left(m_1 \frac{dL_1^2}{dt} + m_2 \frac{dL_2^2}{dt} \right) \quad (93)$$

Substituting (86) in (93),

$$K = \frac{1}{2} m \left(\frac{\mu_E}{a(1-e^2)} (1 + e^2 + 2e \cos \theta) - (\delta^2 - \delta) L^2 \left(\frac{d\theta}{dt} - \frac{d\phi}{dt} \right)^2 \right) \quad (94)$$

And differentiating,

$$\frac{d}{dt} \frac{\partial K}{\partial \dot{\phi}} - \frac{\partial K}{\partial \phi} = -(\delta^2 - \delta) L^2 \left(\frac{d^2 \phi}{dt^2} + 2e \frac{\mu_E}{a^3(1-e^2)^3} (1 + e \cos \theta)^3 \sin \theta \right) \quad (95)$$

The potential energy of the dumbbell satellite system can be expressed as,

$$U = -\mu_E \left(\frac{m_1}{|R + L_1|} + \frac{m_2}{|R + L_2|} \right) \quad (96)$$

$$R + L_1 = \left((1 - \delta)^2 L^2 + \frac{a^2(1 - e^2)^2}{(1 + e \cos \theta)^2} - 2(1 - \delta)L \cos \phi \frac{a(1 - e^2)}{1 + e \cos \theta} \right)^{\frac{1}{2}} \quad (97)$$

$$R + L_2 = \left((-\delta)^2 L^2 + \frac{a^2(1-e^2)^2}{(1+e\cos\theta)^2} - 2(-\delta)L\cos\phi \frac{a(1-e^2)}{1+e\cos\theta} \right)^{\frac{1}{2}} \quad (98)$$

Substituting (97) and (98) in (96) and differentiating w.r.t ϕ ,

$$\begin{aligned} \frac{\partial U}{\partial \phi} = \mu_E m_1 (\delta^2 & \\ & - \delta)L \sin \phi \frac{a(1-e^2)}{1+e\cos\theta} \left(\left((-\delta)^2 L^2 \right. \right. \\ & + \frac{a^2(1-e^2)^2}{(1+e\cos\theta)^2} \\ & \left. \left. - 2(-\delta)L\cos\phi \frac{a(1-e^2)}{1+e\cos\theta} \right)^{-\frac{3}{2}} \right. \\ & - \left((1-\delta)^2 L^2 + \frac{a^2(1-e^2)^2}{(1+e\cos\theta)^2} \right. \\ & \left. \left. - 2(1-\delta)L\cos\phi \frac{a(1-e^2)}{1+e\cos\theta} \right)^{-\frac{3}{2}} \right) \end{aligned} \quad (99)$$

Substituting (95) and (99) in (92),

$$\begin{aligned} \frac{d}{dt} \frac{\partial K}{\partial \dot{\phi}} - \frac{\partial K}{\partial \phi} + \frac{\partial U}{\partial \phi} & \\ = -(1-\delta)(-\delta)l^2 \left(\frac{d^2\phi}{dt^2} \right. & \\ + 2e \frac{\mu_E}{a^3(1-e^2)^3} (1+e\cos\theta)^3 \sin\theta & \\ + \mu_E m_1 (1 & \\ - \delta)(-\delta)L \sin \phi \frac{a(1-e^2)}{1+e\cos\theta} \left(\left((-\delta)^2 L^2 \right. \right. & \\ + \frac{a^2(1-e^2)^2}{(1+e\cos\theta)^2} & \\ - 2(-\delta)L\cos\phi \frac{a(1-e^2)}{1+e\cos\theta} & \\ \left. \left. - \left((1-\delta)^2 L^2 + \frac{a^2(1-e^2)^2}{(1+e\cos\theta)^2} \right. \right. & \\ \left. \left. - 2(1-\delta)L\cos\phi \frac{a(1-e^2)}{1+e\cos\theta} \right)^{-\frac{3}{2}} \right) & \end{aligned} \quad (100)$$

Equation (85) and (100) are the in-plane equations of motion of the dumbbell satellite system as a functions of time, where (85) defines the orbital motion of the centre of mass of the dumbbell satellite system and (100) defines the in-plane attitude motion of the dumbbell satellite system.

Context 2

In this context we use a dumbbell satellite system in an earth orbit with out-of-plane motion for attitude dynamics.

The dumbbell satellite system is modelled with an inertial reference frame X, Y, Z fixed to the centre of the earth E and a non-inertial local reference frame x, y, z fixed to the centre of mass of the dumbbell system O . \vec{R} is the radius vector of the centre of mass of the dumbbell satellite system, θ is the true anomaly of the centre of mass, m_1 and m_2 are the masses of the satellites, M_E the mass of the earth, L_1 and L_2 is the distance between the centre of mass of the dumbbell system and the satellites, ϕ is the angle the tether makes with the x axis of the dumbbell satellite system, while rotating about the y axis and α is the angle between the tether and the y axis while rotating about the x axis.

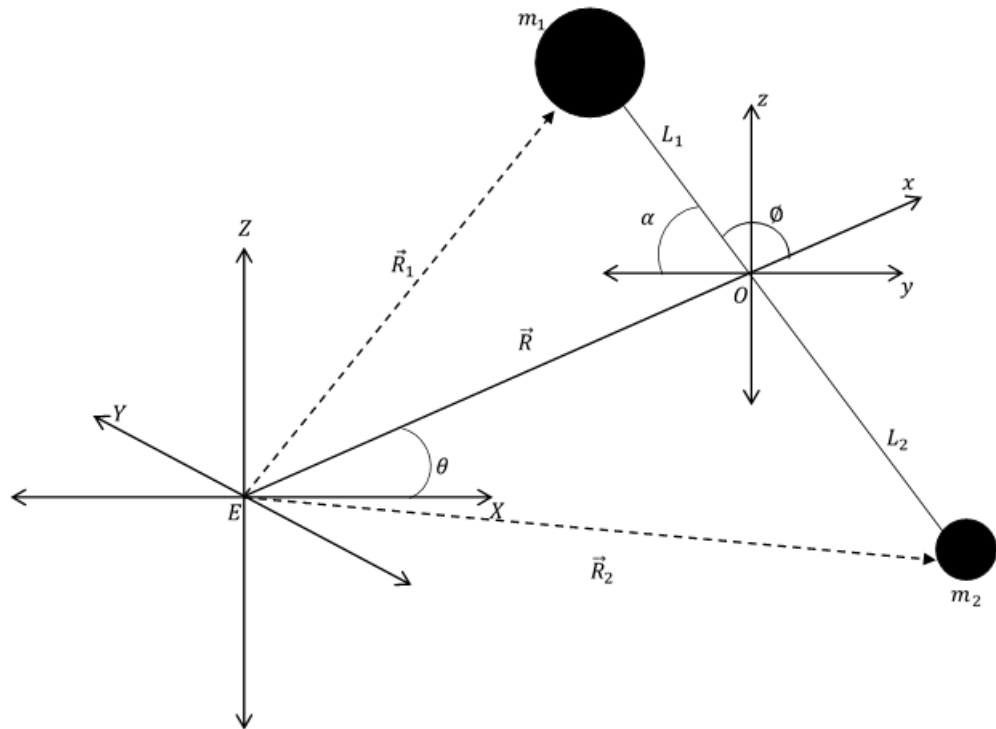


Fig 1.13 Dumbbell Satellite System with an out-of-plane motion

Here R, θ, α, ϕ are the generalised coordinates and are functions of time. The cartesian coordinates of the satellites in the dumbbell system about the centre of the earth E are,

$$x_1 = R \cos \theta + L_1 \cos \alpha \cos(\phi + \theta) \quad (101)$$

$$y_1 = R \sin \theta + L_1 \cos \alpha \sin(\phi + \theta) \quad (102)$$

$$z_1 = L_1 \sin \alpha \quad (103)$$

$$x_2 = R \cos \theta - L_2 \cos \alpha \cos(\phi + \theta) \quad (104)$$

$$y_2 = R \sin \theta - L_2 \cos \alpha \sin(\phi + \theta) \quad (105)$$

$$z_2 = -L_2 \sin \alpha \quad (106)$$

The general expression for finding the length of a vector **(107)** can be used to find the distance between the centre of the earth and the satellites **(108)** and **(109)**,

$$r = \sqrt{x^2 + y^2 + z^2} \quad (107)$$

$$R_1 = \sqrt{L_1^2 + R^2 + 2L_1R \cos \alpha \cos \phi} \quad (108)$$

$$R_2 = \sqrt{L_2^2 + R^2 - 2L_2R \cos \alpha \cos \phi} \quad (109)$$

The equations of motion of the dumbbell system as a function of time can be obtained through the Lagrange Equation **(110)**.

$$\frac{d}{dt} \left[\frac{\partial K}{\partial \dot{q}_i} \right] - \frac{\partial K}{\partial q_i} + \frac{\partial U}{\partial q_i} = Q_i \quad i = 1, 2, \dots, n \quad (110)$$

Where K and U are the kinetic and potential energy of the dumbbell satellite system respectively. In this operational context, the Kinetic Energy of the dumbbell satellite system comprises only the translation of the end bodies and hence from the general expression for the kinetic energy of a system **(111)**, we get the expression for the kinetic energy of the dumbbell satellite system,

$$K = \frac{1}{2} m \left(\frac{dr}{dt} \right)^2 \quad (111)$$

$$K = \frac{1}{2} M_1 \left(\left(\frac{dx_1}{dt} \right)^2 + \left(\frac{dy_1}{dt} \right)^2 + \left(\frac{dz_1}{dt} \right)^2 \right) + \frac{1}{2} M_2 \left(\left(\frac{dx_2}{dt} \right)^2 + \left(\frac{dy_2}{dt} \right)^2 + \left(\frac{dz_2}{dt} \right)^2 \right) \quad (112)$$

Differentiating **(101)**, **(102)**, **(103)**, **(104)**, **(105)** and **(106)** with respect to time and substituting the results in **(112)** we get,

$$K = \frac{1}{2} (M_1 + M_2) \left(\left(\frac{dR}{dt} \right)^2 + R^2 \left(\frac{d\theta}{dt} \right)^2 \right) + \frac{1}{2} (M_1 L_1^2 + M_2 L_2^2) \left[\left(\frac{d\alpha}{dt} \right)^2 + \left(\frac{d\phi}{dt} + \frac{d\theta}{dt} \right)^2 \cos^2 \alpha \right] \quad (113)$$

From the general expression for potential energy **(114)** of a system, the Potential Energy of the dumbbell satellite system can be expressed,

$$U = -\frac{\mu}{r} m \quad (114)$$

$$U = -\frac{\mu_E M_1}{R_1} - \frac{\mu_E M_2}{R_2} \quad (115)$$

$$U = -\frac{\mu_E M_1}{\sqrt{L_1^2 + R^2 + 2L_1 R \cos \alpha \cos \phi}} - \frac{\mu M_2}{\sqrt{L_2^2 + R^2 - 2L_2 R \cos \alpha \cos \phi}} \quad (116)$$

Differentiating (113) and (115) for ϕ, α, θ, R with respect to time, we get the following four equations of motion of the dumbbell system,

$$\begin{aligned} \frac{d^2 \phi}{dt^2} + \frac{d^2 \theta}{dt^2} - 2 \tan \alpha \frac{d\alpha}{dt} \left(\frac{d\phi}{dt} + \frac{d\theta}{dt} \right) \\ + \frac{\mu R \sin \phi \sec \alpha}{L_1 + L_2} \left[(L_2^2 + R^2 - 2L_2 R \cos \alpha \cos \phi)^{-\frac{3}{2}} \right. \\ \left. - (L_1^2 + R^2 + 2L_1 R \cos \alpha \cos \phi)^{-\frac{3}{2}} \right] = 0 \end{aligned} \quad (117)$$

$$\begin{aligned} \frac{d^2 \alpha}{dt^2} + \frac{1}{2} \sin 2\alpha \left(\frac{d\phi}{dt} + \frac{d\theta}{dt} \right) \\ + \frac{\mu R \cos \phi \sin \alpha}{L_1 + L_2} \left[(L_2^2 + R^2 - 2L_2 R \cos \alpha \cos \phi)^{-\frac{3}{2}} \right. \\ \left. - (L_1^2 + R^2 + 2L_1 R \cos \alpha \cos \phi)^{-\frac{3}{2}} \right] = 0 \end{aligned} \quad (118)$$

$$\begin{aligned} (M_1 + M_2) \left(R^2 \frac{d^2 \theta}{dt^2} + 2R \frac{dR}{dt} \frac{d\theta}{dt} \right) \\ + (M_1 L_1^2 + M_2 L_2^2) \left[\cos^2 \alpha \left(\frac{d^2 \phi}{dt^2} + \frac{d^2 \theta}{dt^2} \right) \right. \\ \left. - \frac{d\alpha}{dt} \sin 2\alpha \left(\frac{d\phi}{dt} + \frac{d\theta}{dt} \right) \right] = 0 \end{aligned} \quad (119)$$

$$\begin{aligned} \frac{d^2 R}{dt^2} - \left(\frac{d\theta}{dt} \right)^2 R \\ + \frac{\mu_E}{M_1 + M_2} \left[M_1 (R + L_1 \cos \alpha \cos \phi) (L_1^2 + R^2 + 2L_1 R \cos \alpha \cos \phi)^{-\frac{3}{2}} \right. \\ + M_2 (R - L_2 \cos \alpha \cos \phi) (L_2^2 + R^2 - 2L_2 R \cos \alpha \cos \phi)^{-\frac{3}{2}} \left. \right] = 0 \end{aligned} \quad (120)$$

(117), (118), (119), (120) are the equations of motion of the dumbbell satellite system as a function of time.

Effects of Potential Well Barriers

A gravitational potential well is the region of local minimum of the gravitational potential energy of a spherical body surrounded by the local maximum of the gravitational potential energy of the same spherical body. A smaller body captured in the gravitational potential well of a massive body cannot escape the well without external energy added to the system.

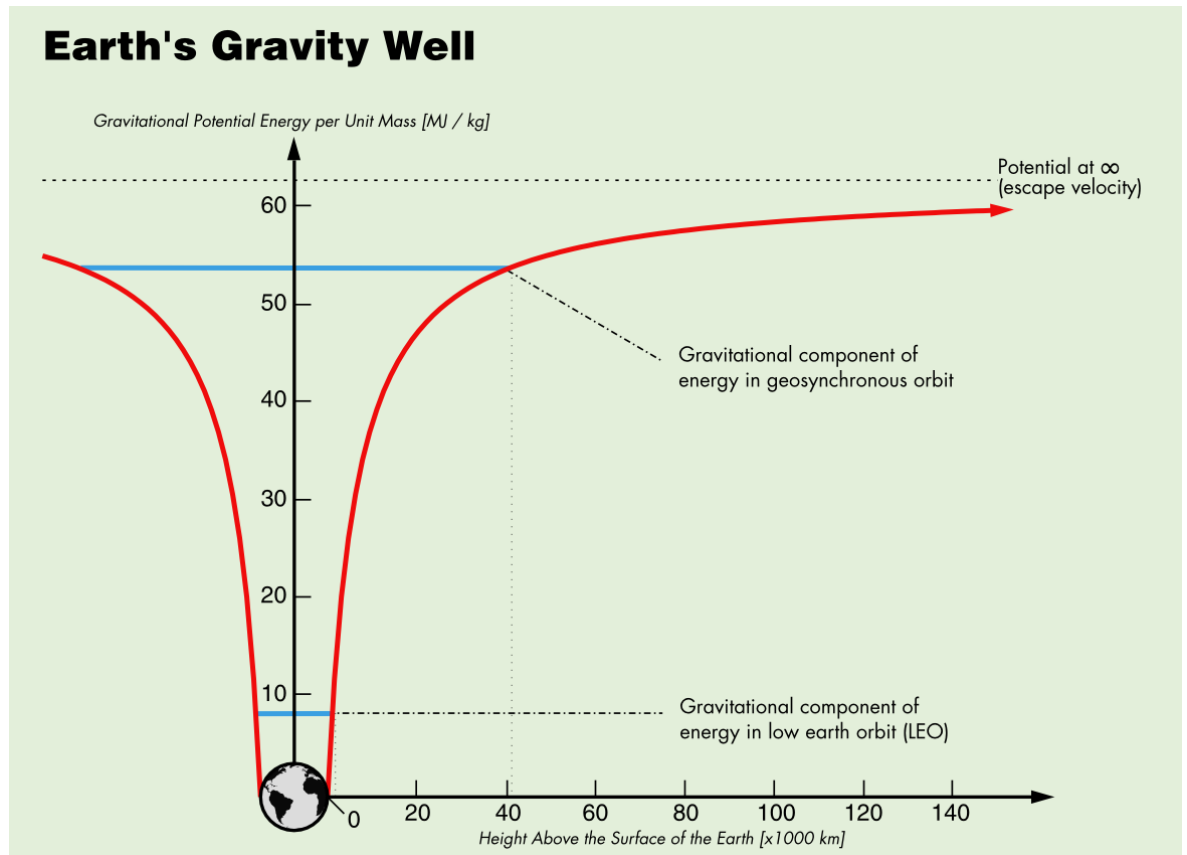


Fig 1.14 Earth's Gravity well

Credit: Nathan Bergey [PSU]

The gravitational potential energy of two masses, m_1 and m_2 , separated by a distance r is,

$$U = -G \frac{m_1 m_2}{r} \tag{121}$$

In the operational contexts discussed earlier, the potential energy and the kinetic energy of the system are,

$$U = -\frac{\mu_E m_{db}}{R} \quad (122)$$

$$K = \frac{1}{2} m_{db} \left(\frac{dR}{dt} \right)^2 \quad (123)$$

The total energy of the system can be expressed as,

$$E = K + U \quad (124)$$

Substituting (122) and (123) in (124), we get (125) and rearranging the equation, we get (126), which is also the expression for the escape velocity.

$$E = \frac{1}{2} m_{db} \left(\frac{dR}{dt} \right)^2 - \frac{\mu_E m_{db}}{R} \quad (125)$$

$$\frac{dR}{dt} = \sqrt{\frac{2\mu_E}{R}} \quad (126)$$

Both the operational contexts of the dumbbell satellite system discussed earlier, are inside the gravitational potential well of the earth, hence it orbits around the earth, and for it to leave the orbit of the earth it should leave the gravitational potential well of the earth. To achieve this, the dumbbell satellite system should have enough energy to surmount the maximum of the well to break free of the barrier, and this can be in the form of kinetic energy.

This energy can be in the form of the kinetic energy and to increase the kinetic energy, the orbital velocity of the body should be increased. But the energy and momentum in a closed system is conserved and hence its energy cannot be increased internally.

If using an external propulsion like motorised tether, which has a motor to spin the system faster, this would impart angular velocity, which would increase the dumbbell system's existing angular velocity about its centre of mass, this in turn would increase the rotational velocities of the end satellites in the system, which would add to the orbital velocity of the centre of mass.

The increase in the orbital velocity of the centre of mass would increase the kinetic energy of the system, and with enough kinetic energy to surmount the maximum of the earth's gravitational well, the dumbbell system would be able to escape the gravitational potential barrier of the earth.

Modelling the system energies

The system energies were modelled based on the approach taken in this thesis, the details of which will be discussed in the following chapters of this thesis. The overall energy of the system, which can be considered as the orbital energy of the dumbbell system can be expressed in (124).

Substituting (94) and (96) in (124) we get the total energy of the system,

$$\begin{aligned}
 E = \frac{1}{2}m \left(\frac{\mu_E}{a(1-e^2)} (1 + e^2 + 2e \cos \theta) \right. \\
 \left. - (\delta^2 - \delta)L^2 \left(\frac{d\theta}{dt} - \frac{d\phi}{dt} \right)^2 \right) \\
 - \mu_E \left(\frac{m_1}{|R + L_1|} + \frac{m_2}{|R + L_2|} \right)
 \end{aligned} \tag{127}$$

$$\text{Where, } \mu_E = 3.986004418 \times 10^5 \text{ km}^3 \text{ s}^{-2}$$

Keeping the length of the tether and the radius of the centre of mass from the centre of the earth constant, the energy of the dumbbell satellite system can be obtained for each value of true anomaly and the angular displacements of both the in-plane and out-of-plane orientation. For simplification, only the orbital energies the satellites in context with in-plane attitude motion is discussed.

The simulation was carried out for one full rotation of the dumbbell satellite system around its centre of mass and the satellites were assumed to be in a closely circular geostationary orbit around the earth and the values considered are as follows.

The radius vector of Satellite1, $R_1 = 36000$ km,

The radius vector of Satellite2, $R_1 = 35800$ km,

The mass of Satellite1, $m_1 = 3500$ kg,

The mass of Satellite2, $m_1 = 3500$ kg,

- Energy of Satellite
- Max Orbital Energy of the Orbit
- Min Orbital Energy of the Orbit
- True Anomaly = 0
- True Anomaly = 180

Fig 1.15 Legend for Fig 1.16 and Fig 1.17

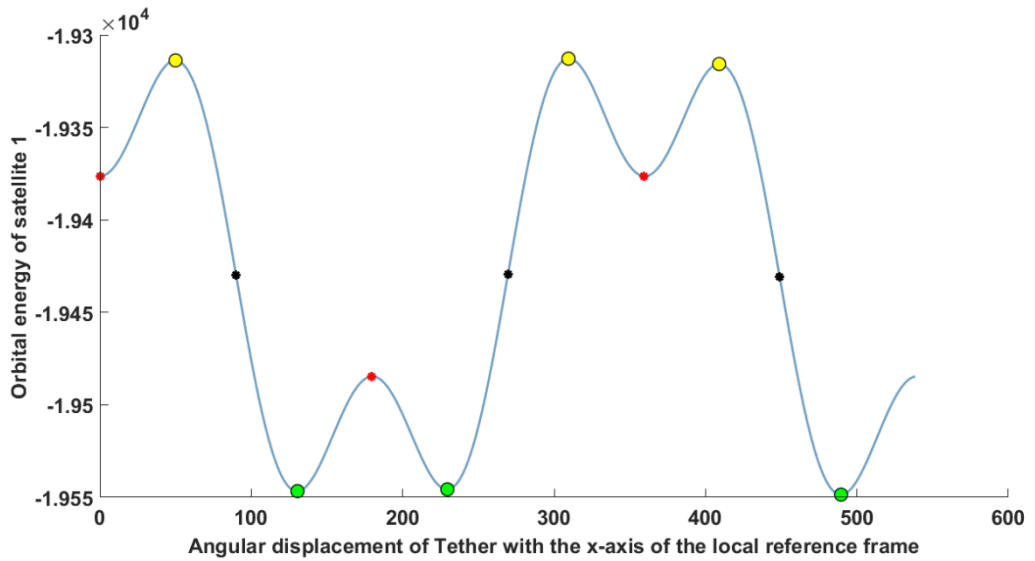


Fig 1.16 Angular displacement Vs Orbital energy of Satellite1

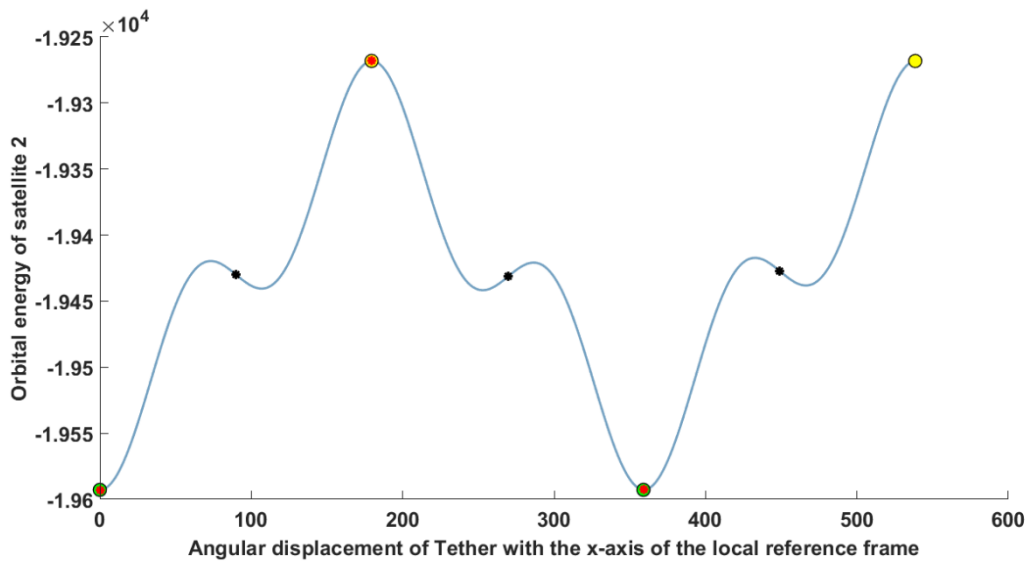


Fig 1.17 Angular displacement Vs Orbital energy of Satellite2

From the obtained plots, it can be observed that the centre of mass of the dumbbell satellite system completed almost three orbits around the earth for one full rotation of the satellites, in the dumbbell system, about the centre of mass.

The maximum and the minimum energy for Satellite1 occurs close to the perigee point than the apogee point for every orbit, and the occurrence of minimum and maximum energies can be observed to occur alternatively for each orbit. It also indicates that the value of the orbital energy at the perigee point is either of two constant values that occurs alternatively, while the orbital energy value at apogee is constant at every orbit. This indicates that the Satellite1 returns to the initial orientation every time it reaches the apogee point, and it reaches the initial orientation at every alternative perigee point. This could be due to the change in the angular velocity of the dumbbell system as it approaches the perigee and apogee points.

The maximum and the minimum energy for Satellite2 occurs at the point of perigee at every orbit, and like Satellite1, the value of for the orbital energies of Satellite2 at perigee is either of two constant values for every alternate orbit. The value of the orbital energy of the Satellite2 at the apogee point remains constant for every orbit.

This similarity in the behaviour of both the satellites for every orbit could be because of the mass ratio, as both the asteroids weigh the same and the length of the tether is very small compared to the distance between the centre of mass and the earth.

Methods of Tether Assisted Deflection

Numerous proposals on tether assisted deflection of an asteroid have been put forward over the years. Not going much into the chronology of the events, it would be helpful to discuss one of these methods to understand the dynamics of such a proposal.

Long Tether and a Ballast Mass

French and Mazzoleni^[52] proposed a method in which a long massless inelastic tether and ballast mass is attached to the asteroid to change its trajectory. This method would affect the trajectory of the asteroid in two ways. First, the connection of a tether and ballast mass would instantaneously change the centre of mass of the system and therefore the orbit. Second, the tether tension would add a perturbing force that would also change the NEO's trajectory.

A study undertaken to run the numerical simulation comparatively with the equation of motion derived through Cowell's and Encke's method proved the latter method convergences to the solution more rapidly. It was concluded with the following points:

- 1) The length of the tether and the mass ratio between the ballast and the asteroid both directly affect the location of the centre of mass after the tether and ballast mass connection
- 2) It further concluded that the effect of orbit size and shape (semimajor axis and eccentricity) can be summarized as follows: smaller more elliptical orbits are more responsive to tether-ballast mitigation than larger, more circular orbits and for orbit size (specifically semimajor axis), this generalisation is limited
- 3) The best point in the orbit at which the tether should be connected to the asteroid is periapsis. This results in a maximum deviation for a given asteroid-tether-ballast configuration

In a follow-up paper^[53], French and Mazzoleni discussed the effect on the predicted motion caused by adding mass and tether flexibility to the tether-ballast model. Here, it was concluded that the most critical metric, the diversion distance resulting from the tether and ballast mass, remained qualitatively consistent with the results found using the massless, inelastic model. Other metrics such as the tether tension however were affected greatly, especially the addition of tether elasticity, and accounting for the case of a slack tether. It was found that the slack tether phenomenon could be mitigated by slightly varying the system initial conditions or design parameters.

If a tether and ballast system were to be used for asteroid mitigation, a two-step procedure could be used to understand and develop a system. First, results obtained using a massless, inelastic simulation model could be used to determine an approximate configuration for the tether and ballast, as it was shown that the introduction of tether mass and elasticity into the modelling process does not greatly affect the diversion performance. Second, the tools presented in this study could then be used to determine an appropriate tether mass and initial condition. Mashayekhi and Misra^[54] proposed an optimization for the above method to increase the diversion achieved by cutting the tether at an appropriate point in the orbit. In a follow-up paper^[55] Mashayekhi and Misra propose a numerical optimisation scheme to determine the best point of tether severance.

Application of Space Tethers

Some of the applications of space tethers are as below:

- 1) Orbit manipulation and manoeuvring

- 2) De-orbiting a satellite at the end of its use life
- 3) Orbit stabilization
- 4) Electrodynamic tethers could be used to generate considerable amount of power, by converting orbital energy into electric power
- 5) Transfer of payloads
- 6) Formation flying

Missions using Space Tethers

The first experiment in using space tethers were conducted in the mid-1960s, there have been numerous experiments since then. Some of the missions using space tethers are^[50]:

- 1) Tethered Satellite System (TSS) is a collaborative programme by NASA and Italian Space Agency (ASI) with the objective of reusable multi-disciplinary facility to conduct space experiments in Earth orbit with a 20-km long electrically conductive tether. The first TSS mission, called TSS-1 was conducted from 31st July to 8th August 1992. Another TSS mission named TSS-1R was deployed on the 22nd of February 1996
- 2) Small Expendable Deployer System (SEDS) was developed by NASA's Marshall Space Flight Center (MSFC), which was primarily responsible for the development of transportation and propulsion technologies. Two SEDS mission named SEDS-1 and SEDS-2 were carried out in 1993 and 1994 respectively
- 3) Tether Physics and Survivability (TiPS) experimental payload was deployed on 20th June 1996. This was a free flying satellite comprising two end bodies separated by a 4.0 km long non-conducting tether. The primary objective was to study the long-term dynamics and survivability of tether systems in space

1.3 Motivation

The current interest and enthusiasm in accessing NEAs either for research or for exploiting the resource has enormous potential for the future human space exploration and settlement, which is a dream, for at least a majority of engineers of the space industry. Though not everyone agrees to the possibility of this becoming a reality, it would be proper to bring to notice that a few decades ago people believed that reaching the moon was impossible. Every

scientific discovery or invention is a matter of time and that era of space transportation is not too far away. In fact, the current trends could be considered as the start of the space age.

The rate of detection of NEAs has increased as shown in **Fig 1.18** due to the advancement in the methods and technology being used to discover them, with this emerges a crowded picture of our solar system, which though raising concerns at times, when viewed optimistically could be considered as a treasure trove for the needs of the ever hungry human expansion. Whether to deflect a hazardous asteroid from earth impact or to exploit the resources in them accessing these celestial bodies is a question to which there has been a lot of contributions.

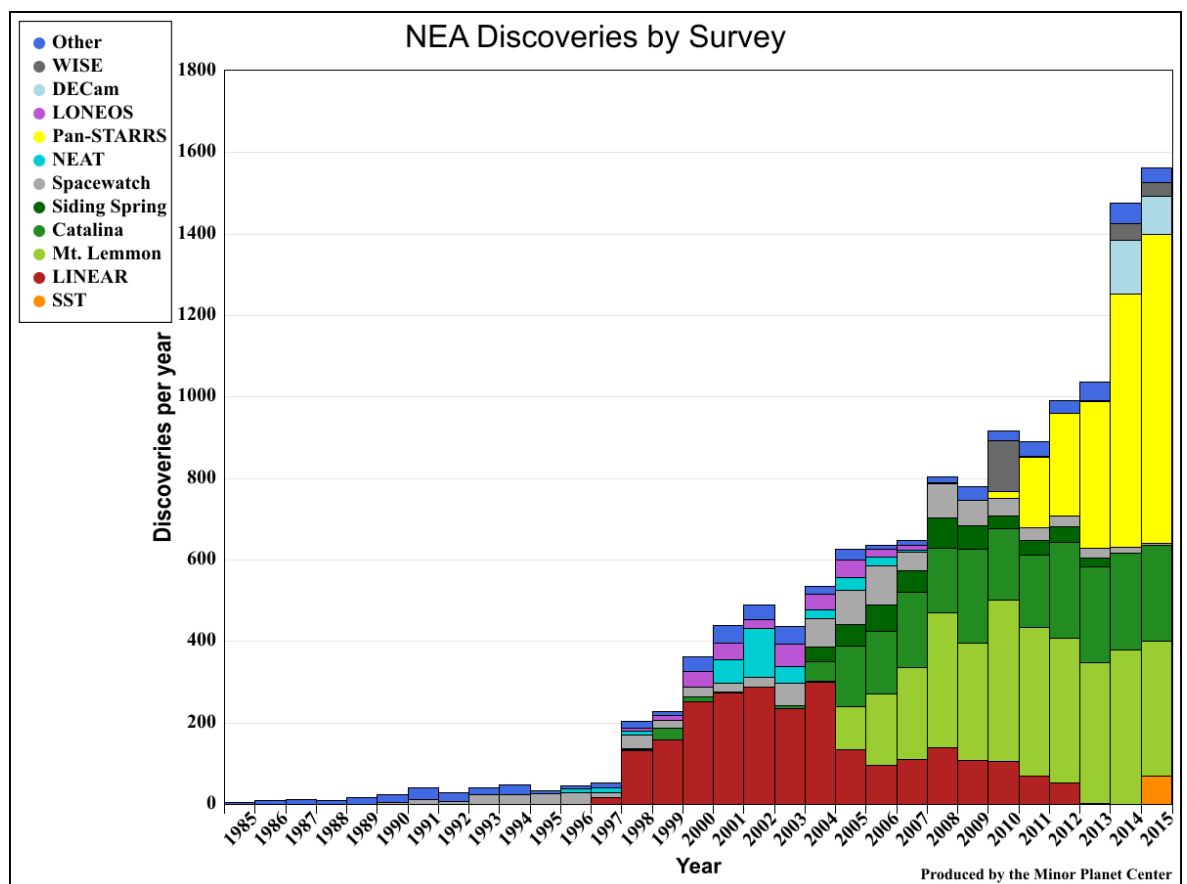


Fig 1.18 NEA Discoveries by Survey (Credit: MPC)

A number of missions being attempted to access these celestial bodies, and a lot of old and new methods have been proposed keeping in mind one important rule, efficiency. The ability to reach regions far away from the vicinity of Earth within a short time and to carry out complicated tasks utilising less resources is a key objective being tried for, and many of the technological advancements in the space industry are in this regard.

Reaching an asteroid is just the initial step, getting resources and transporting them to earth is another. Taking into account the time and efficiency as determining factors, achieving these objectives entirely through the reliance of conventional methods such as chemical propulsion, nuclear propulsion and solar propulsions is not an ideal solution. While these conventional methods could be used to reach an asteroid, using the existing orbital energy of a system to bring the asteroids closer to Earth for capture and exploitation should be given enough consideration.

Considering that at any point in time two asteroids should pass close enough to be connected to each other, the energy from one asteroid could be transferred to the other asteroid, to manipulate and change the trajectory to a desirable one. One of the most practical way of connecting the asteroids is through a tether, which led to the motivation of using tether as a tool in this research. The following sections discuss some of the interesting topics related to the motivation of this thesis.

1.3.1 Asteroid Mining

While Near-Earth-Asteroids could be a threat to the existence of life in the planet, they are also said to contain a variety of resources that can be tapped with proper planning and approach. In fact, a British Broadcasting Corporation (BBC) news article said that platinum, the hypo-allergenic metal, will run out in 20 years if demand continues to increase^[28]. The case is similar with rare Earth metals such as Indium and Dysprosium, and these materials would run out sometime in the near future, as the demand grows, especially to satisfy the needs of the electronics and the Medical industry. And when they do run out, not all of these metals can be artificially replenished, though recycling would help a little, the only permanent way is to prospect them elsewhere. Approximately 95% of the rare Earth materials mined are from China and the entire amount of platinum mined for global consumption comes from four mines and out of this, three are located in the continent of Africa^[29]. The only other possible region that could be thought for replenishment of these precious minerals is out there in the vast spaces of the universe, the asteroids; especially in some NEAs to be specific. In fact, all the amount of these materials currently being mined from the Earth's crust is said to have been brought through the constant bombardment by meteorites after the crust cooled^[30]. In fact, the idea to exploit asteroids is older than the space program, when Konstantin Tsiolkovsky included in "The Exploration of Cosmic Space by Means of Reaction Motors", published in 1903, the "exploration of asteroids" as one of his fourteen points for the conquest of space^[31]. But only recently has this been seen as a commercially and technologically feasible plan. The Apollo program returned 382 kg

of Moon rocks in six missions and with the current technological advancement in space exploration and transportation more could be achieved. To test the validity of this assertion, NASA sponsored the “Asteroid Return Mission Feasibility Study” in 2010 to investigate the feasibility of identifying, robotically capturing and returning to the International Space Station (ISS), an entire small Near-Earth Asteroid (NEA), approximately 2m diameter with a mass of order 10,000kg by 2025 and later the “Asteroid Retrieval Feasibility Study”, otherwise known as the KISS (Keck Institute of Space Studies) report, which eventually settled on the idea that a 7m diameter asteroid with a mass of order 500,000 kg could be put into a high lunar orbit by the year 2025^[32].

1.3.2 In-Situ Resource Utilization

One of the major factors that could contribute to human space expansion would be to find, process and utilize the necessary resource in space. Apart from rare minerals, some of the asteroids, especially Trojans of Jupiter have extractable amounts of water in the form of Ice. Water is an important resource in the quest for space exploration. Before the entry of SpaceX into the launch market, it costed approximately \$10,000 to put a pound of payload into Earth orbit and this cost increased with orbits further in space from Earth^[33, 34, 59]. With the advancement in 3-D printing and moulding, finding resources in space could prove to be a great factor in reducing the cost of access to space, as well as building a new economy in space. Water as a resource in space can be used for:

- 1) Consumption
- 2) Radiation Shielding
- 3) Fuel

Materials for everything from shielding, solar power, storage, oxygen for breathing and propellant, etc. are found in space. It is just a matter of finding, extracting, processing and using these resources.

1.3.3 Scientific Missions

In recent years, a lot of private industries have shown interest in space exploration in general and some in particular on asteroid mining. While companies like Space X, Orbital Sciences Corporation, Blue Origin, and Virgin Galactic are bringing down the cost of accessing space, there are companies such as Planetary Resources, Inc. and Deep Space Industries that are investing in accessing space beyond the immediate vicinity. With powerful and wealthy investors backing these companies, the idea to access the minerals beyond Earth has got a

new life, moving from fiction and theory towards the path to making this a reality. The whole idea started as a way in taking steps to ensure the continuance of life on Earth, leading to a huge amount of data, on collaboration with institutions and organisations from around the world. This huge wealth of data has contributed to some innovative ideas in accessing the resources from space, especially that of Near-Earth Asteroids, which could possibly lead to the next stage in the expansion of human race into colonies in space.

There have been lots of missions to study asteroids through flybys en route to other destinations, like Galileo's flyby of 951 Gaspra in 1991 and 243 Ida in 1993 en route to Jupiter. In 2000, the spacecraft NEAR Shoemaker successfully orbited the S-Type asteroid 433 Eros and impacted in 2001 and continued to operate until a month. This was followed by missions such as the Japanese Aerospace Exploration Agency (JAXA)'s Hayabusa, NASA's Dawn. Currently missions such as the Hayabusa 2 orbiter along with multiple versions of landers are en route to asteroid 162173 1999 JU₃. These missions prove the technological capability of accessing celestial bodies far away from Earth. Private companies such as Planetary Resources, Inc. are building their own prospecting satellites/space telescopes for launch in the near future.

1.3.4 Economics

Considering the fact that the concept of mining an asteroid is an ambitious and risky initiative, the economics of the whole endeavour is very important. Right from the cost of prospecting, through launching, mining, processing and transporting the obtained riches, economics plays an important part. In the years since the entry of SpaceX and other players, the cost of launching a pound of payload has come down from \$10,000 to less than \$2500 per pound^[59], especially for a launch of communication satellites to the Geostationary Orbit (GTO) with the introduction of the Falcon heavy launch vehicles of Space X. This cost is purported to come down further with the introduction of the highly re-useable launch vehicles like the Grasshopper. With the cost of accessing space coming down, it all comes down to the cost accessing the Near-Earth Asteroids and the profit that can be made. With the advent of powerful solar electric propulsion engines, the ability to transport a captured Near-Earth Asteroids has become feasible. This also means that it would cost less than the conventional chemical propulsion.

J. S. Lewis, in his book "Mining the Sky: Untold Riches from the Asteroids, Comets, and Planets", has estimated the amount of money that could be made if the claims from the data analysed from observing the asteroids were true. Taking the smallest known M asteroid,

3554 Amun, as an example of the magnitude and economic value of space resources, he estimates the value of riches waiting in space to be exploited. The asteroid is 2 km in diameter with a mass of 3×10^{10} tons. “Assuming a typical iron meteorite composition, the iron and nickel in Amun have a market value of about \$8,000 billion. The cobalt content adds another \$6,000 billion, and the platinum-group metals (platinum, osmium, iridium, palladium, etc.) add another \$6000 billion.” The total market value is estimated to be \$20,000 billion [30]. Because of it being already present in space, it represents an asset that would cost about \$10 million per ton if launched from Earth. So, in total \$300,000,000 billion can be saved and held as asset in space. This is just from one 2 km sized M-type asteroid. The overall value of all the resource would be impossible to estimate. Of course, there are other factors that would put the value a bit lower, for example reducing the amount of tin that can be added to the terrestrial stockpile, to keep the market price stabilised, but this can be held as equity and borrowed for further expansion.

1.4 Concept used in this research

Two closely passing by asteroids are connected using a tether, resulting in the formation of a dumbbell system with a centre of mass at a point in the line of the tether connecting the asteroids. The position of the centre of mass depends on the mass ratio of the asteroids being connected. The dumbbell system rotates around the centre of mass, as the centre of mass follows a heliocentric orbit. When the tether is disconnected after a certain period of time, the dumbbell system ceases to exist, and each asteroid takes a trajectory, different from the trajectory followed by the asteroids before the connection of the tether. The characteristics of their trajectory depends on the orientation of the tether with the reference axis, the orbital position of the centre of mass and the amount of energy it has gained or lost from the system at the time of disconnection.

1.5 Objectives

Keeping in mind the various necessities or requirements for orbital trajectory manipulation such as the threat posed by the asteroids and reaching asteroid to access their resources, an objective to this research was formed.

The objective of this research is as follows:

- 1) To carry out an initial study, to understand how the orbital trajectory of an asteroid could be manipulated by connecting it with a closely-passing-by asteroid through the means of a tether and later disconnecting

- 2) To study the different parameters that plays an important part in the orbital dynamics of such a method
- 3) To understand the relation between the orbital energy and time of tether cut

Manipulation of the orbital trajectory involves understanding the physics/dynamics behind it and understanding the physics involves setting up of a model that resembles the physical environment to an extent, with acceptable limitations, within the nature and scope of this research. Finally, setting up of a model involves specifying the assumptions considered and defining a proper co-ordinate system for the dynamics, which will be discussed in Chapter 2

The valid model is evaluated using mathematical simulations, wherein multiple resultant orbits with sample cases or scenarios are verified. The physics behind this is to be simulated using a numerical computing environment like MATLAB^[15]. These objectives will set the foundation for future work regarding this specific method of trajectory manipulation.

1.5.1 Study on parameters

Various parameters such as the mass ratio of the asteroids, the tether length between them and the orbital eccentricities of the asteroids before tether connection contribute to the formation of the initial dumbbell model. Although parameters such as the mass ratio of the asteroids and the orbital eccentricities of the initial orbit of the asteroids at tether connection are uncontrollable and are determined in nature, it is better to understand the various scenarios involving these quantities to develop a proper dynamical model. Therefore, different values of these parameters are used in creating multiple scenarios in the creation of the dynamical models for simulations. The relationships between these values are studied to understand how they affect the resulting orbits.

2. Model Description

To understand the dynamics of manipulating the orbital trajectory of an asteroid by manipulating its orbital energy, a mathematical representation of the model has to be defined. This chapter defines a mathematical model by describing the assumptions considered in its definition and the dynamics involved.

2.1 Assumption

Understanding the physics behind any event requires an accurate definition of its environment. For the sake of initial study and analysis within the scope of this research, certain assumptions are considered to simplify the variables involved in the environment:

- 1) Gravitational force is the only force acting on these bodies
- 2) Since the whole scenario is modelled as two body system, the orbital motions of the asteroids are considered to be purely Keplerian
- 3) Asteroids are aligned with the Sun, at the time of tether connection, forming an imaginary line representing the x-axis of the fixed frame of reference “*Ref A*” (**Fig 2.1**) as the heading
- 4) At tether connection, the asteroids are assumed to be at the perihelion point in their respective orbit
- 5) The connection of tether happens instantaneously
- 6) The tether used is massless and inelastic
- 7) Only the ecliptic in-plane motion of the system is considered, due to this being a preliminary study and is complex to predict the dynamics and hence not in the scope of this research. [The inclination of the asteroids is assumed to be zero ($i_1 = 0, i_2 = 0$)]
- 8) All masses are assumed to be point masses. This helps in avoiding motion such as spinning, caused due to structural criteria like micro-porosity, material composition, shape and size of the asteroid

2.2 Representation

The model is represented by two frames of reference as depicted in **Fig 2.1**, where Asteroid1 and Asteroid2 are depicted as A1 and A2 respectively and O_{COM} represents the position of the centre of mass. The centre of mass of a system is the point in a system where the components of weight for each point have a resultant of zero. Reference frame *Ref A* is inertial with the Sun at the origin and is represented by the unit vectors \hat{I} , \hat{J} and \hat{K} . $\vec{r}_{1(0)}$, $\vec{r}_{2(0)}$ and \vec{r}_{COM} are the position vectors of the first asteroid, the second asteroid and the centre of mass respectively. θ_{COM} is the true anomaly of the centre of mass in reference frame *Ref A*. Reference frame *Ref B* is a body fixed, non-rotating reference frame with its origin fixed to the centre of mass of the dumbbell system and moves only in a translational motion along with the centre of mass in a heliocentric orbit. θ is the angular displacement of the tether from the x-axis of frame *Ref B*.

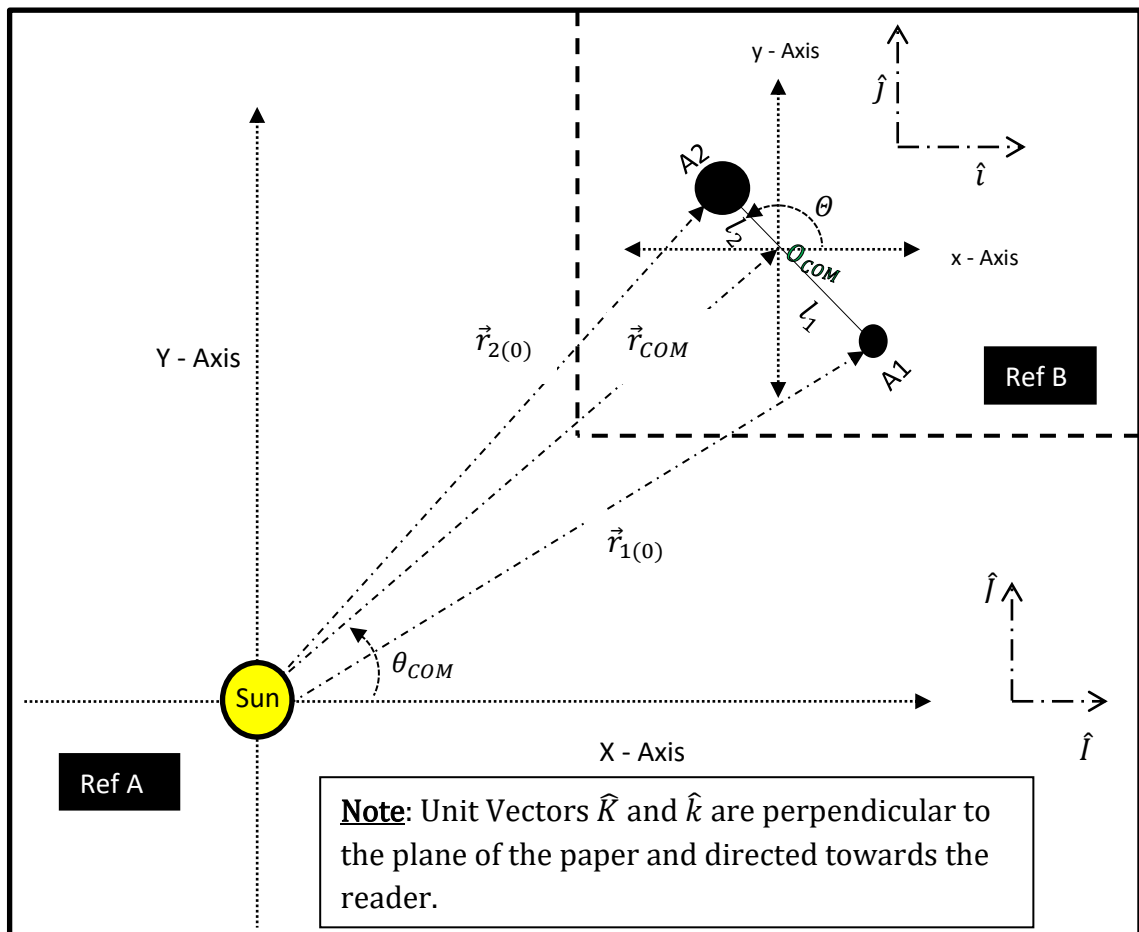


Fig 2.1 Representation of the model

2.3 Dumbbell System

When an asteroid A_1 of mass m_1 with initial position vector $\vec{r}_{1(0)}$ and initial velocity vector $\vec{v}_{1(0)}$ is connected with another asteroid A_2 of mass m_2 with initial position vector $\vec{r}_{2(0)}$ and initial velocity vector $\vec{v}_{2(0)}$, a dumbbell system with a centre of mass O_{COM} of mass m_{COM} with radius vector \vec{r}_{COM} (128) and velocity vector \vec{v}_{COM} (129) is formed:

$$\vec{r}_{COM} = \frac{m_1 \vec{r}_{1(0)} + m_2 \vec{r}_{2(0)}}{m_1 + m_2} \quad (128)$$

$$\vec{v}_{COM} = \frac{m_1 \vec{v}_{1(0)} + m_2 \vec{v}_{2(0)}}{m_1 + m_2} \quad (129)$$

Because the tether is inelastic, the length of tether l , which is actually the distance between the asteroids in the dumbbell system, is fixed throughout the period of tether connection. l_1 (130) (132) is the distance between Asteroid1 and the centre of mass. l_2 (131) (133) is the distance between Asteroid2 and the centre of mass. As depicted in **Fig 2.1** the naming/numbering of the asteroids here are not fixed because of the generalised nature of the representation, and hence could be changed depending on the nature of the objective. Either Asteroid1 or Asteroid2 can be the outer asteroid. In all the simulations carried out in this research, Asteroid1 was considered to be the outer asteroid at the time of tether connection and the appropriate equations for the dynamics were used:

$$\text{If } r_1 > r_2 \left\{ \begin{array}{l} l_1 = r_1 - r_{COM} \quad (130) \\ l_2 = r_{COM} - r_2 \quad (131) \end{array} \right.$$

$$\text{If } r_2 > r_1 \left\{ \begin{array}{l} l_1 = r_{COM} - r_1 \quad (132) \\ l_2 = r_2 - r_{COM} \quad (133) \end{array} \right.$$

Here, there are two motions involved, one is heliocentric translational orbital motion followed by the centre of mass and the other is rotational motion of the asteroids in the dumbbell system about the centre of mass, each defined with their respective frames of reference in **Fig 2.1**.

2.3.1 Attitude Dynamics

The only force acting on the asteroids before tether connection is the gravitational force of the Sun. At the point of tether connection, a centripetal force along the tether causes a moment about the centre of mass resulting in the dumbbell system rotating about its own axis at the centre of mass O_{COM} with an angular velocity ω_v , by an angular displacement θ and the rotational velocities $\vec{v}_{1_{rot}}$ and $\vec{v}_{2_{rot}}$ for Asteroid1 and Asteroid2 respectively, In order to consider a uniform rotation we neglect the gravity gradient.

$$\vec{v}_{1_{rot}} = \vec{v}_{COM} - \vec{v}_1 \quad (134)$$

$$\vec{v}_{2_{rot}} = \vec{v}_{COM} - \vec{v}_2 \quad (135)$$

$$\omega_v = \frac{\vec{v}_{1_{rot}}}{l_1} \text{ or } \omega_v = \frac{\vec{v}_{2_{rot}}}{l_2} \quad (136)$$

$$\theta = \omega_v t \quad (137)$$

Since we have neglected the gravity gradient force, the tension in the tether is only due to the centripetal force acting along the tether. Though the rotational motion of the dumbbell system influences the translational motion of the centre of mass' heliocentric orbit, for simplicity, let us assume that the distance between the point masses (asteroids), i.e. the length of the tether, is much shorter than the distance between the Sun and the point masses, hence the force due to the attitude dynamics on the centre of mass is neglected^[12, 13]. This also means that the orbital dynamics of the dumbbell system is predicted by assuming that the gravitational force acts only on the centre of mass and not on the asteroids during the dumbbell motion.

2.3.2 Orbital Dynamics

Since the state vectors of the centre of mass of the dumbbell system at the time of tether connection (at $t = 0$), with respect to the reference frame *Ref A*, is already represented in the Cartesian co-ordinate system, its use is continued. The centre of mass' heliocentric propagation is predicted at each of time t seconds.

Following Bate^[14], as described in “Orbital Mechanics” by V. A. Chobotov ^[23], the Lagrange coefficients $f_{lag,COM}$ **(140)** $g_{lag,COM}$ **(141)** are used to calculate the position vector of the centre of mass after time t seconds of propagation from the initial time of tether connection t_0 ($t = 0$) with respect to the Sun in reference frame *Ref A*.

$$\vec{r}_{COM(t)} = (f_{lag,COM} \vec{r}_{COM(0)}) + (g_{lag,COM} \vec{v}_{COM(0)}) \quad (138)$$

$$\vec{v}_{COM(t)} = (\dot{f}_{lag,COM} \vec{r}_{COM(0)}) + (\dot{g}_{lag,COM} \vec{v}_{COM(0)}) \quad (139)$$

$$f_{lag,COM} = 1 - \frac{X_{COM}^2}{r_{COM(0)}} C(z_{COM}) \quad (140)$$

$$g_{lag,COM} = t - \frac{1}{\sqrt{\mu_S}} X_{COM}^3 S(z_{COM}) \quad (141)$$

The derivatives $\dot{f}_{lag,COM}$ **(142)**, $\dot{g}_{lag,COM}$ **(143)** of the Lagrange coefficients are used to find the velocity vector after time t seconds in propagation.

$$\dot{f}_{lag,COM} = \frac{\sqrt{\mu_S}}{r_{COM(t)} r_{COM(0)}} (z_{COM} S(z_{COM}) - 1) X_{COM} \quad (142)$$

$$\dot{g}_{lag,COM} = 1 - \frac{X_{COM}^2}{r_{COM(t)}} C(z_{COM}) \quad (143)$$

As discussed earlier in **Section 1.1.4**, The Lagrange coefficients can be obtained from Stumpff functions $C(z_{COM})$ **(144)**, $S(z_{COM})$ **(145)** and universal anomaly X_{COM} .

$$C(z_{COM}) = \frac{(1 - \cos \sqrt{z_{COM}})}{z_{COM}} \quad (144)$$

$$S(z_{COM}) = \frac{(\sqrt{z_{COM}} - \sin\sqrt{z_{COM}})}{\sqrt{z_{COM}}^3} \quad (145)$$

$$z_{COM} = \gamma_{COM} X_{COM}^2 \quad (146)$$

$$\gamma_{COM} = \frac{1}{a_{COM}} \quad (147)$$

$$a_{COM} = \frac{1}{\frac{2}{r_{COM(0)}} - \frac{v_{COM(0)}^2}{\mu_S}} \quad (148)$$

While X_{COM} can be obtained through iteration of (149) with an initial value ($X_{COM(0)}$),

$$F(X_{COM}) = \frac{r_{COM(0)}v_{r,COM(0)}}{\sqrt{\mu_S}} X_{COM}^2 \mathcal{C}(z_{COM}) + (1 - \gamma_{COM} r_{COM(0)}) X_{COM}^3 S(z_{COM}) + r_{COM(0)} X_{COM} - \sqrt{\mu_S} t \quad (149)$$

We need to find the derivative of (149) in order to use it for iteration, and the derivative is (150)

$$F'(X_{COM}) = \frac{r_{COM(0)}v_{r,COM(0)}}{\sqrt{\mu_S}} X_{COM} (1 - \gamma_{COM} X_{COM}^2 S(z_{COM})) + (1 - \gamma_{COM} r_{COM(0)}) X_{COM}^2 \mathcal{C}(z_{COM}) + r_{COM(0)} \quad (150)$$

$$X_{COM(n+1)} = X_{COM(n)} - \frac{F(X_{COM(n)})}{F'(X_{COM(n)})} \quad (151)$$

$$F(X_{COM(n)}) = \frac{r_{COM(0)}v_{r,COM(0)}}{\sqrt{\mu_S}} X_{COM(n)}^2 \mathcal{C}(z_{COM(n)}) + (1 - \gamma_{COM} r_{COM(0)}) X_{COM(n)}^3 S(z_{COM(n)}) + r_{COM(0)} X_{COM(n)} - \sqrt{\mu_S} t \quad (152)$$

$$\begin{aligned}
F'(X_{COM(n)}) &= \frac{r_{COM(0)} v_{r,COM(0)}}{\sqrt{\mu_S}} X_{COM(n)} \left(1 \right. \\
&\quad \left. - \gamma_{COM} X_{COM(n)}^2 S(z_{COM(n)}) \right) \\
&\quad + (1 - \gamma_{COM} r_{COM(0)}) X_{COM(n)}^2 C(z_{COM(n)}) \\
&\quad + r_{COM(0)}
\end{aligned} \tag{153}$$

Initial Value of X_{COM} ,

$$X_{COM(0)} = \sqrt{\mu_S} |\gamma_{COM}| t \tag{154}$$

2.3.3 Dumbbell Propagation

Once the dumbbell system is formed, the dynamics of the asteroids are predicted from the motion of and about the centre of mass of the dumbbell system. The position vectors (155) of the asteroids with respect to the centre of mass of the dumbbell system, in the reference frame *Ref B*, are calculated from the known distance between the centre of mass of the dumbbell system and the respective asteroid and the angular displacement of the tether with respect to the local x-Axis of *Ref B*.

$$\vec{r}_{i_{db}(t)} = l_i [\cos \theta \quad \sin \theta \quad 0] \tag{155}$$

The sum of the position vector (138) of the centre of mass of the dumbbell system relative to the Sun and the position vector of the respective asteroids relative to the centre of mass of the dumbbell system (155) gives the position vectors of the asteroids relative to the Sun (156), represented in the reference frame *Ref A*.

$$\vec{r}_{i_{orb}(t)} = \vec{r}_{i_{db}(t)} + \vec{r}_{COM(t)} \tag{156}$$

The product of the magnitude of the velocity vector of the asteroids with respect to the centre of mass of the dumbbell system, in the reference frame *Ref B*, and the unit vector to the position vector $\hat{r}_{i,t}$ at time t will give the rotational velocity vector (157) of the asteroid with respect to the centre of mass of the dumbbell system in the reference frame *Ref B*.

$$\vec{v}_{i_{rot}(t)} = \hat{r}_{i(t)} v_{i_{rot}} \tag{157}$$

$$\vec{v}_{i_{orb}(t)} = \vec{v}_{i_{rot}(t)} + \vec{v}_{COM(t)} \tag{158}$$

The vector addition of the rotational velocity vector **(157)** of the respective asteroid with respect to the centre of mass of the dumbbell system and the velocity vector **(139)** of the centre of mass with respect to the Sun gives the orbital velocity vector **(158)** of the asteroids with respect to the Sun in the reference frame *Ref A*, after time t .

3. Parameters Affecting Orbit Manipulation

This chapter discusses the various parameters involved in orbit manipulation, such as how energy and angular momentum play a part in the physics of the model. This is followed by a discussion on the parameters that affect the orbit manipulation leading to a case study of some orbital scenarios, where the dynamics involved in the respective cases are discussed.

3.1 Energy and Angular Momentum

Manipulating the orbital trajectory involves manipulating the transfer of orbital energy and orbital angular momentum between the asteroids in the dumbbell system. Before tether connection, it is assumed, that the asteroids were in a closed system with only the Sun as the influencing body. And with respect to each of this closed system, the orbital energy (161) and orbital angular momentum (162) were conserved quantities. The orbital energies of these asteroids are the sum of the potential energy (159) and kinetic energy (160):

$$\varepsilon_i^{pot} = -\frac{\mu}{r_i} m_i \quad (159)$$

$$\varepsilon_i^{kin} = \frac{v_i^2}{2} m_i \quad (160)$$

$$\varepsilon_i^{orb} = \left(\frac{v_i^2}{2} m_i\right) - \left(\frac{\mu}{r_i} m_i\right) \quad (161)$$

$$\vec{h}_i^{orb} = \vec{r}_i \times \vec{v}_i \quad (162)$$

Where ε_i^x is the energy of the respective type and asteroid, and the subscript denotes the asteroid number and the superscript denotes the type of energy, \vec{r}_i represents the radius vector of the asteroid from the Sun and \vec{v}_i denotes the orbital velocity of the asteroids with the subscript denoting the asteroid number, in both cases. After the formation of a dumbbell system the orbit of the asteroids are determined by the orbital motion of the centre of mass of the dumbbell system rather than the orbital motion of the asteroids as individual bodies, this is the assumed model towards the prediction of their dynamics. The orbital energy and the orbital angular momentum about the centre of mass of the dumbbell system are the sum of the orbital energies and orbital angular momentum of the asteroids respectively. The translational kinetic energy of the system transforms into rotational kinetic energy, due to the creation of a couple about the centre of mass of the dumbbell system. This rotational

kinetic energy contributes to an angular velocity **(136)** leading to the rotational motion of the dumbbell system, at an angular displacement $\theta = \omega_v \cdot t$, where t is the time. Now the total energy of the dumbbell system is split into potential **(163)**, kinetic **(164)** and rotational kinetic energy **(165)**:

$$\varepsilon_{db}^{pot} = - \frac{\mu}{r_{com}} m_i \quad (163)$$

$$\varepsilon_{db}^{kin} = \frac{v_{com}^2}{2} m_i \quad (164)$$

$$\varepsilon_{db}^{rot_Kin} = \frac{1}{2} I \omega_v^2 \quad (165)$$

$$\varepsilon_{db}^{total} = \varepsilon_{db}^{pot} + \varepsilon_{db}^{kin} + \varepsilon_{db}^{rot} \quad (166)$$

$$\varepsilon_{db}^{total} = - \frac{\mu}{r} m_i + \frac{v^2}{2} m_i + \frac{1}{2} I \omega_v^2 \quad (167)$$

Where I **(168)**, the moment of inertia about the centre of mass of the dumbbell system is calculated as follows,

$$I = m_1 l_1^2 + m_2 l_2^2 \quad (168)$$

The rotational kinetic energy is actually equal to the sum of the rotational kinetic energy of both the asteroids in the dumbbell system and can also be calculated by:

$$\varepsilon_{db}^{rot_Kin} = \underbrace{\frac{1}{2} m_1 v_{1,rot}^2}_{\text{Asteroid1}} + \underbrace{\frac{1}{2} m_2 v_{2,rot}^2}_{\text{Asteroid2}} \quad (169)$$

While the rotational kinetic energy **(169)** contributes to the rotational motion of the dumbbell system, the potential and kinetic energy contribute to the translational motion of the centre of mass of the dumbbell system, which follows a heliocentric orbit. At the instant when the tether is disconnected after a certain period from the time of tether connection, the dumbbell system ceases to exist, and hence the total energy and the total angular momentum of the dumbbell system gets split and transferred between the two asteroids. This transfer of

angular momentum and orbital energy depends on the orbital position of the centre of mass relative to the Sun, the orientation of the tether with respect to the reference axis, i.e. the x-axis of the reference frame *Ref B* at the time of the tether disconnection, the mass ratio and the eccentricity of the original orbits of the asteroids. The angular momentum and the orbital energy determine the shape, size and orientation of the heliocentric orbit of these asteroids.

3.2 Variation of parameters

The nature of the transfer of orbital energy and orbital angular momentum between the asteroids, especially at tether disconnection, depends on a number of parameters. The amount of orbital energy and orbital angular momentum possessed by an asteroid determines its resulting orbits, i.e. their respective orbits after tether disconnection. Manipulation of these parameters could help in the manipulation of the orbital trajectory of the asteroids. These parameters are:

- 1) Length of the tether
- 2) Mass ratio
- 3) Eccentricity of their initial orbits
- 4) Time of tether disconnection

The mass of the asteroids, the eccentricity of their initial orbits and the length of the tether which depends on the closest approach between the two asteroids, at the point of tether connection, are fixed in nature, at least in the case of using a rigid and inelastic tether. But to understand the extent of how these parameters affect the transfer of orbital energy between the asteroids and the dumbbell system, and hence affect the orbital trajectory manipulation, a parametric study is carried out.

3.2.1 Length of the tether

To understand how the length of the tether would affect the transfer of energy between the asteroids, a test case of fixing the tether for an initial length at about 5×10^7 km (approximately the closest distance between Earth and Mars), then to 3×10^7 km (which is 60% of the initial distance) and finally to 1×10^7 km (which is 20% of the initial distance) was carried out. The following values were set for the test:

1. $e_1 = 0$
2. $e_2 = 0$
3. $m_1 = 10^8$ kg

$$4. m_2 = 10^8 \text{kg}$$

Using the above values as inputs, the orbital energy of the asteroids before tether connection and after tether disconnection was calculated. By the law of conservation of energy, the sum of the orbital energies of Asteroid1 and Asteroid2 before tether connection and after tether disconnection should be equal, proving that the energy is conserved. But contrary to the law, in this case, the value of the sum of the orbital energies of the asteroids after tether disconnection was different to that of the values of the sum of the orbital energies of the asteroids at tether connection. An error percentage was calculated to measure the amount of change in the orbital energy values at tether connection and after tether disconnection.

$$E_{per} = \frac{(\epsilon_{orb,ATD} - \epsilon_{orb,BTC})}{\epsilon_{orb,BTC}} \times 10^2 \quad (170)$$

The results are shown in **Table 3.1** and as it can be seen the difference in the orbital energy values were comparatively very small, but difference between the orbital energies decreased with the decrease in the length of the tether, thus leading to negligible error for shorter tether length.

Tether Length (km)	$5 \times 10^7 \text{ km}$	$3 \times 10^7 \text{ km}$	$1 \times 10^7 \text{ km}$
Orbital Energy BTC (J)	-9.432992×10^{10}	-8.643037×10^{10}	-8.050570×10^{10}
Orbital Energy ATD (J)	-9.369451×10^{10}	-8.626124×10^{10}	-8.049079×10^{10}
Error Percentage	0.6	0.1	0.01

Table 3.1 Error percentage comparison for various tether lengths

The reason for the occurrence of this error is due to the nature of the model considered for the simulation. By Newton's law of universal gravitation, the Sun's gravitational field strength decreases as a body moves away from the Sun. So, the asteroids in the dumbbell system experience different gravitational accelerations, from which their dynamics are determined. But in the model that we have defined, we measure and predict the dynamics of both asteroids from the position and velocity of the centre of mass. This cannot be true, because the centre of mass is not a physical entity but assumed to be at a position where the overall mass of the system would be concentrated. However, for the sake of simplicity of

modelling and hence the calculated state vectors of the centre of mass are not accurate in reality. Since we predict the dynamics and the energy of the asteroids from the state vectors of a non-physical entity, the position and energy of the asteroids are affected by an error.

As noticed in **Fig 3.1**, the error percentage decreases with a decrease in the tether length as the asteroids are practically closer to the position of the centre of mass and in a similar gravitational acceleration with short tethers. So, for shorter tether length the error obtained in the calculation of orbital energy is negligible, and for a longer tether length the error is considerably higher. The value of the angular velocity depends on the initial orbital velocity of the asteroids and the distance between the asteroids and the centre of mass. The orbital velocity of the asteroids varies in time with respect to their motion around the Sun but here we assume the asteroids to be in a locally uniform gravitational field, hence there is no external torque acting on the system and so the angular velocity remains constant.

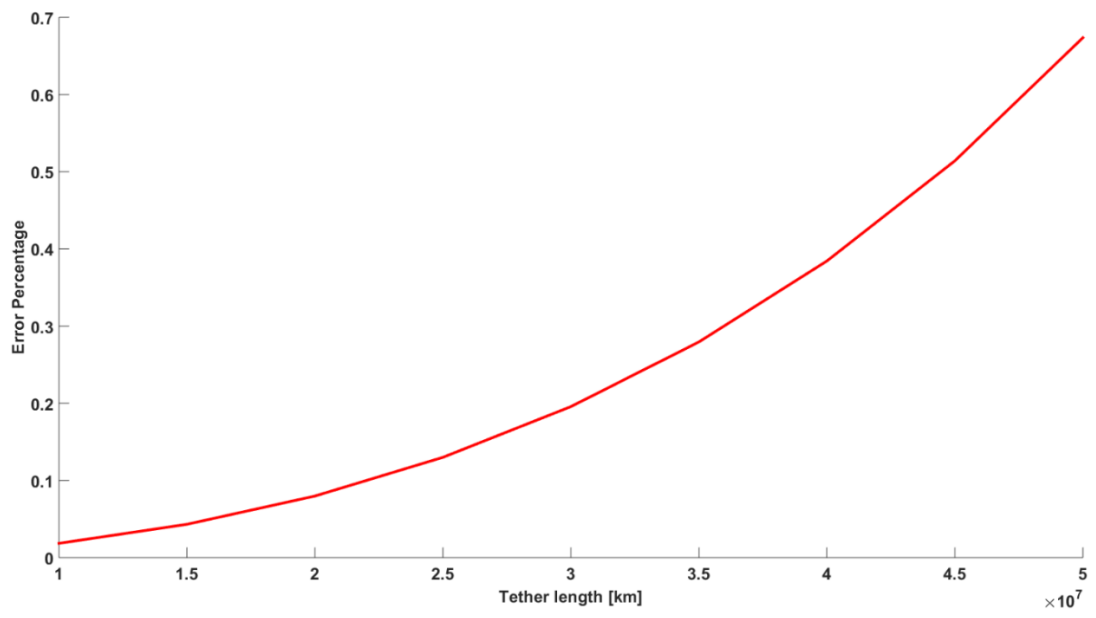


Fig 3.1 Error percentage plot for various tether lengths

Energy Analysis

To understand how the orbital energy varies with respect to the tether length and the angular displacement compared at different true anomalies of the centre of mass, a surface plot was plotted for each asteroid. **Fig 3.2**, **Fig 3.3** and **Fig 3.4** show the variations in the orbital energy plotted for different lengths of the tether against the angular displacement of the tether, for Asteroid1, Asteroid2 and the dumbbell system respectively. In **Fig 3.2** and **Fig 3.3** it can be observed that there exists a broad alternating blue and green striped pattern. The green and blue pattern represents higher and lower values of orbital energy respectively. The x-axis represents the tether length, the y-axis represents the angular displacement and

the z-axis represents the orbital energy with respect to the tether length. Different positions of the true anomaly of the centre of mass are represented as markers to understand the behavioural pattern in the orbital energy. Red markers represent a true anomaly of 90 degrees, green markers represent a true anomaly of 180 degrees, saffron markers represent a true anomaly of 270 degrees and black markers represent a true anomaly of 360 degrees.

As a measure of reference, the plotted distance between the x-axis and the black marker corresponding to the respective value of tether length is denoted as the height of the plotted surface. It could be noticed that height of the plotted surface indicates the relation between the numbers of times the asteroids rotate around the centre of mass of the dumbbell system for one orbit of the centre of mass' motion around the Sun. This can be noted from the lower and higher values of angular displacement for longer and shorter tether respectively. As can be seen, the small height of the plotted surface for a tether length of 5×10^7 km shows that the centre of mass completes one full orbit before the asteroids in the dumbbell system makes one full rotation around the centre of mass. Likewise, the comparatively taller height of the plotted surface for the shorter tether length of 1×10^7 km shows that the dumbbell system makes multiple rotations about the centre of mass before the centre of mass of the dumbbell system completes one full orbit around the Sun.

In **Fig 3.4** it can be seen in the plotted surface that the variation in the orbital energy of the dumbbell system to be altering gradually rather than the alternating broad stripped pattern observed while plotting for individual asteroids of the dumbbell system. This is because the dumbbell system as a whole gets its orbital energy calculated from the position of the centre of mass with respect to the Sun and the centre of mass is a fixed point in *Ref B*, where as the orbital energy of the asteroids are calculated from the dynamics of the centre of mass and the position of the asteroids in *Ref B* keeps changing. A change in the position in *Ref B* indicates a considerable change in the position of the asteroids in *Ref A* as well and hence a considerable change in the orbital energy. This frequency of this change depends on the orbital and angular velocity of the dumbbell system.

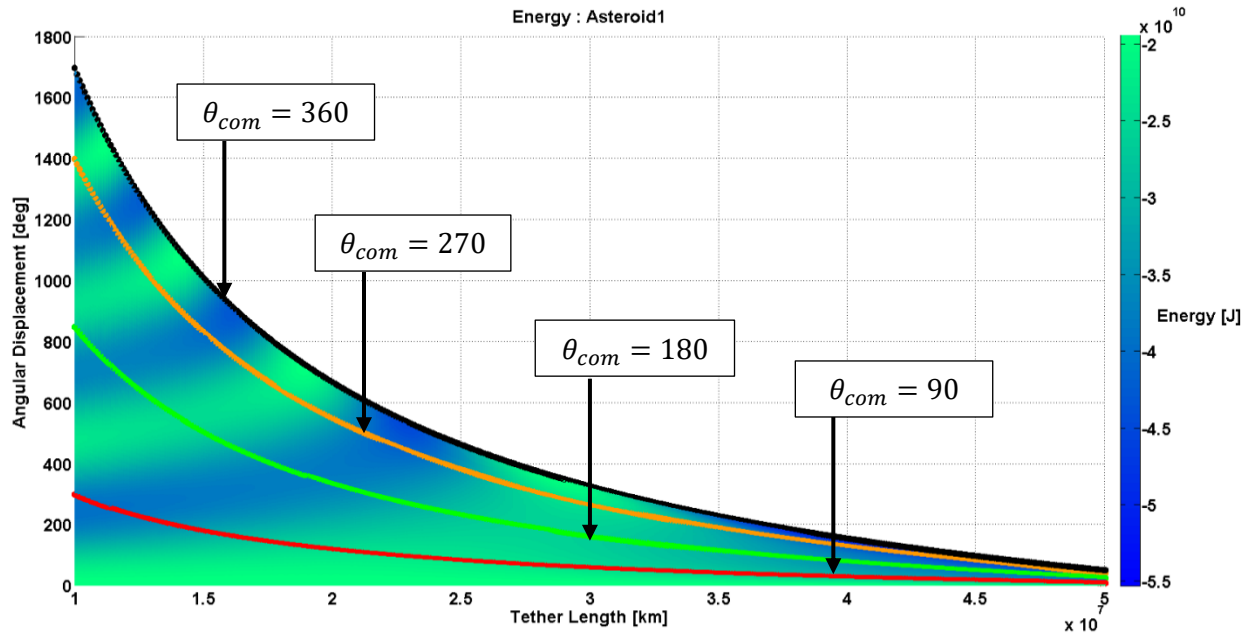


Fig 3.2 Energy of Asteroid1 after tether disconnection for varying tether length and angular displacement

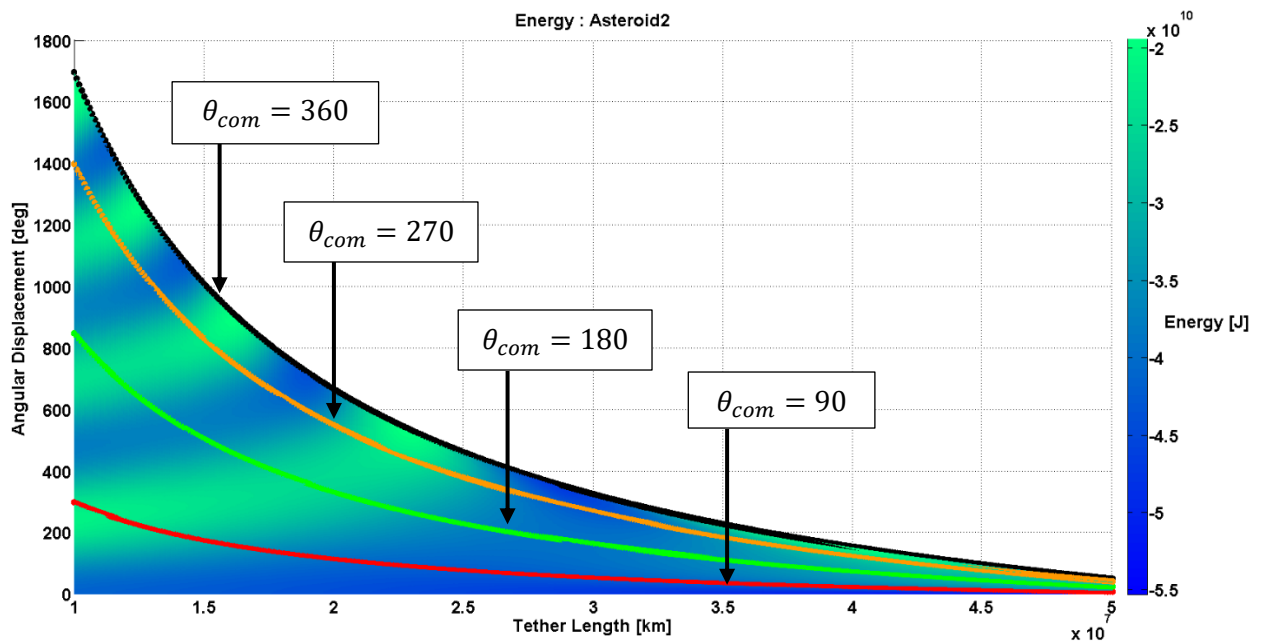


Fig 3.3 Energy of Asteroid2 after tether disconnection for varying tether length and angular displacement

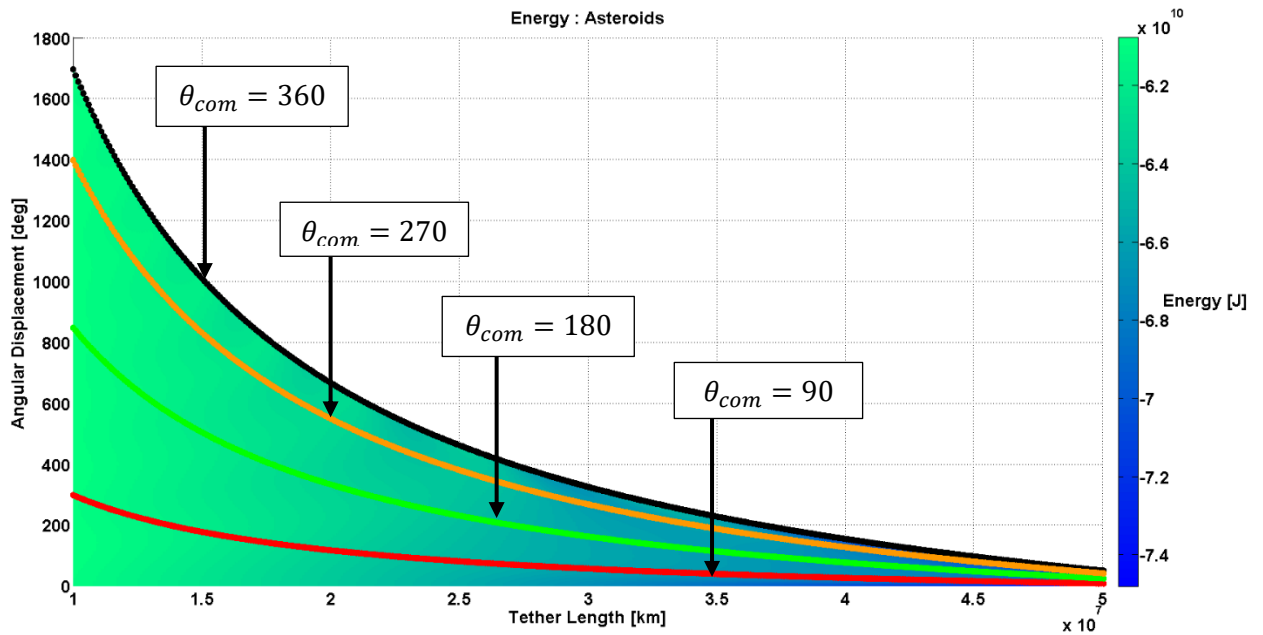


Fig 3.4 Energy of dumbbell system after tether disconnection for varying tether length and angular displacement

In order to have a small error during the course of the simulations as observed earlier in subheading 3.2.1, the length of the tether was fixed to be 1×10^7 km for all other parameter tests.

3.2.2 Mass Ratio

The mass ratio for the asteroids is the relative comparison of the mass of the asteroids in a closed system. It relates how massive one asteroid is with respect to the other and plays an important role in determining the position of the centre of mass of the dumbbell system, which forms the basis for the dynamics of the dumbbell system and the manipulation of the orbital trajectory of the asteroids. One of the parameters affecting the transfer of orbital energy and orbital momentum to and from the dumbbell system is the relative position of the asteroids with respect to the centre of mass. The centre of mass will be closer to the asteroid with a mass larger than the other asteroid. **Fig 3.6, Fig 3.7** and **Fig 3.8** show the difference in the position vector and orbital trajectory of an asteroid for different mass ratios and **Fig 3.5** is the legend for **Fig 3.6, Fig 3.7** and **Fig 3.8**.

The orbit was plotted with the following values for the variables:

1. $e_1 = 0$
2. $e_2 = 0$
3. $r_{p,1} = 17 \times 10^7$ km
4. $r_{p,2} = 16 \times 10^7$ km

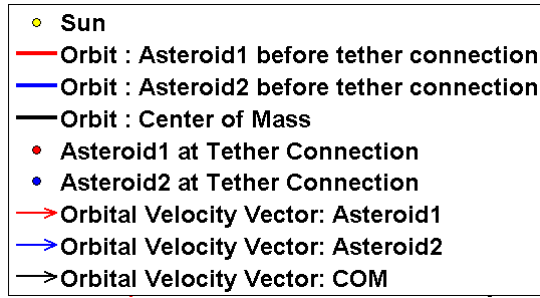


Fig 3.5 Plot legend for initial orbits in Case1, Case2 and Case3

Case 1: Mass ratio 1:1

1. $m_1 = 1 \times 10^8$ kg
2. $m_2 = 1 \times 10^8$ kg

$$\varepsilon_1^{orb} = -3.90330 \times 10^{10} J$$

$$\varepsilon_2^{orb} = -4.14726 \times 10^{10} J$$

$$\varepsilon_{db}^{orb} = -8.03763 \times 10^{10} J$$

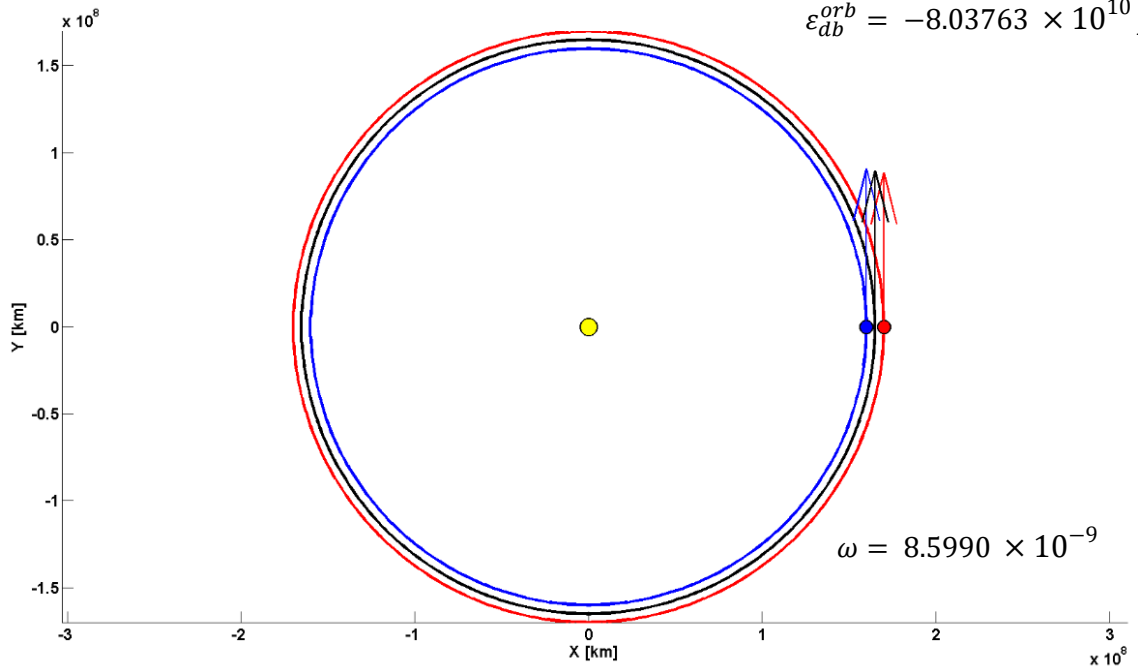


Fig 3.6 Orbits at tether connection with mass ratio 1:1

Fig 3.6 shows that for a mass ratio of 1:1, the position of the centre of mass of the dumbbell system is exactly at the middle of the length of the tether connected between the asteroids, while **Fig 3.7** shows that for a mass ratio of 1:2, the position of the centre of mass of the dumbbell system is closer to Asteroid2 along the tether, as it has a bigger mass than Asteroid1 and **Fig 3.8** shows that for a mass ratio of 2:1, the position of the centre of mass of the dumbbell system is closer to Asteroid1 along the tether, as Asteroid1 has a bigger mass than Asteroid2.

Case 2: Mass ratio 1:2

1. $m_1 = 1 \times 10^8$ kg
2. $m_2 = 2 \times 10^8$ kg

$$\varepsilon_1^{orb} = -3.90330 \times 10^{10} J$$

$$\varepsilon_2^{orb} = -8.29452 \times 10^{10} J$$

$$\varepsilon_{db}^{orb} = -12.1803 \times 10^{10} J$$

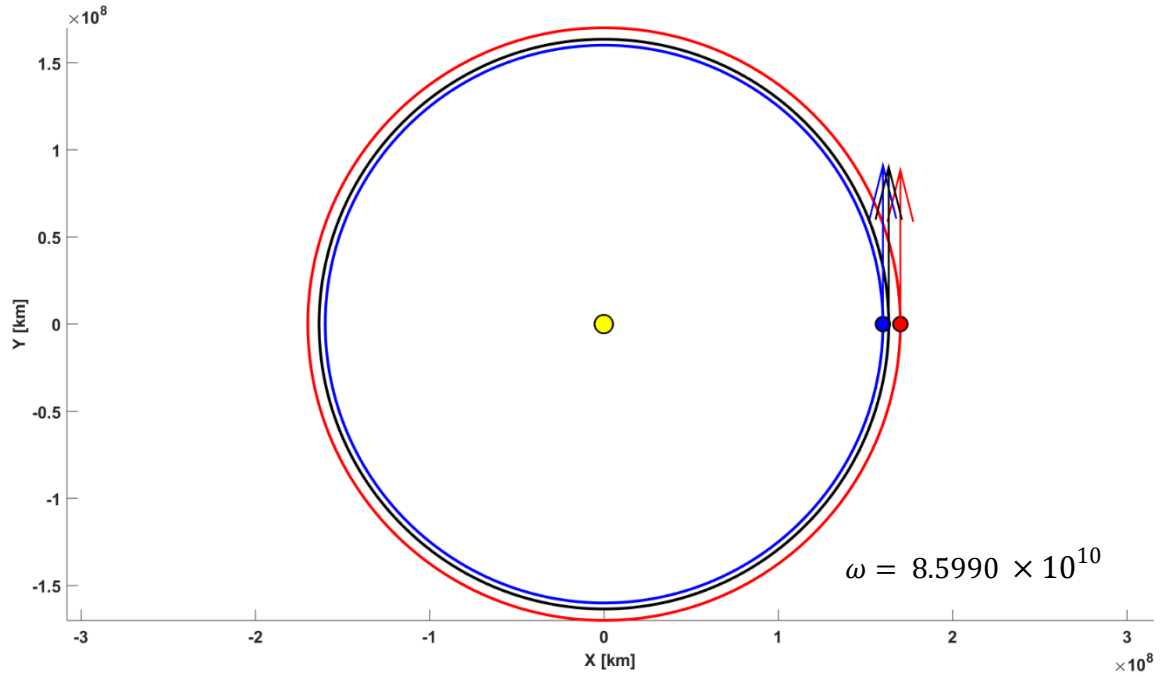


Fig 3.7 Orbits at tether connection with mass ratio 1:2

Case 3: Mass ratio 2:1

1. $m_1 = 2 \times 10^8$ kg
2. $m_2 = 1 \times 10^8$ kg

$$\varepsilon_1^{orb} = -7.80661 \times 10^{10} J$$

$$\varepsilon_2^{orb} = -4.14726 \times 10^{10} J$$

$$\varepsilon_{db}^{orb} = -11.9368 \times 10^{10} J$$

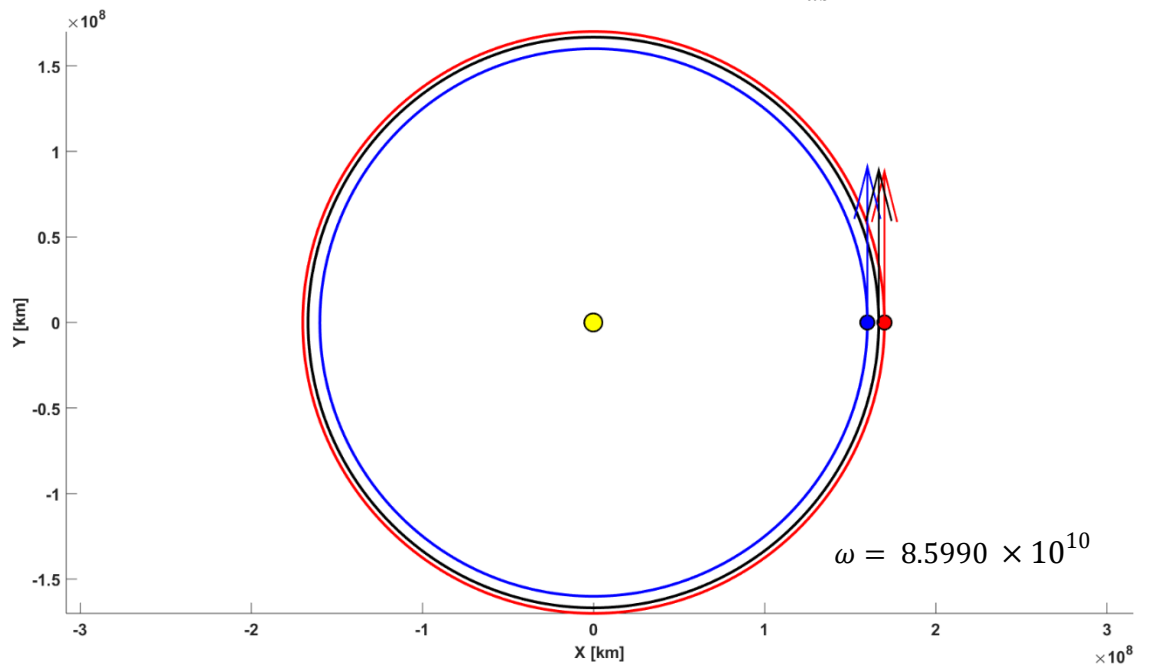


Fig 3.8 Orbits at tether connection with mass ratio 2:1

The cases plotted in **Fig 3.6**, **Fig 3.7** and **Fig 3.8** show that for the same value of eccentricity of the orbit and a constant tether length, a difference in the mass ratio of the asteroids could lead to the formation of an entirely different orbital trajectory of the centre of mass. The orbital energy values for the centre of mass achieved in these orbits differs based on the relative distance of the centre of mass from the Sun and the moment of inertia. The orbital energy possessed by a celestial body is directly proportional to the orbital velocity of the asteroids and hence when the tether is cut the resulting orbital trajectory of each asteroid vary in each case. The orientation of the asteroids in the dumbbell system with respect to the sun at the time of tether disconnection and the magnitude and direction of the rotational velocity vector with respect to the centre of mass contribute to the resulting orbital trajectory after tether disconnection as well, but this will be discussed in a later section of the thesis.

3.2.3 Eccentricity

The eccentricity of an orbit determines how much the orbit deviates from a perfect circle. The value of eccentricity of an orbit is determined from parameters such as the orbital energy, orbital angular momentum, the inertial mass of the two-body system and the coefficient of gravity. The eccentricity for the orbit of the centre of mass of the dumbbell system is determined from the eccentricities of the initial orbits of the asteroids at the time of tether connection. In order to understand the influence of eccentricity of the initial orbit of the asteroids at tether connection, in the determination of the orbital eccentricity of the centre of mass, it is important to understand the energy variations due to the difference in the eccentricity of the orbit of the asteroids at tether connection. This also contributes to the determination of the resulting orbits after tether disconnection. **Fig 3.9** and **Fig 3.10** was plotted to understand this, where the red orbit plot line represents the orbit of Asteroid1, the blue orbit plot line represents the orbit of Asteroid2 and the black orbit plot line represents the orbit of the centre of mass. The arrows represent the orbital velocity of the asteroids at perihelion, where the red, blue and black arrows represent the red, blue and black orbits respectively. From **Fig 3.9** and **Fig 3.10**, it can be seen that the position of the centre of mass and the hence the orbit of the centre of mass does not change in shape and size, irrespective which asteroid among the two in the dumbbell system has that particular value of the eccentric for its orbit.

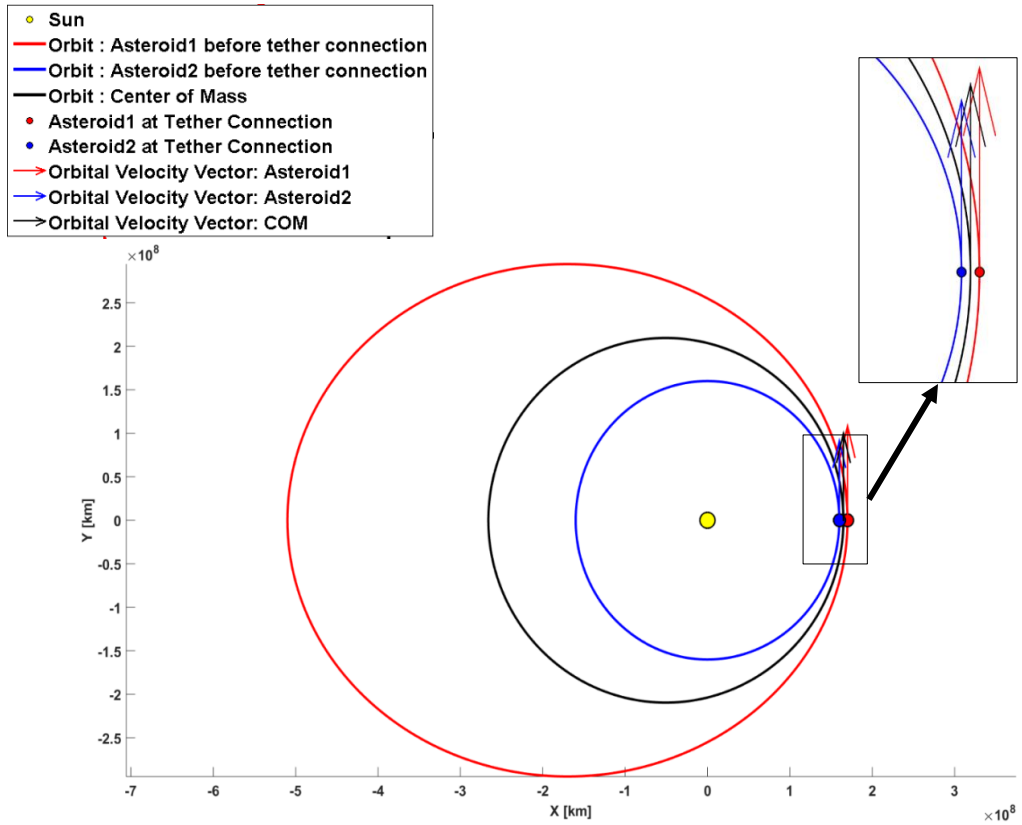


Fig 3.9 Orbits at tether connection with $e_1 = 0.5$ and $e_2 = 0$

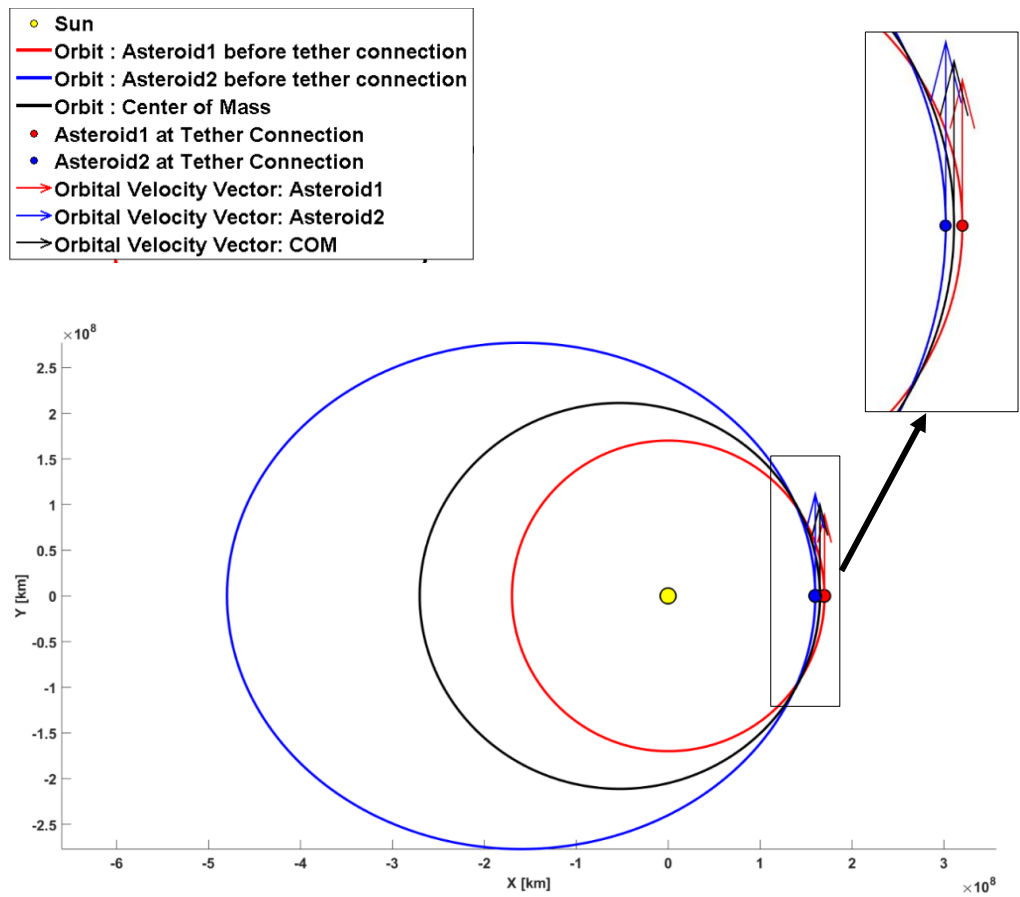


Fig 3.10 Orbits at tether connection with $e_1 = 0$ and $e_2 = 0.5$

4. Resulting Orbits and Wait Times

The true anomaly of centre of mass, at which the tether is disconnected from the asteroids, determines the amount of orbital energy an asteroid has gained or lost from the asteroid-tether-asteroid dumbbell system. This resulting orbital energy determines the magnitude of the velocity possessed by the asteroids, while the orientation of the tether with respect to the x-axis of *Ref B* at the time of tether disconnection determines the direction of the velocity vector of the asteroids. All these parameters contribute towards determining the shape and size of the resulting orbit of the asteroids.

4.1 Energy Distribution over an Orbit

The orbital energy of the centre of mass is constant throughout its heliocentric motion, but the total orbital energy of the centre of mass gets transferred between the two asteroids once disconnected from the dumbbell system. **Fig 4.1** shows this distribution in the orbital energies of the asteroids at tether disconnection, for various points in the centre of mass' orbit at which the tether is cut. The points are represented as the true anomaly of the centre of mass' heliocentric motion and this gives an idea on the energy distribution, the shape and size of the resulting orbit, which will be discussed in the next section. For initial analysis, the following data, chosen at random, was given as the input:

1. $e_1 = 0.5$
2. $e_2 = 0$
3. $m_1 = 10^8$ kg
4. $m_2 = 10^8$ kg
5. $r_{p,1} = 10^7$ km
6. $r_{p,2} = 10^6$ km

The red line represents the orbital energy of Asteroid1, while the blue line represents the orbital energy of Asteroid2, and the circular scatter points superimposed throughout the red and blue lines represents the position of the centre of mass in terms of the true anomaly at which this particular orbital energy value is obtained at the tether disconnection. **Fig 4.1** shows that for a single heliocentric orbital motion of the centre of mass, there exists multiple opportunities of orbit change for the asteroids in the dumbbell system.

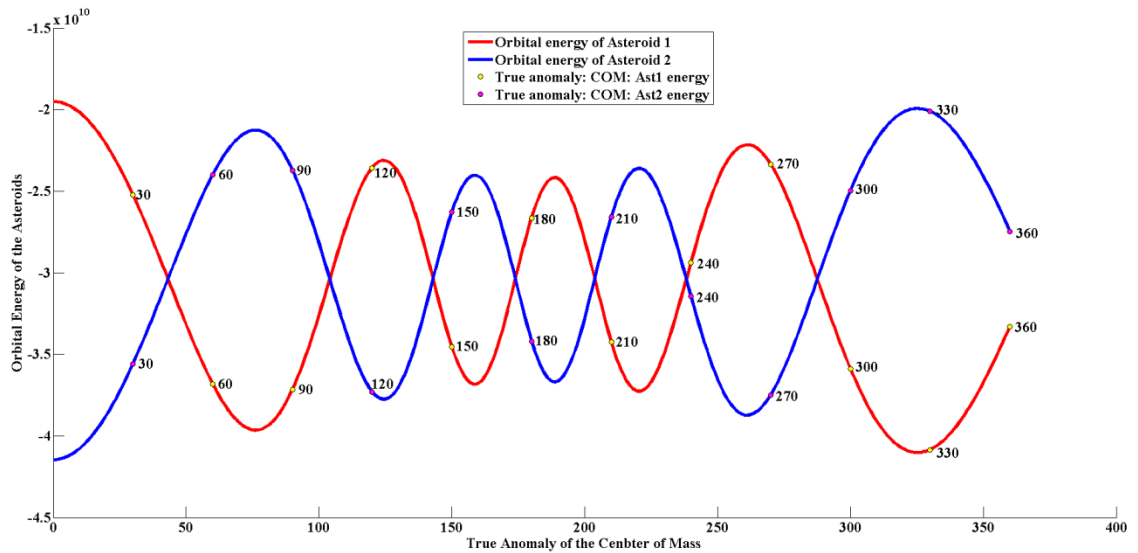


Fig 4.1 Orbital energies of the asteroids with respect to the true anomaly of the centre of mass

4.2 Wait Time

The time to wait for disconnecting the tether depends on parameters such as the achievable resulting orbit and the amount of energy distributed between each asteroid. Determining the energy values for the asteroids at tether disconnection could help in identifying the true anomaly of the centre of mass at which the tether can be disconnected. The value of the orbital energies of the asteroid and the values of the state vectors at the time of tether disconnection determine the shape, size and orientation of the resulting orbit.

Due to the complex nature of the dumbbell system, it is not common for the orbital period of the centre of mass' heliocentric motion and the rotational period of the asteroids in the dumbbell system about the centre of mass to be equal. Due to this, the values of the orbital energies of the asteroids at tether disconnection varies even for the same value of the true anomaly of the centre of mass' heliocentric motion at which the tether is disconnected, but for different number of orbits. This is explained in the flowing sections for shorter waiting time of one orbital revolution of the centre of mass' heliocentric motion and longer waiting time of multiple orbital revolutions of the centre of mass' heliocentric motion, to achieve the desirable resulting orbit with the desirable orbital energies of the asteroids.

4.2.1 Single Orbit

When a single orbit of the centre of mass is enough to cause the necessary diversion or to achieve a desired orbit, a plot like **Fig 4.1** is useful. For the same initial conditions as described for **Fig 4.1**, the resulting orbits were plotted. Plots from **Fig 4.3** to **Fig 4.14** show the resulting orbit that can be achieved with respect to different position of true anomaly of

the centre of mass at which the tether is cut. Plots with continues red and blue line represent the initial orbit, i.e. the orbit before tether connection, of Asteroid1 and Asteroid2 respectively, while plots with dashed red and blue lines represent the resulting orbits, i.e. the orbits after tether disconnection, of Asteroid1 and Asteroid2 respectively. The magenta and cyan dashed lines represent the orbit of the asteroids while in the dumbbell system. The red and blue arrow represent the orbital velocities of Asteroid1 and Asteroid2 respectively, while the magenta and cyan arrows represent the rotational velocities of the asteroids in the dumbbell system. The length of the orbital and rotational velocity vectors determines the magnitude of the respective velocity vectors. While the magnitude of the rotational velocity vectors remains constant, the magnitude of the orbital velocity vectors varies with respect to the centre of mass' true anomaly at which the tether is cut. **Fig 4.3** was plotted for a tether disconnection at the centre of mass' true anomaly value of 30 degrees and it can be seen that at this point Asteroid1 has lost some energy while Asteroid2 has gained some energy and the resulting orbit for both the asteroids are elliptic. The resulting orbit of Asteroid1 has a shorter semimajor axis compared to its semimajor axis before tether connection. And the resulting orbit of Asteroid2 has longer semimajor axis compared to its semimajor axis before tether connection, but still Asteroid1 has a longer semimajor axis than Asteroid2. **Fig 4.2** shows the legend for all the resulting plots.

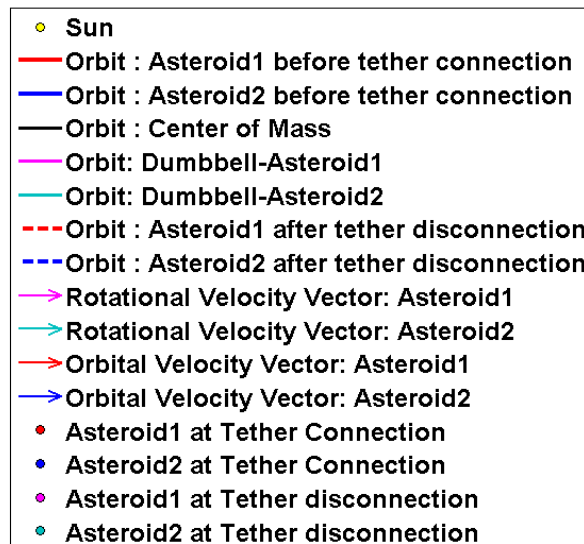


Fig 4.2 Legend for the resulting orbit plots

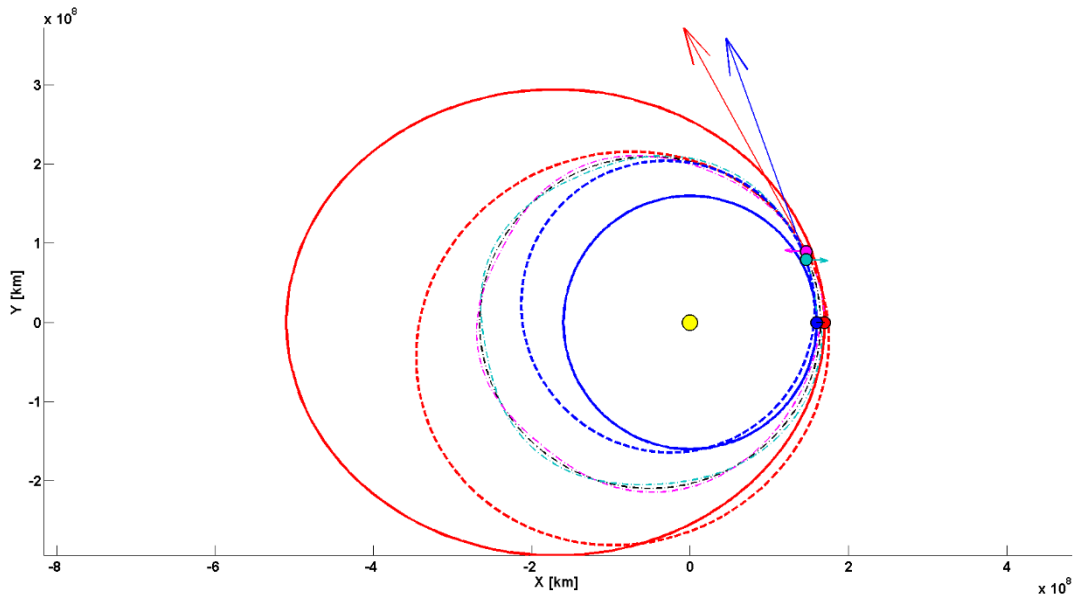


Fig 4.3 Initial, dumbbell and final orbits of the asteroids for a tether cut at true anomaly 30 degrees

Fig 4.4 was plotted for a tether disconnection at the centre of mass' true anomaly value of 60 degrees and it can be seen that, here Asteroid1 has lost a lot of energy and Asteroid2 has gained a lot of energy and the resulting orbits for both the asteroids are elliptic. The resulting orbit of Asteroid1 has a shorter semimajor axis compared to that of its respective initial orbit, while the resulting orbit of Asteroid2 has a longer semimajor axis compared to that of its respective initial orbit. But the resulting orbit of Asteroid2 has a longer semimajor axis than the resulting orbit of Asteroid1. This indicates that the Asteroid2 has gained more energy in this scenario compared to cutting the tether at 30 degrees of the centre of mass' true anomaly.

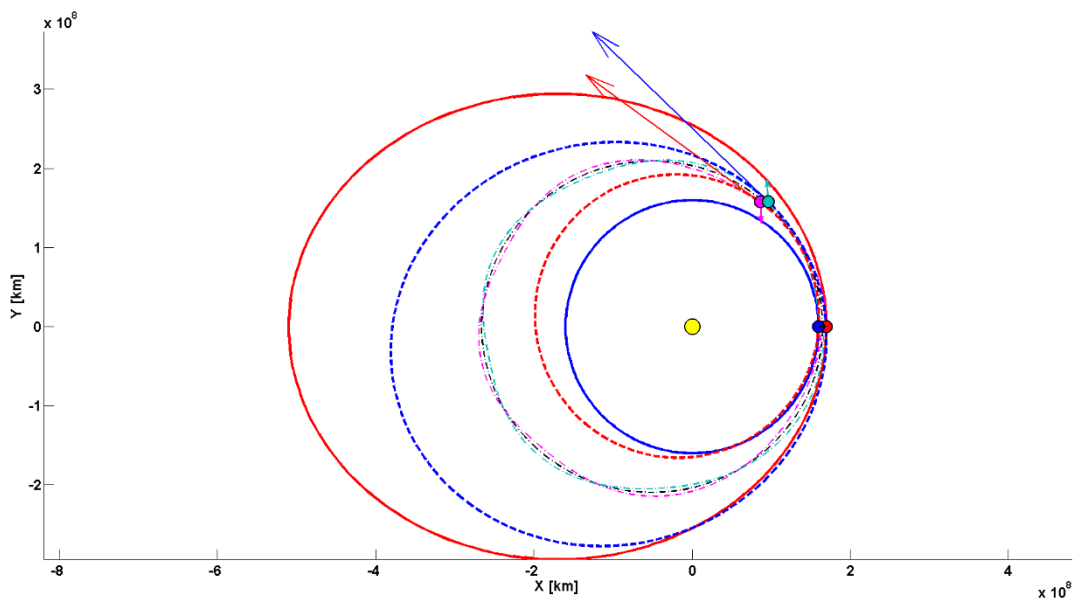


Fig 4.4 Initial, dumbbell and final orbits of the asteroids for a tether cut at true anomaly 60 degrees

Fig 4.5 was plotted for a tether disconnection at the centre of mass' true anomaly value of 90 degrees and it can be seen that Asteroid2 has gained considerably more energy compared to the tether disconnection at the centre of mass' true anomaly value of 30 and 60 degrees and also the shape of Asteroid2 is more eccentric due to the huge gain in the orbital energy at tether disconnection, while the orbit of Asteroid1 is less eccentric and more towards a circular orbit due to the considerable amount of orbital energy lost. The semimajor axis of the resulting orbit of Asteroid2 is longer than its respective initial orbit while it is vice the versa for the resulting orbit of Asteroid1.

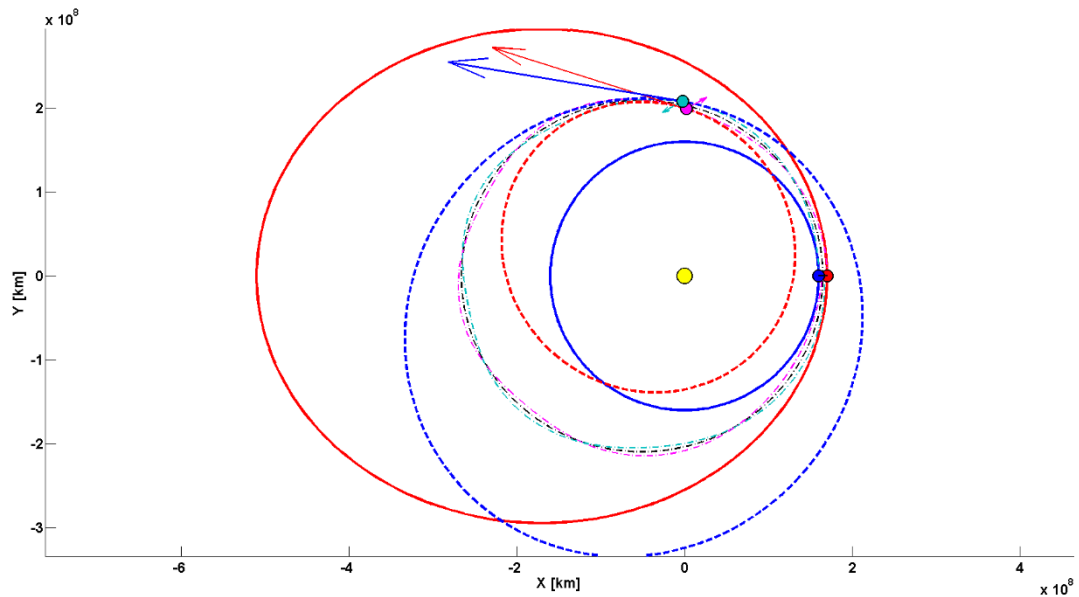


Fig 4.5 Initial, dumbbell and final orbits of the asteroids for a tether cut at true anomaly 90 degrees

Fig 4.6 was plotted for a tether disconnection at the centre of mass' true anomaly value of 120 degrees and here it can be seen that the resulting orbits looks similar to that of the resulting orbits in **Fig 4.5** when the tether was cut at the centre of mass' true anomaly value of 90 degrees, but the only change is that size and shape of the resulting orbits of Asteroid1 and Asteroid2 has interchanged. Within a span of 30 degrees of true anomaly the centre of mass has orbited from its previous position of 90 degrees, a complete reversal in orbital formation has occurred. This can be attributed to the orientation of the tether, which leads to the position of the asteroid with respect to the Sun, at the time of tether connection. The change in the orbital energy between the centre of mass' true anomaly value of 90 degrees and 120 degrees is not considerable, but the change in the orbital velocity vector is, both in magnitude and direction, as can be noted in the respective plots of **Fig 4.5** and **Fig 4.6**. The orbital velocity of Asteroid1 was lesser in magnitude, as shown by its shorter length and the orbital velocity of Asteroid2 is greater in magnitude, as shown by the its longer length in **Fig 4.5**, While it was vice the versa in **Fig 4.6**. This shows the significance played by the direction and magnitude of the orbital velocity vectors.

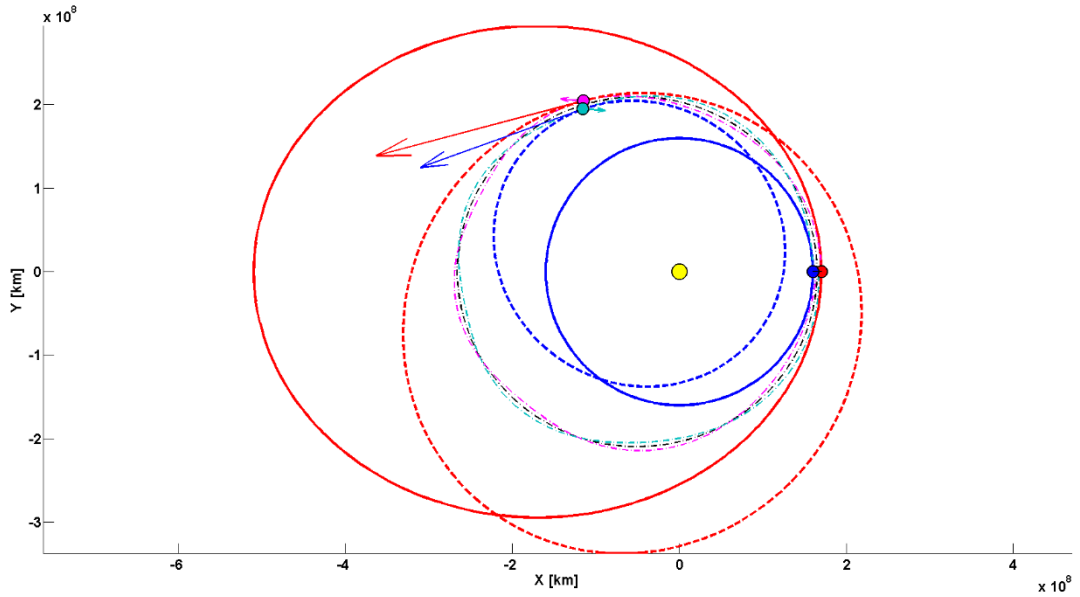


Fig 4.6 Initial, dumbbell and final orbits of the asteroids for a tether cut at true anomaly 120 degrees

Fig 4.7, Fig 4.8 and Fig 4.9 was plotted for a tether disconnection at the centre of mass' true anomaly value of 150, 180 and 210 degrees respectively and follows similar and alternative changes to the resulting orbits as that of tether cut at centre of mass' true anomaly values of 120. The slight variation in the orbits is due to the expected variation in its orbital energy and orbital velocity vectors.

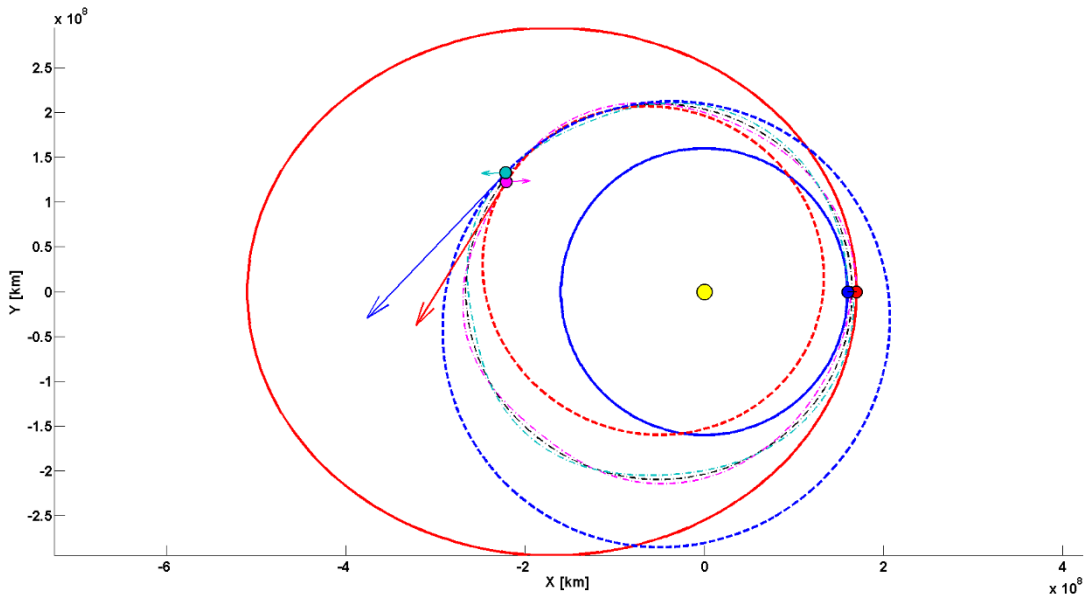


Fig 4.7 Initial, dumbbell and final orbits of the asteroids for a tether cut at true anomaly 150 degrees

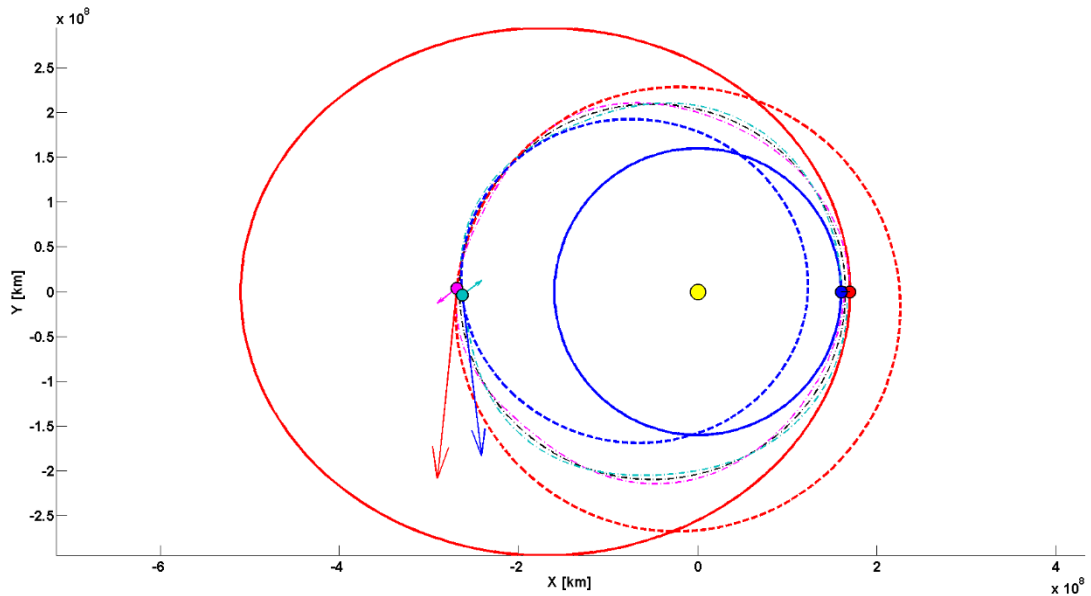


Fig 4.8 Initial, dumbbell and final orbits of the asteroids for a tether cut at true anomaly 180 degrees

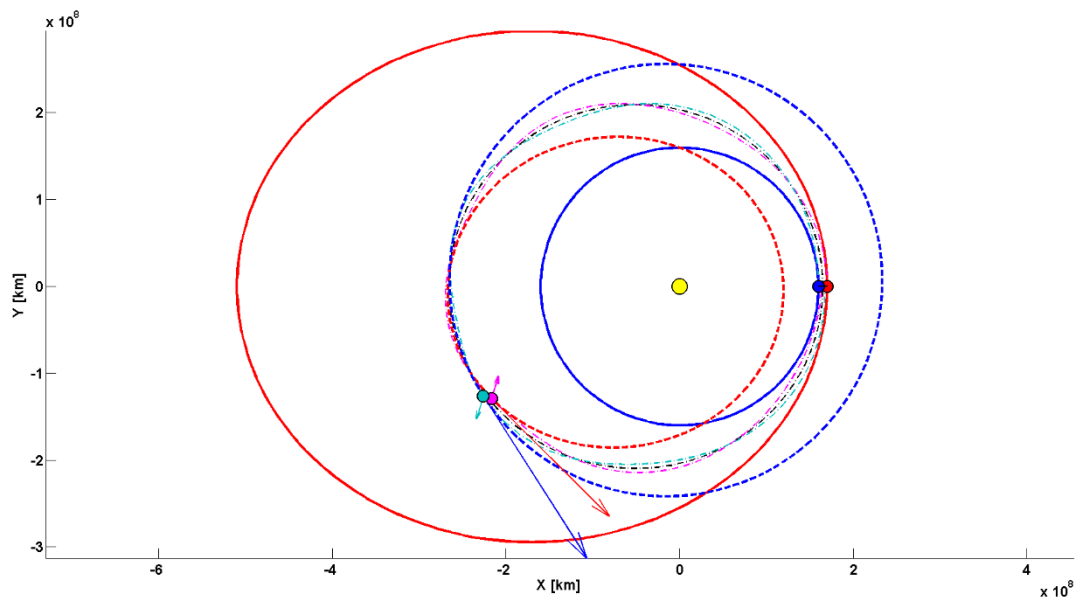


Fig 4.9 Initial, dumbbell and final orbits of the asteroids for a tether cut at true anomaly 210 degrees

Fig 4.10 was plotted for a tether disconnection at the centre of mass' true anomaly value of 240 degrees and shows a considerable reduction in the value of the semimajor axis of Asteroid1's orbit after tether disconnection, compared to the value of the semimajor axis before tether connection. The semimajor axis of the resulting orbit of Asteroid2 is longer than the semimajor axis of the orbit of Asteroid2 before tether connection. This follows a similar trend like that of the orbits of the asteroids after tether cut at true anomalies of 30, 60, 90, 120, 150, 180, 210, except that here, the shape and position of the orbit has shifted to the right of x-axis of the plot, which indicates the part played by the direction of the velocity vectors. The resulting orbits of both the asteroids are closer to each other and have

near similar orbits, along with near similar values of the magnitude of the orbital velocity vectors. This indicates that the orbital energies at tether disconnection were closer to equal for both the asteroids.

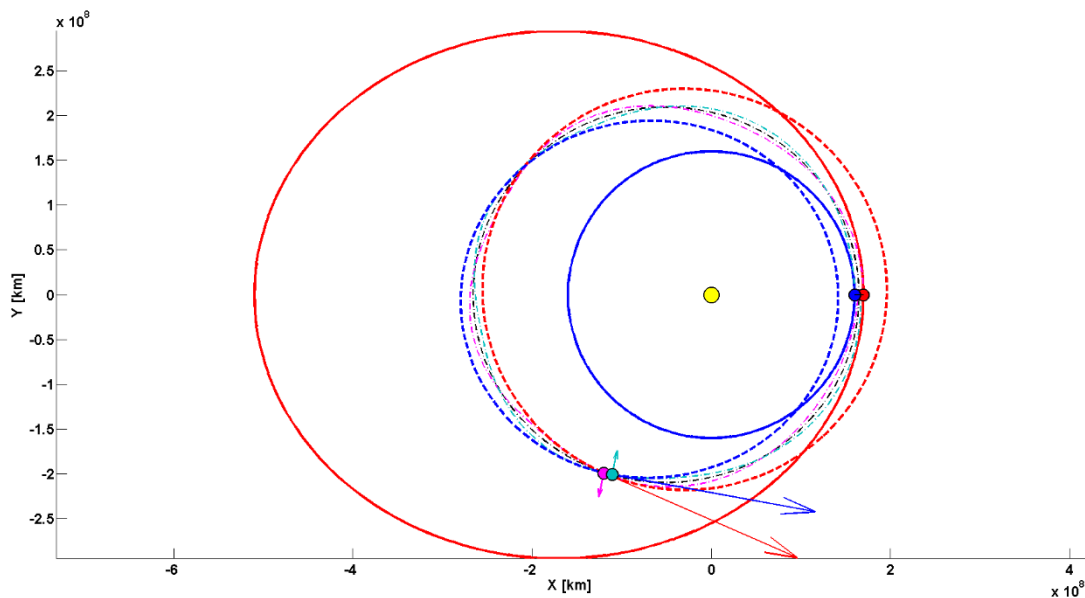


Fig 4.10 Initial, dumbbell and final orbits of the asteroids for a tether cut at true anomaly 240 degrees
Fig 4.11 and **Fig 4.12** are plotted for a tether disconnection at the centre of mass' true anomaly value of 270 and 300 degrees respectively and are similar, but with an interchange in one asteroid taking the orbit of the other. This is another case where the energy transfer is similar between these two scenarios, but for the orientation of the tether and the position of the asteroids with respect to the Sun

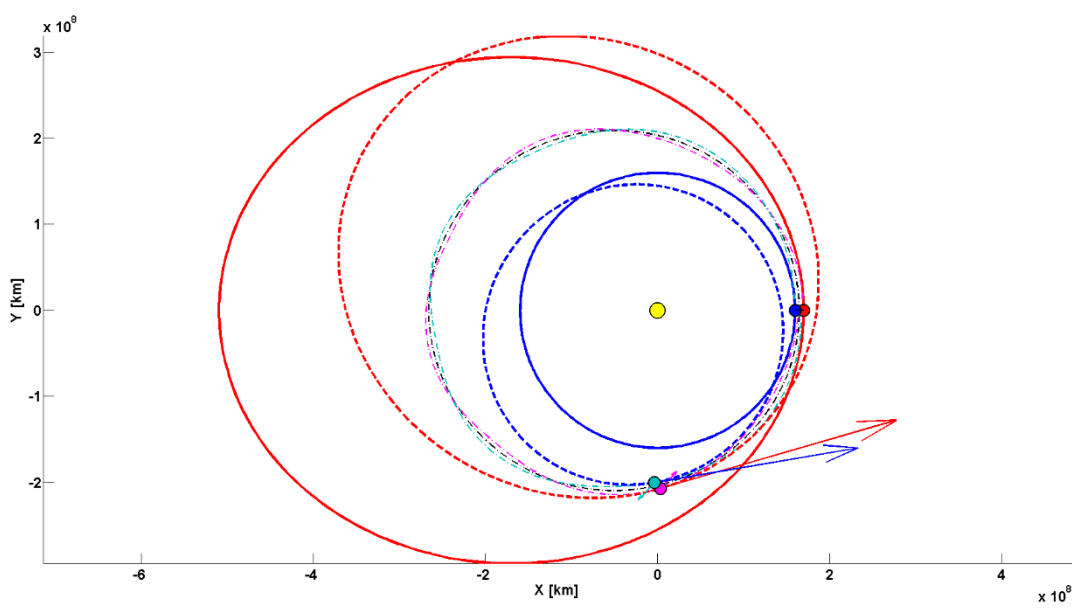


Fig 4.11 Initial, dumbbell and final orbits of the asteroids for a tether cut at true anomaly 270 degrees

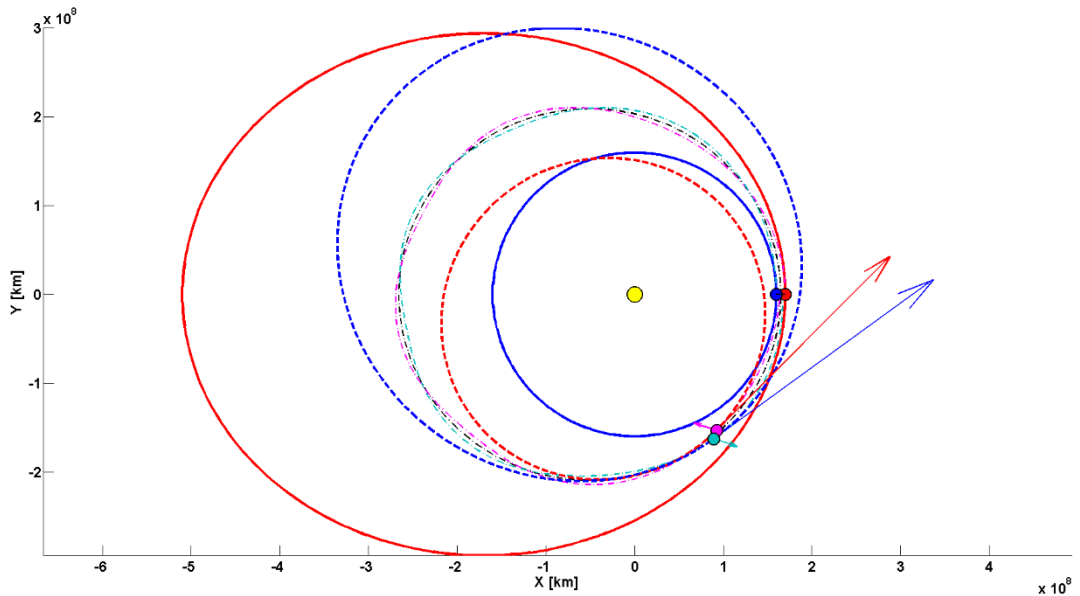


Fig 4.12 Initial, dumbbell and final orbits of the asteroids for a tether cut at true anomaly 300 degrees

Finally, **Fig 4.13** shows a scenario where Asteroid2's resulting orbit takes the place of Asteroid1's initial orbit and Asteroid1's resulting orbit takes the place of Asteroid2's initial orbit. This is the scenario where the orbital energies of Asteroid1 and Asteroid2 are interchanged. The orbits are not exactly an interchange, but this could be due to the errors discussed in the previous section.

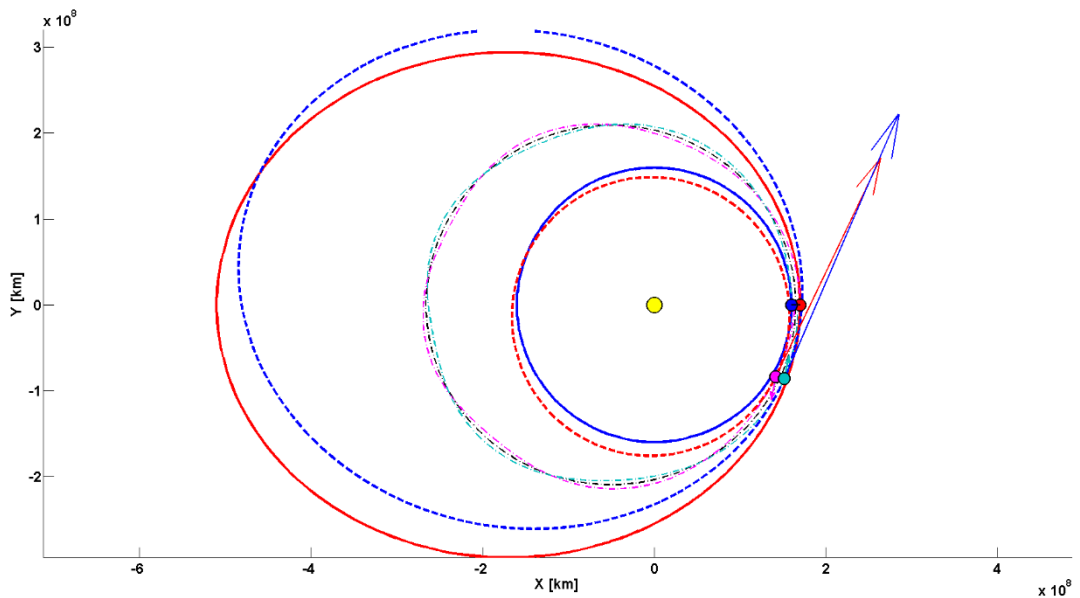


Fig 4.13 Initial, dumbbell and final orbits of the asteroids for a tether cut at true anomaly 330 degrees

Fig 4.14 was plotted for a tether disconnection at the centre of mass' true anomaly value of 360 degrees and shows that it is similar to that of the scenario where the tether was at the centre of mass' true anomaly value of 30 degrees. Here the true anomaly of the centre of mass also indicates the position of 0 degrees, but as discussed before the chances that the

rotational period of the asteroid with respect to the centre of mass being equal to the orbital period of the centre of mass' heliocentric orbit is very and this case shows it clearly. The asteroids are in a different orientation than at the time of tether connection, which is also the reason for the nature of the resulting orbits.

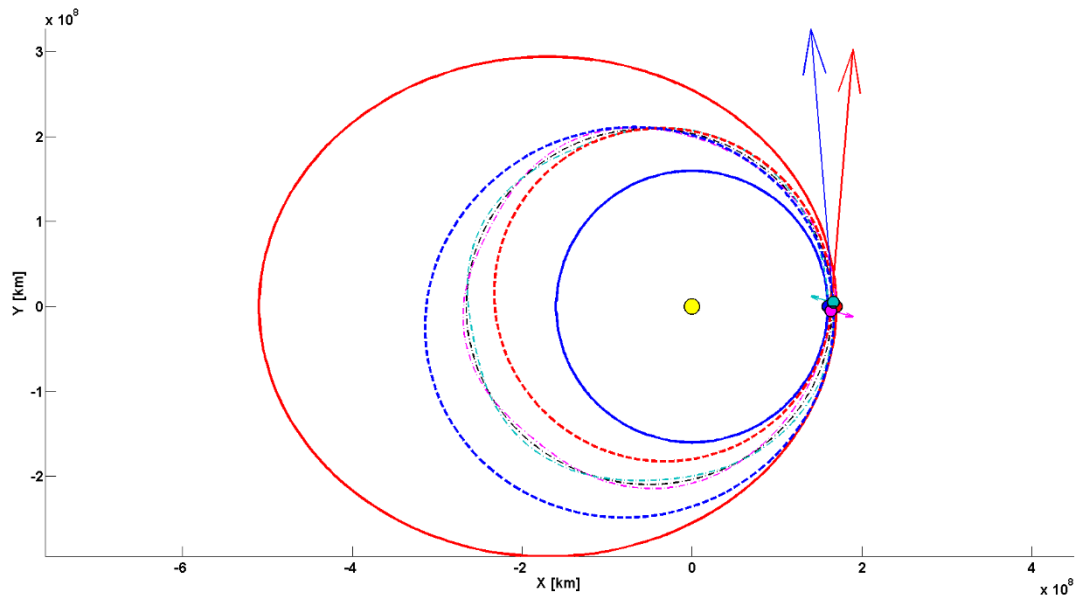


Fig 4.14 Initial, dumbbell and final orbits of the asteroids for a tether cut at true anomaly 360 degrees

In all these scenarios of resultant orbits involving tether disconnection, it can be noticed that Asteroid2 never lost energy and Asteroid1 never gained energy. This could be due to the assumption that at the time of tether connection, the asteroids are at their perihelion and also the fact that Asteroid1 is in an eccentric orbit and farther away from the Sun than Asteroid2 which is in a circular orbit and closer to the Sun, at the tether connection.

4.2.2 Multiple Orbits

Sometimes the required orbital energy for a desirable diversion of an asteroid cannot be achieved in a single heliocentric orbit of the centre of mass. Waiting for multiple orbital revolutions of the centre of mass in a heliocentric orbit for orbital diversion could usually be used for cases where diverting hazardous asteroids away from earth is involved, especially when the threat is identified early enough to achieve the waiting time. To understand the orbital energies obtained over multiple orbital revolutions of the centre of mass' heliocentric motion a sample test case carried out with the following initial conditions were tested:

1. The eccentricity of the Asteroid1, was varied from 0 to 0.9 at a step interval of 10^{-5} ($e_1 = \{0, 0.0001, 0.0002, \dots, 0.9\}$)
2. The eccentricity of Asteroid2, was fixed to be zero ($e_2 = 0$)

3. The radius of perihelion of both the asteroids was fixed at $r_{p,1} = 17 \times 10^7$ km and $r_{p,2} = 16 \times 10^7$ km respectively
4. The value of the rest of the orbital elements were,
 - a. Argument of periapsis, $\omega_1, \omega_2 = 0$
 - b. Longitude of ascending node $\Omega_1, \Omega_2 = 0$
 - c. Initial true anomaly $\theta_1, \theta_2 = 0$

For initial analysis, only the orbital energy of Asteroid1 was observed, and hence only the orbital energy of Asteroid1 was plotted against the angular displacement (the orientation of the tether) of the tether the dumbbell system makes with the x-axis of the reference frame *Ref B* at the time of tether disconnection.

In **Fig 4.18**, **Fig 4.19**, **Fig 4.20** and **Fig 4.21** the orbital energy of Asteroid1 is represented at the y-axis of the plot, while the angular displacement of the dumbbell system is represented at the x-axis of the plot.

The simulation for the change in each value of Asteroid1's eccentricity for the said range was carried out; wherein a limit was set for the maximum number of times the dumbbell system rotates around the centre of mass for one orbit of the centre of mass' motion around the Sun, which was fixed to be 100

This value was identified and fixed by running multiple analyses to understand the highest value of energy an asteroid could attain, on the basis of the orientation of the tether and the position in the orbit at the time of tether disconnection.

The number of times the dumbbell system rotated around the centre of mass during the course of one orbital revolution of the centre of mass is affected by the angular velocity of the dumbbell system. The determination of this angular velocity depends on the initial orbital velocity of the asteroids at the time of tether connection, which in turn depends on the eccentricity of the orbit of these asteroids before and at the time of tether connection. At this point in time we should also remember that the tether connection between the asteroids is made instantaneously when the asteroids lay in-line with the Sun in the ecliptic plane and at the perihelion point. Here, the orbital velocity of Asteroid1 is the highest with respect to its initial orbit while the orbital velocity of Asteroid2 is the same at all point in its orbit around the Sun, as its eccentricity is fixed to be zero, and hence in a circular orbit.

Fig 4.15 (**Fig 4.16** is zoom of **Fig 4.15** at the point of tether connection) is a simple representation of one of the case of the orbit of two asteroids at perihelion at tether connection, the plot shows the velocity vectors of each asteroids at that point. The length of

the velocity vectors directly corresponds to the magnitude of the orbital velocity vector and here it can be shown that the magnitude of the orbital velocity vector of the highly eccentric orbit is higher than the magnitude of the orbital velocity vector of the circular orbit.

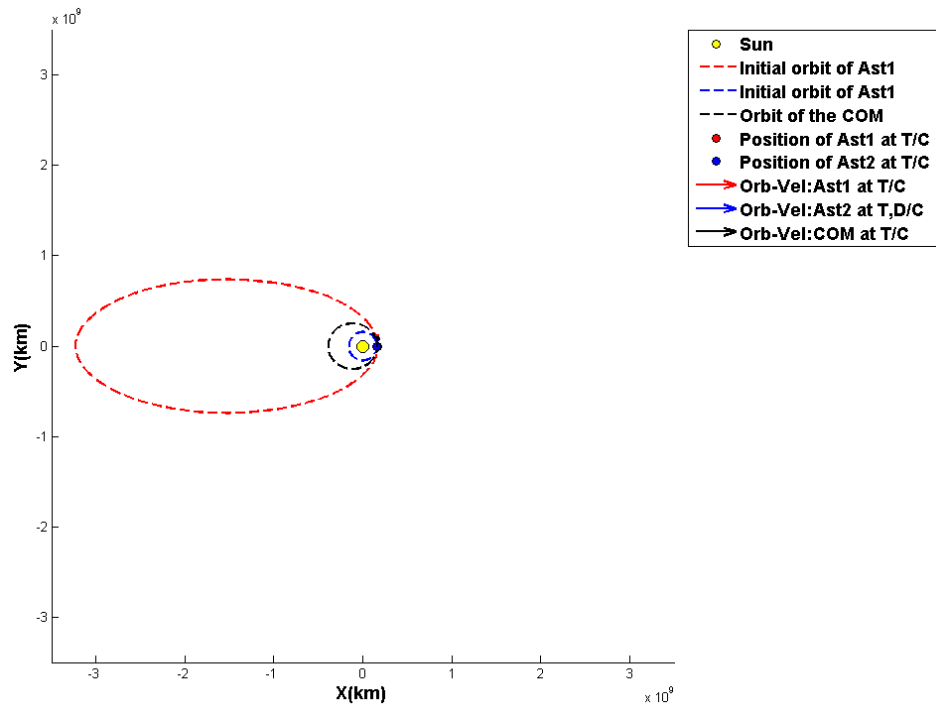


Fig 4.15 Initial orbit plots for the test case

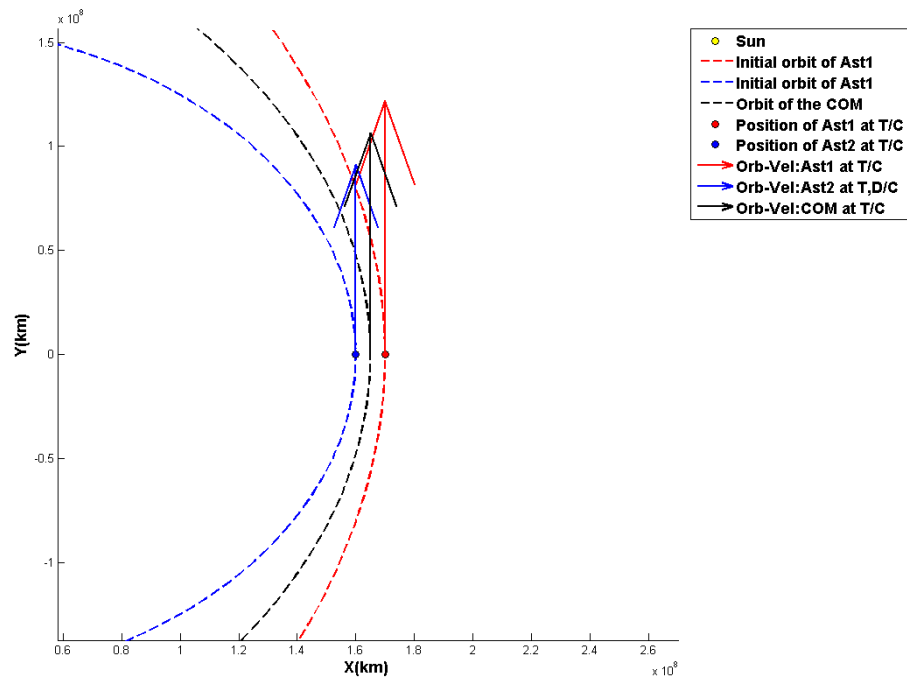


Fig 4.16 zoomed view of Fig 4.15

General Observations

A series of plots were obtained (some of which are shown in **Fig 4.18**, **Fig 4.19**, **Fig 4.20** and **Fig 4.21**) for a range of values of eccentricity of Asteroid1. So that the variation of the orbital energy attained with respect to the orientation of the tether at the time of the tether disconnection, for each value of eccentricity could be observed and understood. Approximately 6000 plots were obtained and keeping in mind the size restriction of the thesis, only a few of the important ones are discussed. Nevertheless, the general observations made from analysing all the plots are mentioned as follows:

1. Variations in the rate at which the dumbbell system rotates for a corresponding number of heliocentric orbital revolutions of the centre of mass for the analysed eccentricity range were observed. The variations observed for the different eccentricity ranges are as follows:
 - a. The rate at which the dumbbell system rotates around the centre of mass decreases from one full rotation for two complete orbits of the heliocentric motion of the centre of mass at an eccentricity of $e_1 = 0$, to one full rotation of the dumbbell system for approximately two thousand complete orbits of the heliocentric motion of the centre of mass at an eccentricity of $e_1 = 0.0625$
 - b. After which it returns to one full rotation of the dumbbell system for two complete orbits of the heliocentric motion of the centre of mass at an eccentricity of $e_1 = 0.1212$,
 - c. Then keeps increasing until approximately twelve complete revolutions of the dumbbell system for approximately one heliocentric orbit of the centre of mass at an eccentricity $e_1 = 0.9$
2. The variation of energy depends on the initial energy possessed by the asteroid at the time of tether connection, and in this case, the energy input to the system keeps increasing throughout, since the velocity at tether connection which is the point of perihelion keeps increasing, which as explained earlier is due to the increasing eccentricity of the orbit
3. The orbital energy of the asteroids varies more unevenly at the lower eccentricities and gets more even and periodic as the value of the eccentricity of Asteroid1 increases
4. For every, one heliocentric orbit of the centre of mass, there exists a maximum and minimum orbital energy that could be attained after tether disconnection.

This value of maximum and minimum energy need not necessarily be equal for the next orbit

5. During the course of the analysis it is found that there is an overall maximum and minimum energy that could be attained by Asteroid1, which is also true for Asteroid2, after tether disconnection. To achieve this overall maximum and minimum orbital energy, the time of tether disconnection has to be determined based on the number of the times the centre of mass orbits around the Sun

Specific Observations

Four eccentricities, namely $e_1 = 0$; $e_1 = 0.0017$; $e_1 = 0.0623$; and $e_1 = 0.9$ are discussed here to understand the behaviour in the energy variations of Asteroid1 in the dumbbell system. Eccentricities $e_1 = 0$; and $e_1 = 0.9$ are chosen because they represent the start and end points of the analysed range of eccentricities. Eccentricities $e_1 = 0.0017$; and $e_1 = 0.0623$ are chosen because of the noticeable change in the occurrence of the maximum and minimum energy in a different way compared to other observed eccentricities.

The blue lines in **Fig 4.18**, **Fig 4.19**, **Fig 4.20** and **Fig 4.21** represent the orbital energy values of Asteroid1 plotted against the angular displacement of the tether. The yellow and green circle markers represent the maximum and minimum energies of Asteroid1 respectively for each of the individual orbits. The red and black asterisks represent a true anomaly of $\theta = 0$ and $\theta = 180$ of the heliocentric orbit of the centre of mass respectively.

Cycles and Repeating Blocks

Local definitions, namely cycle and repeating blocks, are defined for each of the cases studied, and their definition vary with respect to their behavioural dynamics. In general, the definition of cycle is used to define the overall pattern of the case studied, the definition of repeating blocks is used to define repetitive nature of the orbital energy variations within the cycle.

Eccentricity of Asteroid1 at 0

The dumbbell system represented in **Fig 4.18** is such that the asteroids have equal mass and zero eccentricity.

$$m_1 = m_2 = 10^8 \text{ kg}$$

$$e_1 = e_2 = 0$$

Cycles and Repeating Blocks

The number of orbital revolutions of the heliocentric motion of the centre of mass for this scenario was fixed at 400 to show the periodic nature of the pattern of energy occurrence, as after every 400 heliocentric orbital revolution of the centre of mass, the pattern of energy variations repeats. This periodicity for every 400 orbits is defined as a cycle for this case.

Maximum and Minimum Orbital Energies

The plot is split into expansion zones such as **Fig 4.18a** and **Fig 4.18b** apart from the main plot. Expansion **Fig 4.18a** shows the orbital energy values between $\Theta = 2.4 \times 10^4$ and $\Theta = 3 \times 10^4$ degrees of angular displacement of the orientation of the tether and expansion. **Fig 4.18b** shows the orbital energy values between $\Theta = 2.71 \times 10^4$ and $\Theta = 2.79 \times 10^4$ degrees of angular displacement of the orientation of the tether.

This is to show the variations in the obtained energies and to observe the occurrence of maximum and minimum energies for each orbit with respect to the perihelion and aphelion position. The red and blue triangle represent the occurrence of the overall maximum and minimum orbital energies of the orbit of Asteroid1 respectively with each cycle.

It can be observed that in **Fig 4.18** the occurrence of the overall maximum and minimum orbital energy for the cycle occurs approximately at the midpoint of the cycle, showing that the maximum and minimum energies varies gradually between $\Theta = 0$ and $\Theta = 8 \times 10^4$ degrees of angular displacement. Here, $\Theta = 8 \times 10^4$ degrees indicate the number of 360-degree tether rotations the dumbbell system has had in the cycle.

Initially, the value of maximum energy for each individual orbit keeps increasing until about approximately $\Theta = 4 \times 10^4$ degrees of angular displacement, where it reaches the maximum orbit for the cycle and then it gradually reduces until about $\Theta = 7.8 \times 10^4$ degrees of angular displacement of the tether after which a new cycle starts.

It can also be noticed that there is an alternating pattern of maximum and minimum energies for every alternate orbit, with even numbered orbits having a higher local maximum energy value and higher minimum energy value than odd numbered orbits, this can be evident from the different directions taken by two lines of yellow markers.

The line that goes up is for even number of orbits and the line that goes down is for odd number orbits. This alteration is due to the change in the orientation of the asteroids with respect to the Sun at every orbit. Initially at tether connection the position is aligned with the Sun, but after every orbit the orientation of the asteroids changes and is no longer aligned with the Sun when the centre of mass reaches the perihelion point in the next orbit.

It can be noted that the maximum and minimum orbital energy for odd orbits starts occurring at the perihelion point at about $\Theta = 2.8 \times 10^4$ degrees of angular displacement and it continues up until the next cycle, this is shown clearly in expansion **Fig 4.18a** and **Fig 4.18b**.

In expansion **Fig 4.18b**, the convergence is shown in comparison of the previous alternate odd and even orbit. This indicates that at each point of maximum orbital energy in the odd orbits the asteroids are closer to the sun in terms of its orientation of the tether and the true anomaly of the centre of mass and when the closest point coincides with the perihelion of the centre of mass the maximum energies of that particular orbit coincides with the true anomaly of the centre of mass at perihelion.

The achievement of the maximum and minimum energy for the orbit is very useful in terms of waiting for the opportune moment to cut the tether, so as to achieve the required deflection in the orbital trajectory of the asteroid in focus.

For eccentricity $e_1 = 0$ the occurrence of maximum energy happens in alternate orbits, thereby making it necessary to wait for every two orbits to achieve maximum or minimum deflection. Also, the overall maximum and minimum energy obtained is higher and lower respectively to the maximum and minimum energy of all other orbit. **Fig 4.18** also shows that the motion is periodic for every 204 dumbbell rotations.

-
- Energy of Asteroid 1
 - ▲ Overall Max Orbital Energy
 - ▲ Overall Min Orbital Energy
 - Max Orbital Energy for the cycle
 - Min Orbital Energy for the cycle
 - True Anomaly = 0
 - True Anomaly = 180

Fig 4.17 Legends for Fig 4.18, Fig 4.19, Fig 4.20 and Fig 4.21

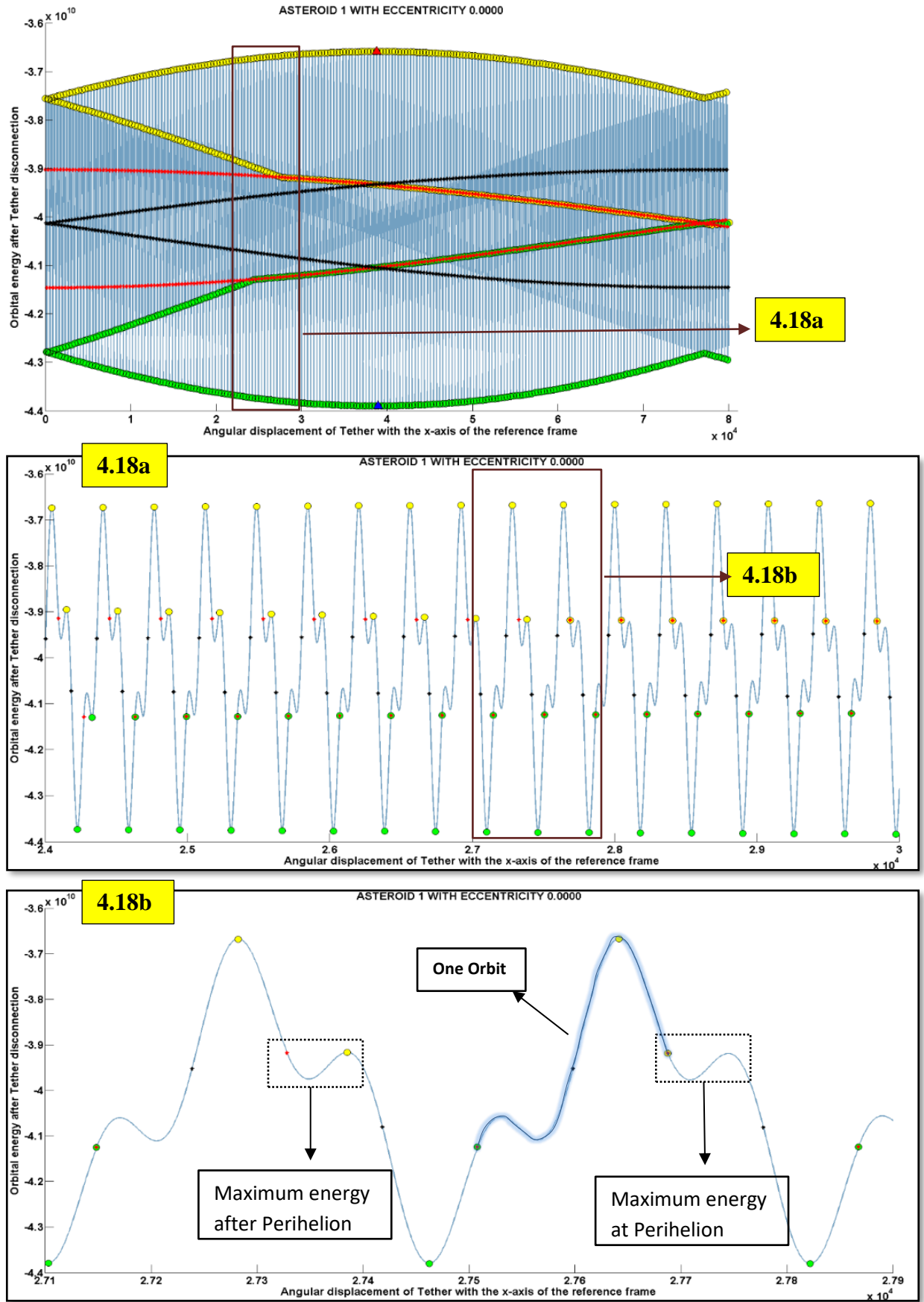


Fig 4.18 Energy variation of Asteroid1 against angular displacement of the tether for an eccentricity value of 0

Eccentricity of Asteroid1 at 0.0017

The dumbbell system represented in **Fig 4.19** is such that the asteroids have equal mass and Asteroid1 is in an orbit with an eccentricity of $e_1 = 0.0017$.

$$m_1 = m_2 = 10^8 \text{ kg}$$

$$e_1 = 0$$

$$e_1 = 0.0017$$

The dumbbell system makes approximately one dumbbell revolution for two orbital revolutions of the centre of mass' heliocentric motion.

Cycles and Repeating Blocks

The number of orbital revolution of the centre of mass' heliocentric motion was fixed at 154, which is defined as one orbit cycle in this case, to study the periodicity in the occurrence of the value of the orbital energy.

It can be noticed that the overall maximum energy occurs early in the cycle and the overall minimum energy occurs later in the cycle. This value of overall maximum and minimum orbital energy is actually one of the maximum energy of a repeating block. Here a repeating block can be defined as a block containing 20 consecutive orbits.

The block contains alternating pattern of orbital energy, where every odd orbit has less maximum energy than every even orbit and the maximum energy in odd orbits intersect with the perihelion point of the centre of mass between the 9th and 35th orbit spanning two repeating blocks, while the minimum energy point for every even orbit intersects with the perihelion point of the centre of mass between 8th and 34th orbit. This case is an example of the asteroids in the dumbbell system returning to the initial orientation when the centre of mass passes through the perihelion point for every 20 orbits.

Maximum and Minimum Orbital Energies

Cases like this lead to the overall maximum and minimum orbital energy to be periodic and of similar values, which could lead to a shorter wait time if the tether needs to be cut at the overall maximum or overall minimum orbital energy the asteroid could make with a considerable period of wait time at the least.

Eccentricity of Asteroid1 at 0.0623

The dumbbell system represented in **Fig 4.20** is such that the asteroids have equal mass and Asteroid1 is in an orbit with an eccentricity of 0.0623.

$$m_1 = m_2 = 10^8 \text{ kg}$$

$$e_1 = 0$$

$$e_1 = 0.0623$$

Cycles and Repeating Blocks

In this case, one revolution of the dumbbell system leads to 527 heliocentric orbital motion of the centre of mass and this is due to the fact that the angular velocity of the dumbbell system is slower compared to other cases.

Here one cycle is defined by one dumbbell revolution, in which there are 189,720 heliocentric orbits of the centre of mass.

Maximum and Minimum Orbital Energy

The maximum orbital energy for individual orbit coincides with the point of perihelion at the start and end of the cycle, after which the perihelion point deviates, and the maximum orbital energy coincides with the aphelion of the centre of mass at 180 degree of angular displacement of the tether. Similarly, the minimum orbital energy for an orbit coincides with the aphelion of the centre of mass at the start and end of the cycle, after which the aphelion deviates, while the minimum energy of the orbit coincides with the perihelion of the centre of mass at 180 degree of the angular displacement of the tether.

To wait for the maximum energy for tether connection, this case needs less wait time. Most of the orbits in this case have similar maximum and minimum orbital energy values because the rate at which the orientation of the tether changes with respect to the change in the true anomaly of the centre of mass is very less.

Eccentricity of Asteroid1 at 0.9

The dumbbell system represented in **Fig 4.21** is such that the asteroids have equal mass and Asteroid1 is in an orbit with an eccentricity of 0.9.

$$m_1 = m_2 = 10^8 \text{ kg}$$

$$e_1 = 0$$

$$e_1 = 0.0623$$

Because of the huge difference in the eccentricity of the orbits of Asteroid1 and Asteroid2, the angular velocity in this case is very high, which leads to multiple dumbbell revolution for one heliocentric orbital motion of the centre of mass. For one heliocentric orbit of the centre of mass, the dumbbell system rotates around 12.5 times about the centre of mass. This is in contrast to the cases in **Fig 4.18**, **Fig 4.19** and **Fig 4.20**, where the number of dumbbell rotation about its centre of mass was slower than the motion of the centre of mass of the dumbbell system around the Sun. This is due to the very high eccentricity of Asteroid1, which leads to higher orbital velocities and hence higher angular velocities leading to the faster rotational motion of the dumbbell system about the centre of mass.

Cycles and Repeating Blocks

Here one cycle is defined as 7 heliocentric orbits of the centre of mass and one repeating block is defined with 4,500 degrees of angular displacement of the tether, which is 12.5 times the rotation of the dumbbell system.

Maximum and Minimum Orbital Energies

From **Fig 4.21**, it can be observed that the occurrence of maximum and minimum orbital energies of the cycles is not strictly regular, although we can consider it to be approximately or close to regular. But, with every single orbit, there are at least one occurrences each of maximum and minimum orbital energies that has a closer value to the overall maximum and minimum orbital energies for the cycle. The maximum and minimum orbital energies appear to be alternating in their occurrence close to periapsis and never near apoapsis. While the value of the overall maximum and minimum orbital energy and value of the maximum and minimum energy for each orbit is not much different, the change is negligible. This shows that the opportunity for tether disconnection for a desired orbit with corresponding orbital energy occurs repeatedly over a short period of time compared to the other cases observed earlier and hence contributes to shorter wait time.

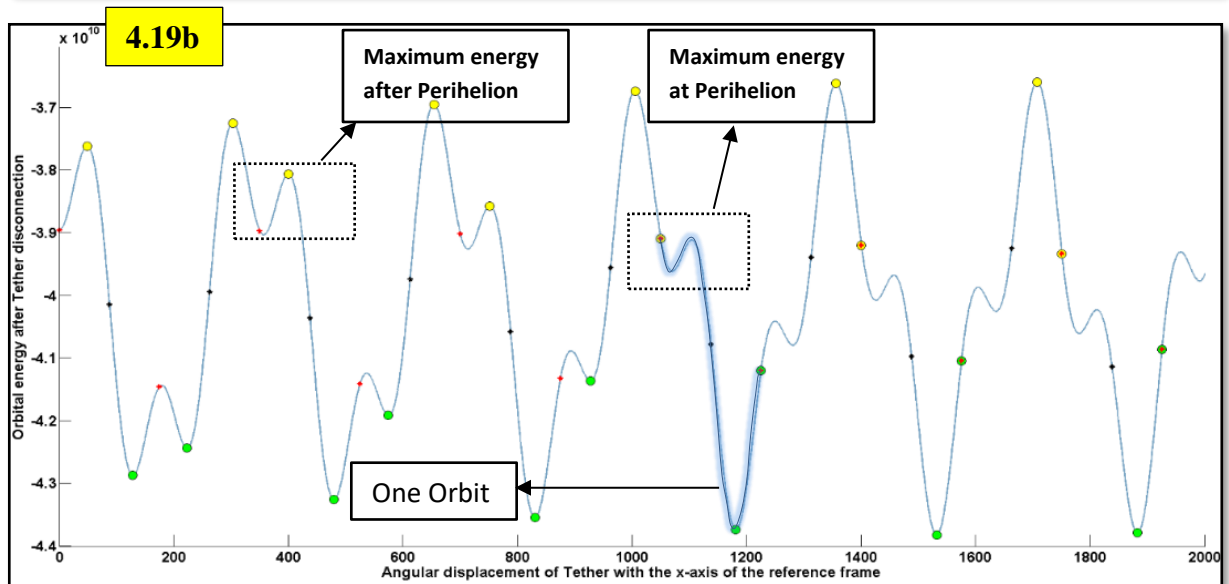
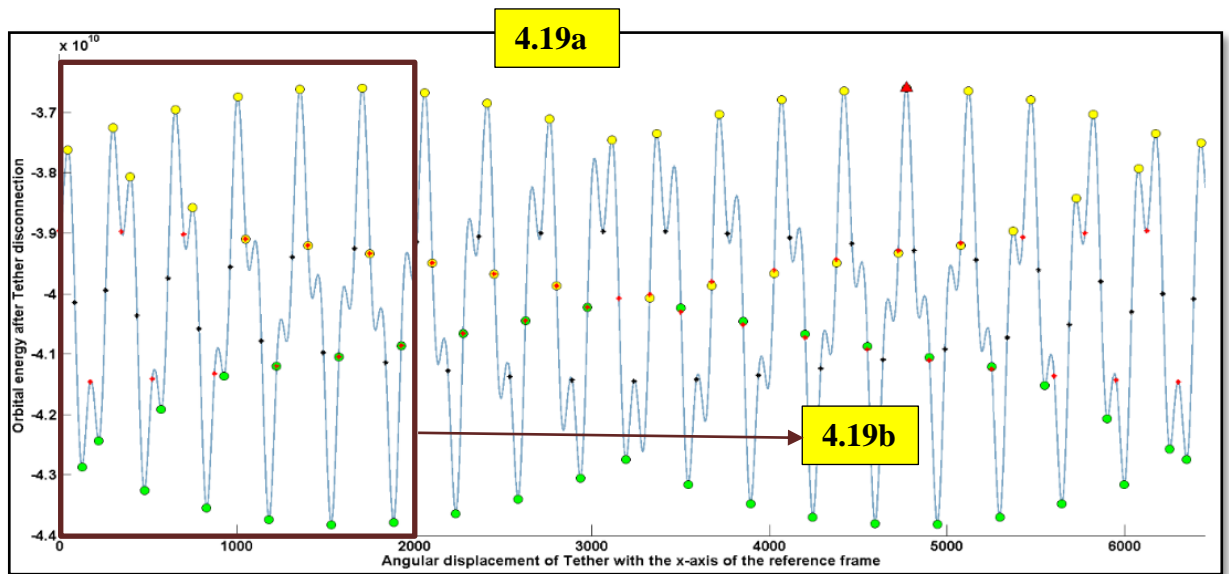
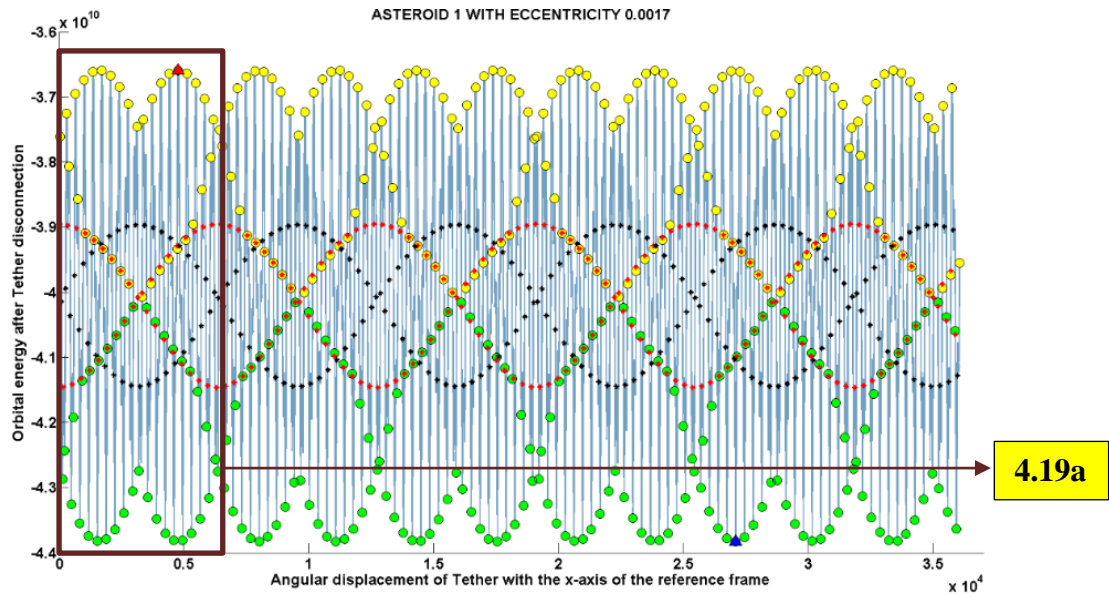


Fig 4.19 Energy variation of Asteroid1 against the angular displacement of the tether for an eccentricity value of 0.0017

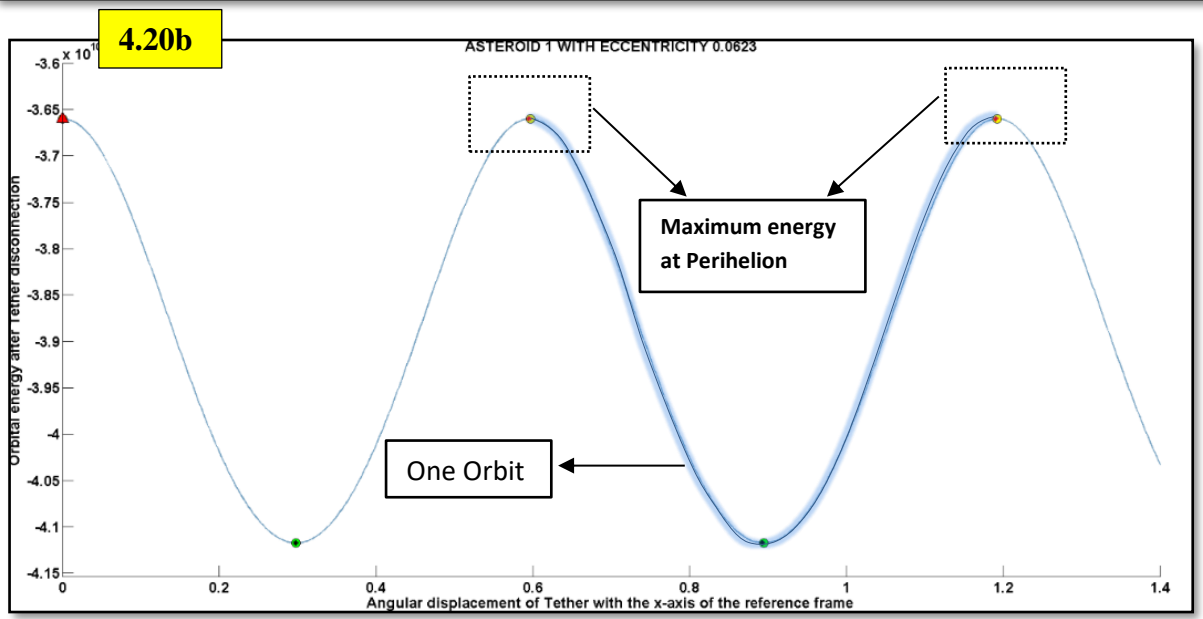
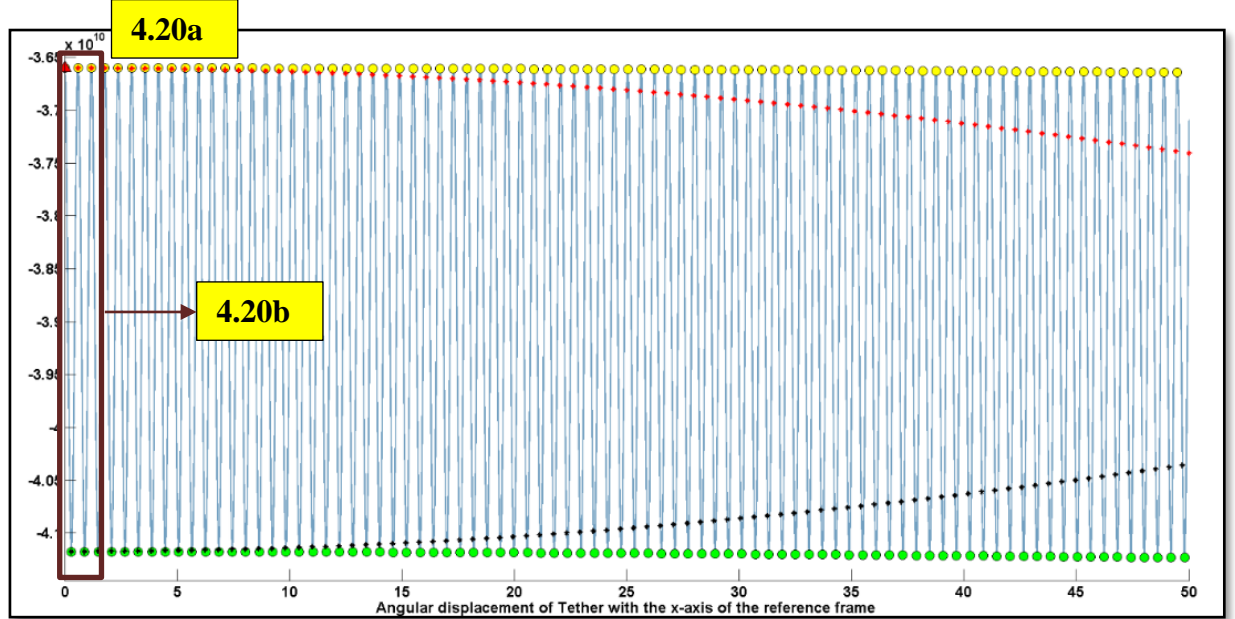
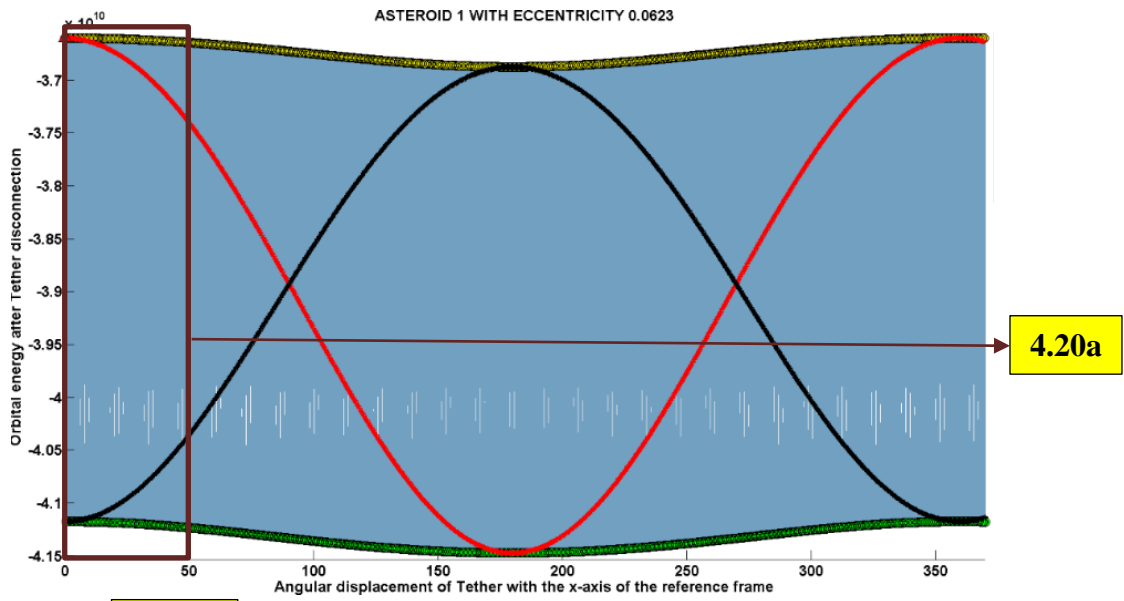


Fig 4.20 Energy variation of Asteroid1 against the angular displacement of the tether for an eccentricity value of 0.0623

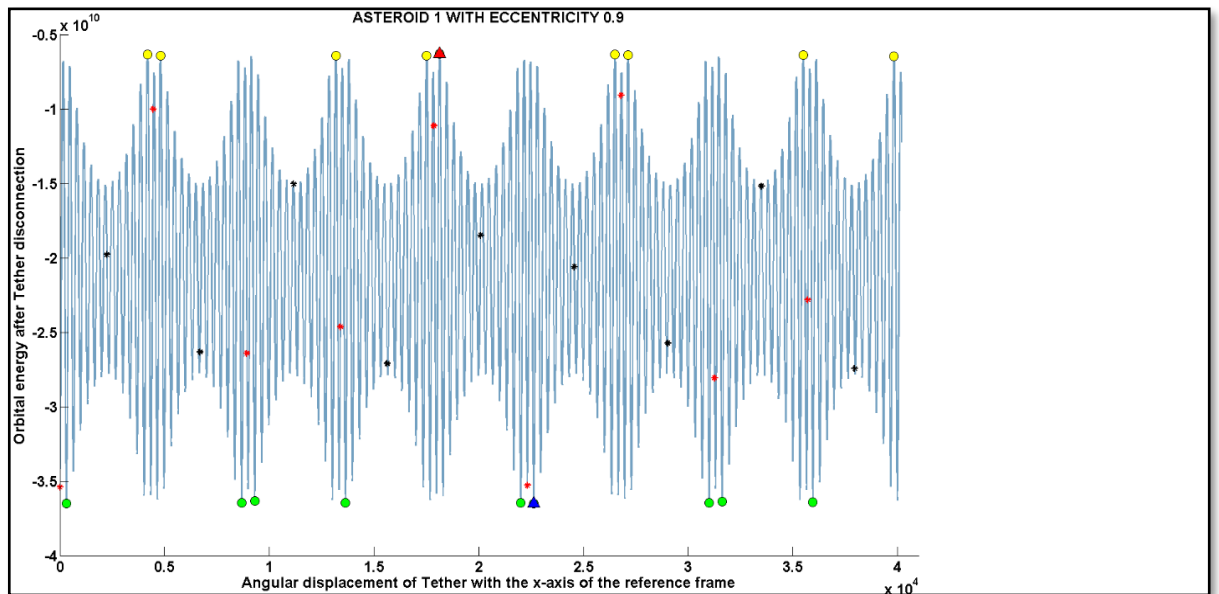


Fig 4.21 Energy variation of Asteroid1 against the angular displacement of the tether for an eccentricity value of 0.9

The values and data in the above cases are not of significance and these are general imaginary cases used to study the behavioural dynamics of the asteroid-tether-asteroid dumbbell system.

5. Conclusion

This thesis presented a study on manipulating the orbital trajectory of an asteroid by connecting the asteroid to a closely-passing-by asteroid through the means of a tether. The study included the analysis of the various parameters affecting such type of orbit manipulation and also analysed the different ways to achieve orbit diversion. The dynamics involved in the orbit manipulation was discussed, including how the manipulation of the orbital energy of the asteroids could lead to the manipulation of the orbital trajectory of the asteroid.

5.1 Summary

Chapter 1 discussed the historical view of the asteroids, starting from its first discovery, etymology and how the view on asteroid changed over time with a change in our understanding about them. Then the different ways to classify asteroids and their detailed classification leading to their composition and their relevance to humanity was discussed. Then the nature of asteroids from the perspective of them being a threat as well as important resource was discussed. A short description of the different methods of asteroid diversion was presented. A detailed analysis on tether assisted asteroid diversion was presented followed by the motivation involving the need for resources, asteroid mining, and economics, ending with the objectives for the research.

Chapter 2 discussed the assumption involved in the creation of the model, and the representation of the model developed for the study to fulfil the objectives. The study of the orbital and attitude dynamics of the setup which involved discussing the physics involved in the trajectory manipulation was analysed and represented by the equation of motion. The overall concept of connecting two closely-passing-by asteroids by means of a tether to manipulate the transfer of the orbital energy between the asteroids in the dumbbell system, in order to manipulate the orbital trajectory of the asteroids were elaborated.

Chapter 3 discussed about the different parameters that affected the trajectory manipulation through the asteroid-tether-asteroid dumbbell system. An analysis of how the various parameters such as the length of the tether, the mass ratio of the asteroids and the eccentricity of the initial orbits affected the orbital trajectory manipulation was carried out and the results presented along with a description about the dynamics of the energy pattern that is observed during the trajectory manipulation.

Chapter 4 dealt with describing in detail the part played by orbital energy of the asteroids in the orbital trajectory manipulation, the time needed to wait before a desirable orbital diversion can be achieved by cutting the tether at the correct orbital energy value.

5.2 Objectives Achieved

The following objectives were achieved:

- 1) A mathematical model was developed with the help of MATLAB, with limitations made possible through assumptions input into the model
- 2) The dynamics involved in changing the orbital trajectory of the asteroids through the formation of asteroid-tether-asteroid dumbbell system were studied, understood and explained
- 3) The parameters that affect the formation of the dumbbell system and those involved in the dynamics of the dumbbell system were studied and important points were concluded
- 4) Since orbital energy plays an important part in the whole idea, the relation between the orbital energy and the time of tether cut was studied in detail to understand how the system would behave to give out various resultant orbits could be achieved

5.3 Remarks

The following points are mentioned as observations made from carrying out the study and analysis involved in the orbit manipulation process using this method:

- 1) Assumptions played an important part in making it easy for the model to be setup and the dynamics to be simple
- 2) Though the time of tether cut is an important factor in the formation of the resultant orbits, the real quantities at play here are the orbital energy and orbital velocity. These quantities determine the size, shape and orientation of the resultant orbit
- 3) It could be noticed that the change in the orbital trajectory of the asteroids is achieved not only by cutting the tether after a certain time since dumbbell formation, but also due to the formation of the dumbbell system itself. The tether connection creates a dumbbell system with a centre of mass, which sets the trajectory of the dumbbell

system and hence the asteroids are in the dumbbell system the asteroids follow the path of the dumbbell system

- 4) It can be noticed from the resultant orbits achieved in the sample cases of single orbital tether disconnection scenario, that Asteroid2, which is closer to the Sun than Asteroid1 at tether connection and in a circular orbit does not seem to lose energy
- 5) The physics involving the scenarios, in which the awaiting time of tether cut spanned multiple orbital revolutions of either the centre of mass around the sun or the dumbbell rotations around the centre of mass, has patterns for every combination of eccentricity that could be helpful in determining the tether cut time

5.4 Feasibility of the Idea

On the question of feasibility, the whole concept could be divided into multiple streams, they are:

- 1) The concept of connecting two closely-passing-by asteroids through the means of tether
- 2) Controlling the dynamics of the tether
- 3) Achieving the desired change

While the concept is feasible in the sense of the physics behind it, this could be only made possible through various parameters involved. The parameters are explained below, and it is expected to be a while before tethers become stronger and dynamic to support concepts such as this.

5.4.1 Asteroids

The dynamics studied in this research involved a lot of limitations through mathematical assumptions to make the study simple. But in reality, the dynamics of the asteroids are more complex. One of the major processes involved would be to de-spin tumbling asteroids either about one axis or multiple axis. One of the methods proposed is angular momentum drain to de-spin an asteroid proposed by A. D. Dobrovolskis and J. A. Burns ^[56] another method is to use sun oriented tethers ^[51].

5.4.2 Tether

Tethers are crucial to this concept and parameters such as the strength of the tethers, the different types of tethers that could be used to control the dynamics are important. While the research involving tethers has been on-going for several years, it is mostly confined to the realm within the vicinity of the earth and involving comparatively smaller masses such as satellites and probes.

5.5 Future Work

This research established that the physics in the concept of connecting two asteroids to manipulate the orbital trajectory could be a reality and the feasibility of the concept could be achieved after considerable research and development on tethers and dynamics involving asteroids are carried out.

5.5.1 Orbital Energy Range

This topic could be a concept for study for any follow up research conducted based on this thesis.

For any scenario, the orientation of the tether over the course of the motion of the dumbbell system is determined by the initial conditions such as the mass of the asteroids, the orbital size, shape, orientation and the true anomaly of the two asteroids at the time of tether connection. For each value of true anomaly of the centre of mass' heliocentric orbit, the tether can have different orientation and the orientation of the tether for every value of true anomaly of the centre of mass varies from orbit to orbit within a single case. The best result in diverting an asteroid could be achieved by getting the right combination of the tether orientation and true anomaly of the centre of mass. This is the wait time discussed previously, where waiting for the right time to disconnect the tether once the desirable orbital energy is achieved leads to the expected resultant orbit. This desirable orbital energy is achieved from the right combination of the orientation of the tether and the true anomaly of the centre of mass.

Except in very few cases such as that of the one discussed in **Fig 4.20**, not all possible tether orientations are achieved in a dumbbell's motion and hence not all possible orbital energies achieved, and these orientations and orbital energies could be called as missed or hidden orientations and missed or hidden orbital energies respectively. Each value of orbital energy in combination with the orbital velocity vectors help in the resulting orbit during tether

connection. So, to identify all possible resulting orbits from a particular scenario, a study on the different combinations of tether orientation for different value of true anomaly of the centre of mass' heliocentric orbit that are hidden due to undisturbed dumbbell dynamics could be carried out, which would lead to the identification of right combinations of the missed tether orientations and energies.

For a particular scenario, creating a surface plot by plotting all the orbital energy for all possible tether orientation for all possible true anomaly value of the dumbbell system gives an idea on the energy ranges for that particular case. This is just to study the possibility of the missed or hidden combinations and hence the method used to obtain these hidden orientations is not discussed.

5.5.2 Other Future Research

- 1) The first point in the course of any future work would first require refining the current research. To minimize the complexity of the model, so as to form the basis of the idea and carryout the base analysis. Restrictions such as fixing of orbit to in-plane orbits were assumed in this research, to remove such restrictions and considerations of other forces such as the solar radiation pressure, Yarkovsky effect, etc. could be added for further analysis
- 2) To identify real cases of closely passing-by asteroids and use them as the basis of the research to get more realistic data
- 3) Discuss different ways that can be used to capture asteroids

References

- 1) NASA\JPL, <http://nssdc.gsfc.nasa.gov/planetary/text/asteroids.txt>
(Archive <http://archive.is/2X3HU>) (Date Accessed: 17th Feb, 2018)
- 2) C. J. Cunningham, B. G. Marsden and W. Orchiston, “How the First Dwarf Planet Became the Asteroid Ceres”, *Journal of Astronomical History and Heritage*, vol.12, pg.240-248, 2009
- 3) C. J. Cunningham and W. Orchiston, “Who invented the word asteroid - William Herschel or Stephen Westen”, *Journal of Astronomical History and Heritage*, vol.14, no.3, pg.230-234, 2011
- 4) T. Gehrels, “Asteroids”, *University of Arizona Press*, 1979
- 5) C. T. Kowal, “Asteroids: Their Nature and utilization (Second Edition)”, *John Wiley and Sons*, 1996
- 6) L. W. Alvarez, W. Alvarez, F. Asaro, H.V. Michel, “Extraterrestrial cause for the Cretaceous–Tertiary extinction”, *Science*, vol.208, no.4448, pg.1095–1108, 1980. doi:10.1126/science.208.4448.1095
- 7) NASA\GSFC, <http://nssdc.gsfc.nasa.gov/planetary/comet.html>
(Archive <http://archive.is/Ec82w>) (Date Accessed: 17th Feb, 2018)
- 8) J. L. Remo, “Near Earth Objects: The United Nations International Conference”, *Annals of the New York Academy of Sciences*, vol.822, pg.1, 1997
- 9) D. Morrison et al, “The impact hazard”, in T. Gehrels, “Hazards due to comets and asteroids”, pg. 60, 1994
- 10) D. Morrison et al, “The Spaceguard Survey: Report of the NASA International Near-Earth-Object Detection Workshop”, pg.1, 1992
- 11) A. Celletti, V. Sidorenko, “Some properties of the dumbbell satellite attitude dynamics”, *Springer*, 2008
- 12) P. Williams, “Libration Control of Tethered Satellites in Elliptical Orbits”, *Journal of spacecraft and rockets*, vol.43, no.2, March–April 2006
- 13) H. Kojima, Y. Furukawa, P. M. Trivailo, “Experimental Verification of Periodic Libration of Tethered Satellite System in Elliptic Orbit”, *Journal of guidance, control and dynamics*, vol.34, no.2, March–April 2011
- 14) H. Curtis, “Orbital Mechanics for Engineering Students (Third edition)”, *Elsevier Aerospace Engineering Series*, pg.174
- 15) MATLAB[®] is a high-level language and interactive environment for numerical computation, visualization, and programming -

- <http://www.mathworks.co.uk/products/matlab/>
(Archive <http://archive.is/FNXNr>) (Date Accessed: 17th Feb, 2018)
- 16) United Nations Office for Outer Space Affairs, “Recommendations of the Action on Near-Earth Objects for an international response to the Near-Earth Object impact threat”, *Press Hand-out*, 20 February 2013
- 17) G. H. Stokes, J. B. Evans and S. M. Larson, “Near-Earth Asteroid Search Programs”, in W. F. Bottke Jr., A. Cellino, P. Paolicchi & R. P. Binzel (eds), “Asteroids III”, *Tucson: University of Arizona Press*, pg.45
- 18) NASA Office of audits of the Inspector General’s office,” NASA’s Efforts to Identify Near-Earth Objects and Mitigate Hazards”, 2014
- 19) Armagh Observatory, <http://www.arm.ac.uk/neos/>
(Archive <http://archive.is/f3GvQ>) (Date Accessed: 17th Feb 2018)
- 20) NASA\JPL, NEO Program <http://neo.jpl.nasa.gov/glossary/h.html>
(Archive <http://archive.is/nmjAH>) (Date Accessed: 17th Feb, 2018)
- 21) Database, *Minor Planet Center (MPC)*
- 22) C. R. Chapman, “Calibrating asteroid impact”, *Science*, vol.342, pg.1051, 2013
- 23) V. A. Chobotov, “Orbital Mechanics”, *AIAA Education Series*, Third Edition, pg.68, 2002
- 24) NASA, <http://www.hq.nasa.gov/pao/History/conghand/traject.htm>
(Archive <http://archive.is/pz7pI>) (Date Accessed: 17th Feb, 2018)
- 25) J. R. Wertz and W. J. Larson, “Space Mission Analysis and Design”, Third Edition, pg.134, 2005
- 26) M. L. Nelson, D.T. Britt and L. A. Lebrofsky, “Review of Asteroid Compositions”
- 27) NASA, “Near-Earth Object Survey and Deflection Analysis of Alternatives: Report to Congress”, 2007
- 28) BBC, <http://www.bbc.com/future/story/20140314-the-worlds-scarcest-material>
(Archive <http://archive.is/G0Dw9>) (Date Accessed: 17th Feb, 2018)
- 29) B. R. Blair, “The role of Near-Earth Asteroids in Long Term Platinum Supply”, EB535 Metals Economics, Colorado School of Mines, 2000
- 30) J. S. Lewis, “Mining the Sky: untold riches from the asteroids, comets and planets”, Helix Books, 1996
- 31) K. Tsiolkovskii, “The Exploration of Cosmic Space by Means of Rocket Propulsion”, 1903
- 32) NASA-JPL, KISS, “Asteroid Retrieval Feasibility Study”, 2012

- 33) NASA, <http://www.nasa.gov/centers/marshall/news/background/facts/astp.html>
(Archive <http://archive.is/Yq9EA>) (Date Accessed: 17th Feb, 2018)
- 34) V. Badescu, ‘Asteroids: Prospective Energy and Material Resources’, pg.81, 2013
- 35) A. Storrs et al, “Imaging Observations of Asteroids with Hubble Space Telescope”, *Icarus*, Vol.137, pg. 260-268, 1999
- 36) J. P. Sanchez, “Asteroid hazard mitigation: deflection models and mission analysis”, PhD thesis, University of Glasgow, 2009
- 37) T. J. Ahrens, A. W. Harris, “Deflection and fragmentation of near-Earth asteroids”, *Nature* 360, pg. 429-433, 1992
- 38) H. J. Melosh, I. V. Nemchinov and Yu. I. Zeter, “Non-nuclear strategies for deflecting comets and asteroids”, *Hazards due to comets and asteroids*, University of Arizona Press, 1994
- 39) T. Lu, S. G. Love, “A Gravitational Tractor for Towing Asteroids”, *Nature*, Vol 438, pg. 177-178
- 40) H. J. Melosh and I. V. Nemchinov, “Solar asteroid diversion”, *Nature*, Vol 366, pg. 21-22, 1993
- 41) National Research Council, “Defending Earth, Near-Earth-Object surveys and Hazard Mitigation Strategies”
- 42) D. Izzo, “Optimization of Interplanetary Trajectories for impulsive and continuous Asteroid Deflection”, *Journal of Guidance, Control, and Dynamics*, Vol 30, No.2, March-April 2007
- 43) D. Scheeres and R. Schweickart, “The mechanics of moving asteroids”, 2004 planetary Defense Conference: Protecting Earth from Asteroids, AIAA, 2004-1446, 2004
- 44) D. Izzo, J. Olympio, C. H. Yam, “Asteroid Deflection Theory: Fundamentals of orbital mechanics and optimal control”, 1st IAA Planetary Defense Conference, 2009
- 45) B. Wei, “Astrodynamics Fundamentals for Deflecting Hazardous Near-Earth Objects”, IAC, 2009
- 46) William E. Wiesel, “Spaceflight Dynamics”, Irwin McGraw-Hill, Second Edition, 1995
- 47) R. Fitzpatrick, “An Introduction to Celestial Mechanics”, Cambridge University Press, 2012
- 48) V. S. Aslanov and A. S. Ledkov, “Dynamics of tethered satellite systems”, Woodhead Publishing, 2012

- 49) A. K. Maini, V. Agarwal, "Satellite Technology: Principles and Applications", Wiley, 2004
- 50) M. L. Cosmo and E. C. Lorenzini, "Tethers in space Handbook", Smithsonian Astrophysical Observatory, Third edition, 1997
- 51) N. Melamed, "Deflection of tumbling asteroids by means of sun oriented tethers", IAS, 2012
- 52) D. B. French and A. P. Mazzoleni, "Asteroid Diversion Using a Long Tether and Ballast", Journal of Spacecrafts and Rockets, Vol.46, No.3, May-June 2009
- 53) D. B. French and A. P. Mazzoleni, "Modelling tether-ballast asteroid diversion systems, including tether mass and elasticity", acta astronautica, 103, pg. 282-306, 2012
- 54) M. J. Mashayekhi and A. K. Misra, "Tether assisted near earth object diversion", acta astronautica, 75, pg. 71-77, 2012
- 55) M. J. Mashayekhi and A. K. Misra, "Optimization of Tether-Assisted Asteroid Deflection", Journal of Guidance, Control and Dynamics, Vol. 37, N0.3, May-June 2014
- 56) A. R. Dobrovolskis and J. A. Burns, "Angular momentum drain: A mechanism for despinning asteroid", Icarus, Vol.57, pg. 464-476, 1984
- 57) Yury I. Loanovsky, "Refind Parameters of Chelyabinsk and Tunguska Meteoroids and their Explosion Modes", IRKUT Corporation
- 58) P.G. Brown et al, "A 500-kiloton airburst over Chelyabinsk and an enhanced hazard from small impactors", Nature, pg. 238, Nov. 14, 2013
- 59) Hearing before the senate subcommittee on science, technology and Space, "The Space Shuttle and future Space launch vehicles", U.S. Govt Publishing Office, pg. 42, 2016
- 60) V. A. Chobotov, "Orbital Mechanics", *AIAA Education Series*, Third Edition, pg.28, 2002
- 61) Gerald R. Hintz, "Orbital Mechanics and Astrodynamics- Techniques and Tools for Space Missions", Springer, pg. 4, 2015
- 62) Richard Fitzpatrick, "An Introduction to Celestial Mechanics", Cambridge University Press, pg. 8, 2012.
- 63) Ashish Tewari, "Atmospheric and Space Flight Dynamics", Birkhäuser, pg. 99, 2007.
- 64) R. R. Bate et al, "Fundamentals of Astrodynamics", Dover Publications Inc, pg. 198, 1971.

- 65) H. Curtis, "Orbital Mechanics for Engineering Students (Third edition)", *Elsevier Aerospace Engineering Series*, pg.76.
- 66) R. R. Bate et al, "Fundamentals of Astrodynamics", Dover Publications Inc, pg. 191-193, 1971.
- 67) V. A. Chobotov, "Orbital Mechanics", *AIAA Education Series*, Third Edition, pg.59, 2002